Addis Ababa University

Addis Ababa Institute of Technology

School of Mechanical and Industrial Engineering

Mathematical modeling for thermo-mechanical stress field associated with a propagating crack in homogenous isotropic materials

A thesis submitted to the School of Mechanical and Industrial Engineering of Addis Ababa University in partial fulfillment of the requirements for the Degree of Masters of Science in Mechanical Engineering (mechanical design Stream)

Prepared by: Haile Simachew

ID: GSR/5250/11

Advisor: Addis Kidane (Ph.D.)

Associate Professor of Mechanical Engineering

University of South Carolina

Addis Ababa, Ethiopia

September, 2020 G.c

Declarations

This is to certify that the thesis presented by Haile Simachew, entitled as "**Mathematical modeling for thermo-mechanical stress field associated with a propagating crack in homogenous isotropic materials**" and submitted to the School of Mechanical and Industrial Engineering in the partial fulfillment of the requirements for the award of the degree of masters of science in Mechanical Design Engineering with the regulations of the university, and meet accepted standards with respect to originality and quality.

Haile Simachew	_____	_____
Name	Signature	Date

This thesis has been submitted for examination with approval as a university advisor

Addis Kidane (Ph.D.)	_____	_____
Advisor	Signature	Date

Addis Ababa University

Addis Ababa Institute of Technology

School of Mechanical and Industrial Engineering

Mathematical modeling for thermo-mechanical stress field associated with a propagating crack in homogenous isotropic materials

Addis Kidane (Ph.D.)	_____	_____
Advisor	Signature	Date
Samuel Tesfaye (Ph.D.)	_____	_____
Internal examiner	Signature	Date
Behailu Mamo (Ph.D. candidate)	_____	_____
External examiner	Signature	Date
Araya Abera (Ph.D. candidate)	_____	_____
Mech_Design chairman	Signature	Date
Yilma Teddesse (Ph.D.)	_____	_____
Char_Man SiME	Signature	Date
Ermiyas Tesfaye (Ph.D.)	_____	_____
Director of post graduate	Signature	Date

Acknowledgment

As long as I am a poor creature of GOD, I am strongly grateful for his permission to be healthful, breathing O_2 for 24 hours, for his unmeasurable mercifulness and gift as well as for the chance to fellow my MSc program in Addis Ababa University as well as for giving permission to perform each and every tasks of MSc program including this research. Next, I would like to say thanks to Dr. Addis Kidane for giving his unlimited advice how to write research proposal, gave the particular research title to be conducted for the thesis submitted to the School of Graduate Studies of Addis Ababa University impartial fulfillment of the Degree of Masters of Science in Mechanical Engineering (design stream). Moreover, he gave necessary materials for the research and I am grateful for his unlimited guide for the accomplishment of this final research work. Finally, thanks to our classmate that helps me by sharing ideas.

Abstract

The main objective of this research is to develop mathematical modeling of the thermos mechanical stress field associated with the propagating crack in homogeneous isentropic materials by using a temperature field that can be replicated in real world application. In most of existing work, the temperature field is obtained by assuming the heat flux to be singular at the crack tip. However, such assumption could lead to a theoretical solution practically generating a temperature field where the heat flux singular at the crack tip is not attainable. The mechanical design of engineering structure in accordance with preexisting flaws is analyzed based on mechanical loading and mixed mode thermo-mechanical stress field by using asymptotic solution of the steady state 2D temperature field equation. The solution is developed for the mixed mode thermo-mechanical loading condition when the crack propagates at a constant velocity in homogeneous isentropic materials using an asymptotic approach. The solution is obtained by simultaneously solving equation of motion defined as a function of displacement potentials, and perturbation theory for the solution of two-dimensional steady state temperature field equation. The perturbed temperature field equation is used to derive the first three terms of thermo-mechanical stress field equations by superimposing with the mechanical loading equation for the steady state propagating crack. The thermo-mechanical stress field developed by the superimposition and the developed stress fields evaluated for the crack tip introduce at the center single edge when the value of θ expressed by the interval $[-\pi, \pi]$. Around the crack tip from the crack tip plasticity approximations theory with the distance $r = 0.002m$ at $\theta = 0$ from the crack tip the thermo-mechanical stress field is zero. And the graph of stress intensity factors interpreted on the behalf of stress field since the stress and stress intensity factors have direct relationships. As the temperature and the heat flux increases the principal thermo-mechanical stress field such as σ_{xx}, σ_{yy} and τ_{xy} increases and similar trend is observed for the stress intensity factors that the material is overstressed to propagate the initial crack.

Key words: - Thermo-mechanical loading, Isentropic materials, Perturbation, Asymptotic approach, Stress fields,

Contents

List of figures

Chapter One

1. Introduction

It is known that the ultimate goal of applied solid mechanics is to be able to design structures or components that are capable of safely withstanding static or dynamic service loads for a certain period of time. And fracture mechanics is a field of solid mechanics that deals with the mechanical behavior of cracked bodies under different loading conditions and many researchers and authors conducted the investigation on the failure behavior of cracked body to estimate the maximum crack size that a material can sustain safely, to relate the crack size to the applied load, to know the amount of the critical load to extend a crack of known size, to know the crack extension behavior is stable or unstable according to the applied load, and to estimate the propagation of crack with time. Homogeneous identical properties at all points and isotropic materials are characterized by the particular property that does not vary with direction, and this work is intended to conduct on this type of material.

(Achenbach, 1975) explored an elasto dynamic explanation of running crack bifurcation by considering the semi-infinite body in a state of anti-plane strain that contains a two-Dimensions edge crack by the balance of rates of energies within the assumption of quasi-static increase of the external loads gives rise to rapid crack propagation at time t = 0, with an arbitrary and time-varying speed. The general finite-element model is employed to deal with coupled transient thermo elastic problems of fracture in an edge-cracked plate, especially with longer transient periods (Tei-Chen and Cheng-I, 1991). The pattern of crack growth during solidification after welding and a coupled thermo-mechanical analysis was conducted to achieve the stresses induced by welding processes using stress intensity factor (SIF)-based analysis by establishing SIF cracked model geometrically identical to an uncracked seam element based on the Lemaitre strain equivalence principle (Chen *et al.*, 2018). Methods of using the J-line integral to extract the magnitude of crack tip stress intensity factors from finite element solutions for thermal stress crack problems are presented (Wilson and Yu, 1979). The crack propagation in thermo-anisotropic elastic materials was model by using the extended finite element method (XFEM) based on the discontinuity at the crack surface is located and modeled using the level set principle whereas the singularity at the crack tip

is handled using special branch enrichment functions derived from the asymptotic analysis following Lekhnitskii's formalism in anisotropic media (Bouhala, Makradi and Belouettar, 2015). Thermo-mechanical crack propagation in aircraft engine vane was predicted based on a combined FEM (finite element method) – DBEM (dual boundary element method) approach through which starting from a three-dimensional FEM mesh for the uncracked structure a subdomain is identified, in which crack initiation and propagation are simulated by DBEM (Citarella *et al.*, 2013). The three-dimensional interfacial crack growth simulations using coupled finite element and element free Galerkin (FE-EFG) approach under mechanical and thermoelastic loading was investigated using an extrinsic partition of unity (PU) enrichment technique has been employed to model a crack in the domain (Pathak, Singh and Singh, 2016). (Vshivkov *et al.*, 2019) conducted experimental and theoretical study of heat dissipation at the fatigue crack tip during mixed-mode loading based on the plane samples of stainless steel (AISI 304) were weakened by a notch to initiate fatigue crack for uniaxial loading and biaxial loading conditions. Mixed-mode dynamic crack growth behavior in functionally graded materials (FGMs) under thermo-mechanical loading is studied by using asymptotic analysis in conjunction with displacement potentials to develop thermo-mechanical stress field(Kidane *et al.*, 2010). Mixed-mode dynamic crack growth along an arbitrarily smoothly varying path in functionally graded materials (FGMs) under thermo-mechanical loading is studied asymptotic analysis in conjunction with displacement potentials is used to develop the stress fields around propagating cracks in FGMs (Abotula *et al.*, 2012). The solutions in problems concerning steady-state crack propagation, either in infinite, or in strip-like elastic plates, based on complex-variable methods was presented when the crack is assumed semi-infinite and propagating, either in plane extension or in anti-plane shear under the action of constant stresses over a segment of the crack faces (Georgiadis and Theocaris, 1985). Thermo-mechanical stress field equations are developed for a mixed-mode crack propagating at constant velocity in homogeneous and isotropic materials using an asymptotic approach along with displacement potentials (Kidane, Chalivendra and Shukla, 2010).

Fracture is common in the engineering system that is operated with high temperatures and the above works do not consider the combined effects of the thermo-mechanical loading conditions as well as developed the stress field equations for these couple of effects to predict the fracture behavior of engineering structures. Some of the investigations developed the stress field equations

that enable to estimate of the fracture behavior of the engineering system but the temperature filed they developed was theoretical and is not experimentally verified. They utilized only asymptotic approach for the temperature field by assuming it will be singular at the crack tip, but it will not happen in the real-world scenarios. This paper aimed to forward the stress field equation the thermo-mechanical loading conditions associated with a propagating crack in engineering materials with a temperature field equation that will satisfy the real operating conditions. For the development of the new thermo-mechanical stress field equations we replace their assumptions of the singularity of the temperature field at the crack tip, by the real operating temperature by utilizing the ordinary solution principles of steady heat equation with perturbation theory. This theory enables to solve the temperature equation that satisfies the boundary values.

1.1. Statement of the problem

In the mechanical design of engineering structures in accordance with pre-existing flaws that could initiate crack and failure was investigated by many researchers and authors by considering mechanical loads, and also various equations that can be applied to forecast or predict the failure behavior of the systems were established. However, there are engineering systems that are exposed to high operating temperatures such as aircraft engine, engine, furnace, heat exchangers, heat pump, turbine rotor blades, vanes for aircraft engines, etc. in which their behavior of failure according to fracture mechanics was established according to mechanical load only. Some systems that are operating in thermo-mechanical loading condition will be exposed to thermo-mechanical fatigue, creep, and crack propagation.

In literature (Kidane *et al.*, 2010) utilized the asymptotic approach for the solution of the 2D steady state temperature field to be singular at the crack tip like the mechanical stress, but this is not attainable in the real world scenario. Thus, this work will come up with the stress field equations to estimate fractural failure characteristics of the engineering structure under thermo-mechanical loading conditions by considering temperature field that can be generated in real world application. This is due to their assumptions of the temperature field is singular at the crack tip, and to realize their assumption they utilize the asymptotic approach. But the singularity at the crack tip can't be obtained really. Therefore, in this research we utilize the ordinary solution principles of steady state heat equation and perturbation theory to obtain the solutions of heat equation that

is suitable to superimpose with mechanical stress field as well as to obtain the solution that satisfies the boundary condition and obtained in real scenarios.

1.2. Objectives

1.2.1. General objectives

The overall objective of this work is the mathematical modeling of the thermo-mechanical stress field associated with a propagating crack in homogenous isotropic materials.

1.2.2. Specific objectives

In order to deliver the equation of the thermo-mechanical stress field associated with propagating cracks in engineering materials, the following tasks should be performed.

- ✓ To develop the temperature field equation that can be generated in the real operating conditions.
- ✓ To define the equation of motion as a function of the displacement potentials ϕ and ψ
- ✓ To superimpose the developed fields to get the final verified and illustrated thermo-mechanical stress field associated with crack.

1.3. Delimitation

This research aimed to perform the mathematical modeling for the thermo-mechanical stress field associated with a propagating crack in homogenous isotropic materials since there is a wide range of engineering materials. Engineering materials have been conveniently grouped into three basic classifications: metals, ceramics, and polymers. Further metals are classified as ferrous and nonferrous metals. However, this research will be conducted on the engineering materials that have identical properties at all points and the particular property does not vary with direction. The mathematical modeling will allow different methods like asymptotic analysis, Galerkin methods, differential methods, and will employ a series of ordinary and partial differential equations. The research is proposed to achieve the thermo-mechanical stress field equation and extended up to the depiction and verification of the field equation using the software. But in this research the proposed task is developing the thermo-mechanical stress fields according to the in-plane stresses (σ_{xx}, σ_{yy} and τ_{xy}), will analyze the effect of temperature field on the magnitude and also the effect of temperature on the crack tip velocity analytically.

1.4. Limitation

As the scope the research is limited to analyze and verify the results experimentally for the developed thermo-mechanical stress field equations. In this research it is assumed that the material

is isentropic and homogeneous, but when we apply the temperature the materials properties will vary at all points as well directions. In this research we set it as a limitation since it didn't consider the variation of the properties due to the applied load. And also in the graph of the stresses fields and stress intensity factors are below the isothermal values, such that forth the stress field in y direction σ_{yy} and stress intensity factor it becomes below the isothermal for the θ in between -2 and -3.14 rad as well for the stress field in x direction σ_{xx} and stress intensity factor it becomes below the isothermal for the θ in between 2 and 3.14 rad and it is limited to interpret this situation in the real world scenarios.

1.5. Methodology

Technically this research will use different approaches that will give the best solutions and these strategical methods will start with data collected directly from the primary source and indirectly from the secondary source of books, kinds of literature and website. The collection of the data will include the properties of materials, operating conditions of the selected system that operated in thermo-mechanical loads, the boundary conditions or the limiting conditions and the operating temperature to develop the temperature field equations. In this work, the proposed types of data will include the temperatures that are imposed on the mechanical system, the mechanical load that applied to the systems that are exposed to combine mechanical and thermal loadings, the boundary conditions also the other data needed in this work. The chemical composition and the mechanical properties of the material are also the other data that need to be analyzed and evaluated in this work to be utilized for the stress field equations. The methodology that will employ to this work is the other critical information to be selected properly by using scientific reasons and selection. The suitable methods for the derivation of the temperature field and the heat flux equation will be selected such as the asymptotic approach, Galerkin method, extended finite element method, finite element methods, etc.

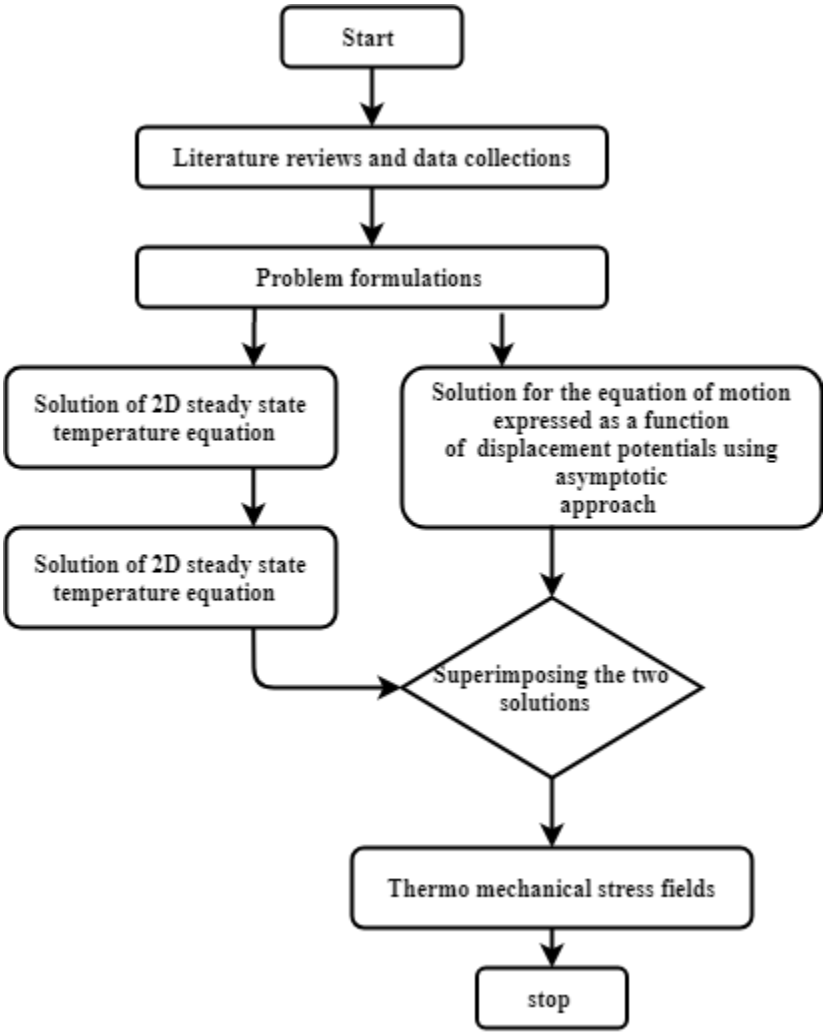

Figure 1:- The expected methodology of the research

The stress fields from the mechanical loading conditions and the stress intensity factors will be determined. Using these thermo-mechanical stress fields, various stress components are developed, and the effect of temperature on these stresses and the effects of temperature field and crack-tip velocity on crack growth angle will be discussed.

1.6. Expected outcomes

At the end of this research, the thermo-mechanical stress field equations on isotropic homogeneous materials using a series of ordinary and partial differential equation will be forwarded for the materials in which the initial crack is introduced and the governing equation, as well as the response of the material due to both thermal and mechanical load, will be established. The equation ensures that the designers, the researcher as well as the concerned personnel will study the fractural

behaviors for different materials based on the established equations. This newly derived equation enables the other researcher to conduct fractural experiments for the materials that are loaded both mechanical and thermally, and also the derived equation will enable the researchers to perform further derivations for the rest of materials such as within isentropic, non-homogenous, composites, non-ferrous, polymers, and ceramics within the similar methodology. This work will forward the thermo-mechanical stress fields by the development of the equations of the stress, strain, and displacement and also the effect of temperature on the parameters such as the in-plane stresses (σ_{xx}, σ_{yy} and τ_{xy}), on the magnitude and the profile of the maximum shear stress τ_{max} and principal stress σ_1, crack tip velocity will also be forwarded.

Chapter Two

2. Literature reviews

H. G. GEORGIADIS, P. S. THEOCARIS(1985), formulated the solutions in problems concerning steady-state crack propagation, either in infinite, or in strip-like elastic plates, based on complex-variable methods by assuming the crack to be semi-infinite and propagating, either in-plane extension or in anti-plane shear under the action of constant stresses over a segment of the crack faces. And they also reported the methods of the solution is particularly useful in treating problems of infinite strips over other methods. In the solution principles (Georgiadis and Theocaris, 1985) assumed that yielding occurs in a narrow wedge-shaped zone R, the material in the zone is under uniform tensile yield stress, a_o, a Tresca yield criterion is obeyed and the material outside the zone is elastic.

CHENG LIU, ARES J. ROSAKIS (1994), aimed to understand the nature of the mixed-mode asymptotic field that dominates the region near a transiently propagating and curving crack tip. They developed a new methodology to obtain the higher-order transient asymptotic elasto dynamic field near the tip of a crack that propagates non-uniformly along an arbitrary and smoothly curved path and also they focused on crack growth in a homogeneous, isotropic, and linearly elastic material in which there is an arbitrarily propagating crack on the origin of the cartesian coordinates at t=0 and at t>0 the crack will propagates to an arbitrary order point ($X_1(t)$, $X_2(t)$). (Liu and Rosakis, 1994) developed a procedure for obtaining the higher-order transient asymptotic representation of the elasto dynamic field around the tip of a propagating crack and stated that the crack propagates transiently along a smooth but otherwise arbitrary path.

D. E. KATSAREAS AND N. K. ANIFANTIS (1995), analyzed fractured planar bodies associated with thermal shock load type loads by utilizing a time-domain boundary-only element method through solving the uncoupled quasi-static thermo elasticity equation without the necessity of domain discretization. The authors exhibited the singularity comportment of the temperature and displacement fields in the vicinity of the crack tip based on the quarter-point elements. The researchers used the well-known displacement and traction formulas to estimate the transient thermal stress as well as heat flux by using the calculated nodal values. These authors compare and contrast their results with the analytical and computational ones reserved from the previous

research and literature to verify the results obtained according to the accuracy of the method, the stability of the solution and the dependence on space-time discretization. They selected two representative thermally shocked fracture problems such as edge cracked infinite strip and edge cracked finite plate.

Vijaya Bhaskar Chalivendra (2007), considered transient mixed-mode elasto dynamic crack growth along arbitrary smoothly varying paths in functionally graded materials (FGMs), and they utilized the various properties of FGMs by varying the shear modulus, and mass density exponentially along the gradation direction. They used the asymptotic approach to develop crack tip out of displacement fields and their gradients for the propagating curved cracks of arbitrary velocity. In addition to the asymptotic analysis super positioning was utilized to get the mode-mixity due to the inclination of curved crack as well the expansion of the displacement fields and their gradients around the crack tip were driven in power series of radial coordinates with coefficients of expansion based on the local curvature of the crack path time rate of crack tip-speed, and time derivatives of mode-I and mode-II stress intensity factors. As a result to understand the effect of transient terns associated with the parameters such as the instantaneous value of the local curvature of the crack path, crack-tip speed, time derivatives of crack-tip speed, and time derivative of mode-I and mode-II stress intensity factors in crack-tip field equations (Chalivendra, 2007), plotted both opening and mixed-mode loading for the effect of listed parameters whereas extracting fracture parameters from experimentally determined out of plane displacement fields, analytical out of plane displacement contours for various values and these contours show that the transient effects cause significant spatial variation in out of plane displacements around the crack-tip. In the nutshell the authors concluded that the properties around the crack tip in FGM during crack propagation and therefore hey postulated FGM is likely to be transient with the crack speed and dynamic stress intensity factors changing as a function of time and also the author suggested that it is vital to consider the curvature, rate of change of velocity and rate of change of fracture parameters terms in the growth for a curved crack in extracting fracture parameters from experimentally determined crack-tip field.

Addis Kidane, Vijaya B. Chalivendra, Arun Shukla, Ravi Chona (2010), studied mixed-mode dynamic crack growth behavior in functionally graded materials (FGMs) under thermo-mechanical loading by utilizing the asymptotic analysis in conjunction with displacement

potentials to develop thermo-mechanical stress fields for a mixed-mode propagating crack in an FGM. These authors assumed the shear modulus, mass density, thermal conductivity and coefficient of thermal expansion for the FGM to vary exponentially along the gradation direction as well Poisson's ratio was assumed constant. (Kidane, Chalivendra and Shukla, 2010) also neglected the thermo-elastic cooling and the transient effects, temperature field generated due to crack-tip propagation. As the methodology, the authors primarily drove, asymptotic temperature fields for an exponential variation of thermal conductivity and in the second phase, these temperature fields were used to drove stress fields. Mainly the researchers used asymptotic thermo-mechanical stress fields to generate the variation of maximum shear stress, circumferential stress and strain energy density as a function of temperature around the crack tip. The authors evaluated the crack growth direction as a function of temperature, non-homogeneity parameter, and crack-tip velocity by applying both circumferential stress and minimum strain-energy density criteria. As well as using the developed equations, the angular variation of the maximum shear stress is plotted as a function of temperature around the crack tip. The authors utilized the developed stress field to evaluate the variation of stress components hoop stress $\sigma_{\theta\theta}$, maximum principal stress $\sigma 1$ and maximum shear stress τ_{max} the in-plane σ_{xx}, σ_{yy} and σ_{xy} near the crack tip as a function of angular position θ for the temperature field associated with different q_o. The direction of crack growth was predicted theoretically through minimum strain energy density (S-criterion) and maximum circumferential stress ($\sigma_{\theta\theta}$ -criterion). Finally (Kidane, Chalivendra and Shukla, 2010) summarized their study as the thermo-mechanical stress fields around the crack tip are significantly affected by the non-homogeneity parameter, the temperature coefficients considered in this study show little variation in the stress fields, the crack extension angle depends on the crack-tip velocity, the crack deviates from the original path and starts to kink after the crack tip velocity reaches a critical value (about $c/cs > 0.5$), the crack extension angle increases with the increase in crack-tip velocity, the increases in temperature field increases the crack extension angle in the case of FGMs with decreasing stiffness along the crack direction.

Addis Kidane · Vijaya B. Chalivendra · Arun Shukla (2010), developed thermo-mechanical stress field equations for a mixed-mode crack propagating at constant velocity inhomogeneous and isotropic materials using an asymptotic approach along with displacement potentials. The authors used the asymptotic approach to develop the temperature field for steady-state temperature fields

on insulated crack face boundary conditions, then after the developed temperature field equations are used to derive the first three terms of thermo-mechanical stress field equations for a steady-state propagating mixed-mode crack. (Kidane, Chalivendra and Shukla, 2010) used the developed thermo-mechanical stress field for the determination of various components of stresses as well by applying strain energy density and circumferential stress criteria to observe the effect of temperature and the crack tip velocity on the crack growth direction. Finally, (Kidane, Chalivendra and Shukla, 2010) concluded that the developed crack-tip field equations can be successfully used to estimate fracture behavior from experimental stress and deformation fields when the materials are subjected to thermo-mechanical loading as well as the effect of temperature on in-plane stress, qualitative profiles of in-plane stresses, maximum shear stress, hoop stress, the principal stress around the crack tip, and crack growth angle for a given crack-tip velocity were suggested.

Sandeep Abotula, Addis Kidane, Vijaya B. Chalivendra, Arun Shukla (2012), investigated Mixed-mode dynamic crack growth along an arbitrarily smoothly varying path in functionally graded materials (FGMs) under thermo-mechanical loading. They also changed shear-modulus, mass density, thermal conductivity and coefficient of thermal expansion FGMs to get various properties for the study exponentially along the gradation direction as well they employed asymptotic analysis in conjunction with displacement potentials to develop the stress fields around propagating cracks. thermo-mechanical stress field was developed primarily by utilizing asymptotic analysis for the temperature filed and then they super positioned with mechanical stress fields, and then after based on the developed thermo-mechanical stress fields various components of stresses were established for a curving crack in FGMs. Finally (Abotula *et al.*, 2012) established and discussed the effect of curvature parameters, crack-tip speeds, non-homogeneity values and temperature gradients on crack growth directions on the basis of minimum strain energy density criterion and contours of maximum shear stress were plotted to show the effect of curvature terms and gradation around the crack-tip.

R. Citarella, G. Cricrì, M. Lepore, M. Perrella (2013), the main issue of these researchers was the dimensional decrement of newly generated jet engines due to the requirements of cruelly reduced fuel consumptions and causes thermo-mechanical fatigue, creep, and crack propagation. Also, the authors stated that the combined effect of mechanical and thermal stresses leads to a mixed-mode loading in which by using a suitable crack propagation tools must be capable to

forecast mixed mode crack propagation of a randomly curved cracks in three dimensional space through a combined FEM(finite element method)-DBEM(dual boundary element method) approach. They started from three-dimensional FEM mesh for the crack-free structure and identified the subdomain, and then after the crack initiation and propagation are simulated by DBEM. They also extract subdomains from the FEM domain and imported together with its boundary conditions (that are calculated by utilizing the previous thermal stress FEM analysis) in the DBEM environment were performed a linear elastic multiple crack growth analysis. (Citarella *et al.*, 2013)suggested the iteration procedure of their work as once the direction of the crack propagation determined new crack increment can be calculated for the new crack front and this procedure repeated until failure as well in this procedure allows the consideration of the spectrum effects and creep effects: both conditions determine residual stresses and determines the residual stresses that the crack will encounter during the propagation. They also tested the proposed procedure gas turbine vane, getting sound results, and can be made fully automatic based on the CAD modeling, FE and BE analysis, fracture mechanics, creep, meshing and sub-modeling issues, and is aimed at an accurate prediction of crack growth.(Citarella *et al.*, 2013) have taken the thermal boundary conditions of the imposed temperature in the internal cooled surface (T=913K), on the suction side (T=1113K) and the pressure side (T=1138K) of the airfoil and they assumed the adiabatic conditions for the sake of simplicity on the rest of the surfaces(hub and casing) as well as in the DBEM analysis the thermal (conductivity and expansion coefficient) and mechanical (Poisson ratio and Young Modulus) material properties. They also automatically extract the portion of the domain in which the crack propagates and can read from the FEM result temperature and displacements to be applied on the subdomains using the DBEM. The researchers compared the maximum principal stresses on a small (still uncracked) aero foil portion as provided respectively by a FEM and a DBEM global thermal-stress analysis (the latter based on the boundary conditions coming from the global FEM analysis).

Lyazid Bouhala, Ahmed Makradi, Salim Belouettar (2015), reported the model for the crack propagation in thermo-anisotropic elasticity and demonstrated the influence of anisotropy on crack propagation paths. In their work they utilized XEFM to solve the transient state heat transfer problem and then they super positioned to the couple solution with the thermo-mechanical problem, and their main target was to develop the enrich functions relevant to the phenomena

subjected in the temperature and displacement field at the crack surface and also to drive the relevant functions suitable to model the singularity of the heat flux and stress at the crack tips.(Bouhala, Makradi and Belouettar, 2015) located the discontinuity at the crack surface and also modeled by utilizing level set principles whereas they handled the singularity at the crack tip based on the special branch enrichment function that is driven from the asymptotic analysis following Lekhnitskii's formalism in anisotropic media. Then based on the established methods the authors observed that the crack starts to propagate when the maximum circumferential strength ratio was satisfied and also, they validate the numerical model by comparing the computed stress intensity factors (SIFs) with the existing ones for the static cracks and finally they utilized several simulations to investigate the effect of anisotropy.

Himanshu Pathak, Akhilendra Singh and Indra Vir Singh (2016), forwarded the simulation of three-dimensional interfacial crack growth using coupled finite element and element free Galerkin (FE-EFG) enrichment method has been employed to the model a crack in the domain and also the researchers employed Extrinsic partition of unity (PU) enrichment procedure to model a crack in the domain. (Pathak, Singh and Singh, 2016) modeled the crack face by Heaviside and they modeled the crack front by asymptotic branch enrichment functions, as well as a material interface, has been modeled by a signed distance function. The researchers evaluated the individual stress intensity factors using a modified domain-based interaction integral approach. The authors also performed the life prediction of interfacial cracked geometries using Standard Paris law of fatigue crack growth and finally, they solved numerous interfacial fatigue crack growth problems have been by the coupled EF-EFG approach.

Amin Memari, Mohammad Reza Khoshravan Azar (2019), investigated transient stress intensity factors of two- or three-dimensional cracked specimen by the meshless method with linear test function by considering different mechanical and thermal shock loads. The researchers also investigated the effect of crack length, density and Lord-Shulman relaxation time on stress intensity factors, and mainly the effect of the crack length on the stress intensity factor will be postulated.

(Memari and Khoshravan Azar, 2019) used different theoretical and real values of relaxation time to show how thermal stress intensity factor curves change when modified Fourier heat conduction law is employed compared with classical Fourier law. The authors studied various crack problems

based on the stress intensity factor investigations by meshless local Petrov-Galerkin method(MLPG) and they supported the study by examples to examine the efficiency of the proposed method as well 2D, 3D specimens of stationary cracks and static(steady) state, dynamic(transient) problems using homogeneous and functionally graded (FG) materials are considered. (Memari and Khoshravan Azar, 2019)the utilized linear coupled thermoelastic governing equation that includes equation of motion and classic energy relation with the stress tensor, material density, displacement vector, spatial coordinate vector, time variable, heat flux vector, specific heat, temperature difference, and initial temperature. The authors also take into account the effect of different crack length and they concluded that despite the pure mechanical stress intensity factors, thermal stress intensity factors which obtained from thermal shock loads, and different responses were obtained for temperature, heat flux, and heat convection load, as well the effect of specimen size on the temporal variation of thermal stress intensity.

A. Vshivkov, A. Iziumov, R. Yarullin, V. Shlyannikov, O. Plekhov (2019), tested series of specimens prepared from stainless steel within the specified geometries and these specimens were subjected to cyclic load with constant stress amplitudes and different biaxial coefficients. In the experiments, the authors employed contact heat flux sensor and sensor-based on See beck effect to analyze the energy dissipation at the crack tip. The researchers hypothesized that the quantity of heat and its sign depends on the type of materials, the direction and strength of the electric current. (Vshivkov *et al.*, 2019) targeted to examine different specimens of stainless steel that were subjected to biaxial load test and to record the crack length and the heat flux, as a result, they have gotten the crack propagation rate of 10e-7-10e-4 m/cycle. The authors observed from the Paris curve and crack length curve, in the first stage crack rate is proportional to the power of heat flux and the crack length and in the second stage the power of heat flux. The plastic deformation at the fatigue crack tip also estimated theoretically. The study revealed a qualitative agreement between the energy approach to the description of the fatigue crack propagation and the classical approach, which is based on the use of the stress intensity factor.

Different researchers performed the effect of the temperature and mechanical loading in the separated mode and also some literature depicted that there are the researchers conducted on the combined mode of temperature and mechanical loading by utilizing different techniques such as the steady-state crack propagation, either infinite or in strip-like elastic plates by using the complex

variables. The authors also established different assumptions, working conditions, problem formulations, and also, they employed the different methodologies of the result, and they also concluded their findings by correlating the objectives of the research with the result of it.

Most of these literature objectives and the target of this paper that is the mathematical modeling of the thermo-mechanical stress field associated with a propagating crack in homogenous isotropic materials are slightly different but their methodology, verifications of the result techniques, problem or theoretical formulation techniques, presentation methods of the results and findings will help our work as the benchmarks. Although (Liu and Rosakis, 1994)asymptotic analysis of a non-uniformly propagating dynamic crack along an arbitrary path they didn't include the effect of temperature in the combined with the mechanical loads, and also they used existed equation to predict the fractural behavior of smooth curved path under two-dimensional conditions. (ANIFANTIS, 1995)analyzed fractured planar bodies associated with thermal shock load type loads by utilizing a time-domain boundary-only element method through solving the uncoupled quasi-static thermo elasticity equation without the necessity of domain discretization but they failed to include the effect of mechanical load in combined with the temperature effect and failed to analyze the thermo-mechanical singularity at the crack tip and most of the literature conducted fractural stress field analysis individually for thermal effect or mechanical loading conditions. But (Kidane, Chalivendra and Shukla, 2010), (Kidane *et al.*, 2010) and (Abotula *et al.*, 2012)conducted the investigation on Thermo-mechanical stress fields and strain energy associated with a mixed-mode propagating crack, Mixed-mode dynamic crack propagation in graded materials under thermo-mechanical loading and Dynamic curving cracks in functionally graded materials under thermo-mechanical loading respectively but their estimation of the fracture behavior of the engineering system but the temperature filed they developed was theoretical and is not experimentally verified that is they formulated the simplest a theoretical equations using asymptotic analysis for the simplicity of the equation, this leads to unachievable temperature field equations.

Chapter Three

3. Methodology

3.1. A two-dimensional Heat equation

Figure 2 represents the heat flow in two-dimensional object (thin plate). Representing the plate by a region in the xy plane and let T(x,y) the temperature of plate at a position (x, y) .

Under ideal assumption, (e.g. uniform density, uniform specific heat, perfect insulation along faces, no internal heat source etc.). One can show that T satisfies the two-dimensional heat equation, which is steady or does not dependent on time.

Let us assume; the plate is rectangular represented by $R = [0, a] \times [0, b]$

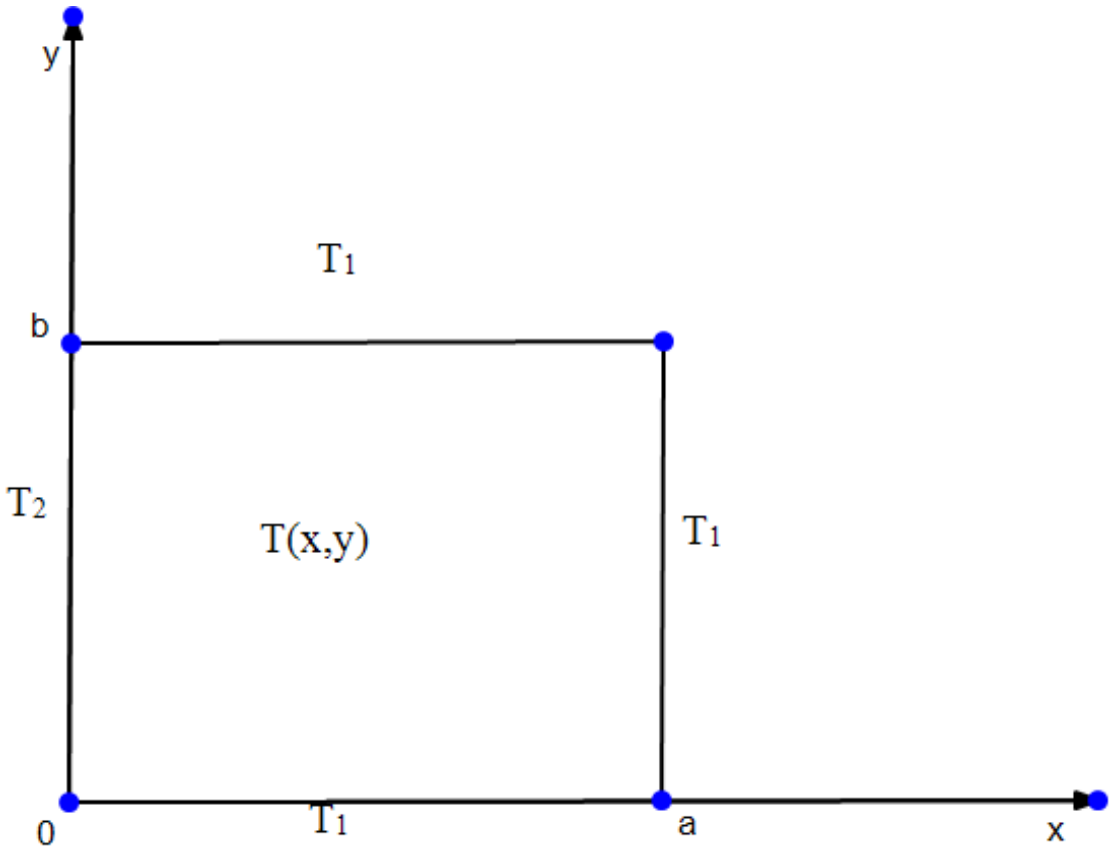

Figure 2:- The rectangular plate exposed to temperature

The plate is imparted with some initial temperature T(x,y)=f(x,y), (x,y)εR

The edges of the plate are held at zero degree

Inhomogeneous boundary conditions

Steady state solution and Laplace equation. 2D heat problems with inhomogeneous Dirichlet's boundary conditions can be solved by the homogenizing procedure used in 1D case.

1) Find and subtract the steady state ($T_t = 0$)
2) Solve the resulting homogeneous problem
3) Add the steady state results of step 2

We will focus on finding the steady state part of the solution.

Setting $T_t = 0$ in the 2D heat equation gives, the Laplace equation solution of which are harmonic functions.

$$K\frac{\partial^2 T}{\partial x^2} + K\frac{\partial^2 T}{\partial y^2} = 0 \qquad [3.1]$$

Here the temperature applied on the 2R is T(x, y)=f(x, y) where the region is rectangle $R = [0, a] \times [0,\ b]$the boundary conditions will give on each edge separately as

$$\begin{aligned} T(x,0) &= f_1(x) \\ T(x,b) &= f_2(x) \\ T(0,y) &= g_1(y) \\ T(a,y) &= g_2(y) \end{aligned} \qquad for\ \ 0 < x < a\ and\ 0 < y < b \qquad [3.2]$$

Solving the Dirichlet problem on the rectangle

Homogenizing and super positioning

Strategy reduce to four simpler problem and use superposition.

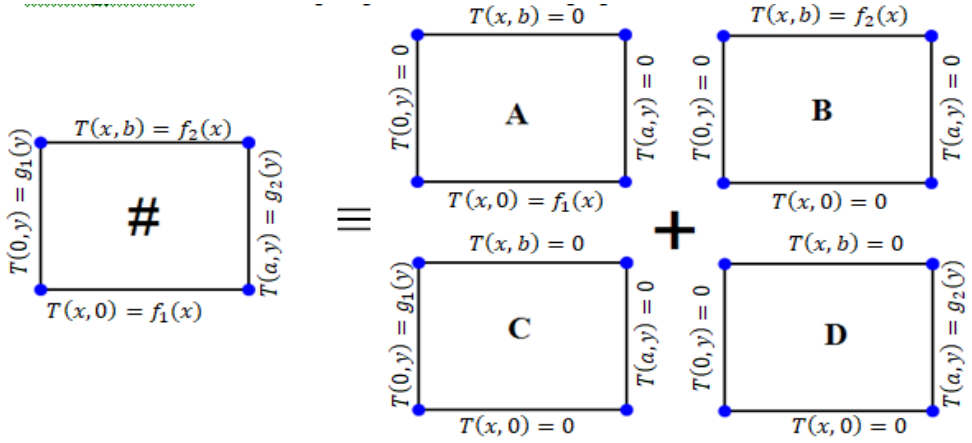

Figure 3:- The homogenizing and super positioning of a plate

1) If T_A, T_B, T_C and $T_D$solve the dirichlet problems A, B, C and D then the general solution to # is the sum
2) Note the boundary conditions in A_D are all homogeneous with the exceptions of single edge.
3) Problems with inhomogeneous Neumann and Robin boundary conditions or (combination of these there if) can be reduced in similar manner.

Solution of the Dirichlet problem or rectangle case B.

Solve the boundary value problem B $\Delta T = 0, \quad 0 < x < a, \qquad 0 < y < b$

$T(x,0) = 0 \quad T(x,b) = f_2(x) \qquad 0 < x < a$

$T(0,y) = 0 \quad T(a,y) = 0 \qquad 0 < y < b$

Setting T(x,y)=X(x)Y(y) leads to the following differential equation based up on the law of separable equation (Kreyszig, 2012).

$$X" + KX = 0 \qquad [3.3]$$

$$Y" - KY = 0 \qquad [3.4]$$

For X(0)=X(a)=0 and Y(0)=Y(b)=0.

For non-trivial solution for x are given by;

$$X(x) = X_n(x) = \sin(\mu_n x) \qquad [3.5]$$

Where $\mu_n = \frac{n\pi}{a}, \quad and\ K = {\mu_n}^2$

The hyperbolic trigonometric cosine and sine function are $coshy = \frac{e^y + e^{-y}}{2}$ and $sinhy = \frac{e^y - e^{-y}}{2}$ and satisfies the following identities and derivatives.

$$cosh^2 y - sinh^2 y = 1$$
$$\frac{\partial}{\partial y} coshy = sinhy \qquad [3.6]$$
$$\frac{\partial}{\partial y} sinhy = coshy$$

Then the general solution for the ordinary differential equation of [3.4] can also be written as follows for $K = {\mu_n}^2$

$$\mathrm{Y(y)} = Y_n(\mathrm{y}) = \mathrm{Acosh}(\mu_n y) + Bsinh(\mu_n y) \qquad [3.7]$$

Then for $Y_n(0) = 0$ we get $Y_n(\mathrm{y}) = B_n sinh(\mu_n y)$

This yields the separated solution;

$$\mathrm{T(x,y)} = \mathrm{X(x)Y(y)} = B_n sin(\mu_n x) sinh(\mu_n y) \quad [3.8]$$

And super positioning gives the general solution.

$$T_n(x,y) = \sum_{n=1}^{\infty} B_n sin(\mu_n x) sinh(\mu_n y) \quad [3.9]$$

Finally, the top edge boundary condition requires that;

$$f_2(x) = T(x,b) = \sum_{n=1}^{\infty} B_n sin(\mu_n x) sinh(\mu_n b) \quad [3.10]$$

Appealing to the formula for sine series coefficient we can now summarizes our findings. If $f_2(x)$is a piecewise smooth the solution to the dirchelet problem (Kreyszig, 2012).

$\Delta T = 0 \qquad 0 < x < a \qquad 0 < y < b$

$T(x,y) = 0 \qquad T(x,b) = f_2(x) \qquad 0 < x < a$

$T(0,y) = T(a,y) = 0 \qquad 0 < y < b$

$$T_n(x,y) = \sum_{n=1}^{\infty} B_n sin(\mu_n x) sinh(\mu_n y) \quad [3.11]$$

Where,

$$B_n = \frac{2}{\mathrm{asinh}(\mu_n b)} \int_0^a f_2(x)\, sin(\mu_n x) dx \quad [3.12]$$

Solution of the Dirichlet problem on rectangle case A and C

Separation of the variables shows that the solution to A is;

$$T_A(x,y) = \sum_{n=1}^{\infty} A_n sin\left(\frac{n\pi}{a}x\right) sinh\left(\frac{n\pi}{a}(b-y)\right) \quad [3.13]$$

Where,

$$A_n = \frac{2}{\mathrm{asinh}(\frac{n\pi}{a}b)} \int_0^a f_1(x)\, sin\left(\frac{n\pi}{a}x\right) dx \quad [3.14]$$

Likewise, the solution to case C is;

$$T_C(x,y) = \sum_{n=1}^{\infty} C_n sinh\left(\frac{n\pi}{b}(a-x)\right) sin\left(\frac{n\pi}{b}y\right) \quad [3.15]$$

$$C_n = \frac{2}{\mathrm{bsinh}(\frac{n\pi}{b}a)} \int_0^a g_1(y)\, sin\left(\frac{n\pi}{b}y\right) dy \quad [3.16]$$

Similarly, for case D;

$$T_D(x,y) = \sum_{n=1}^{\infty} D_n sinh\left(\frac{n\pi}{b}x\right) sin\left(\frac{n\pi}{b}y\right) \quad [3.17]$$

Where,

$$D_n = \frac{2}{b\sinh(\frac{n\pi}{b}a)} \int_0^a g_2(y)\, sin\left(\frac{n\pi}{b}y\right) dy \quad [3.18]$$

Then the complete solution for $T_{xx} + T_{yy} = 0$ for the non-homogeneous boundary condition is;

$$T(x,y) = T_A(x,y) + T_B(x,y) + T_C(x,y) + T_D(x,y) \quad [3.19]$$

$$T(x,y) = \sum_{n=1}^{\infty} A_n sin\left(\frac{n\pi}{a}x\right) sinh\left(\frac{n\pi}{a}(b-y)\right) + \sum_{n=1}^{\infty} B_n sin(\mu_n x) sinh(\mu_n y) + \sum_{n=1}^{\infty} C_n sinh\left(\frac{n\pi}{b}(a-x)\right) sin\left(\frac{n\pi}{b}y\right) + \sum_{n=1}^{\infty} D_n sinh\left(\frac{n\pi}{b}x\right) sin\left(\frac{n\pi}{b}y\right) \quad [3.20]$$

Where the coefficients $A_n, B_n, C_n \; and \; D_n$ are given by the equation [3.12] [3.14] [3.16] and [3.18] respectively.

At this stage let's check the solution for the two-dimensional equation whether it satisfies the boundary condition or not.

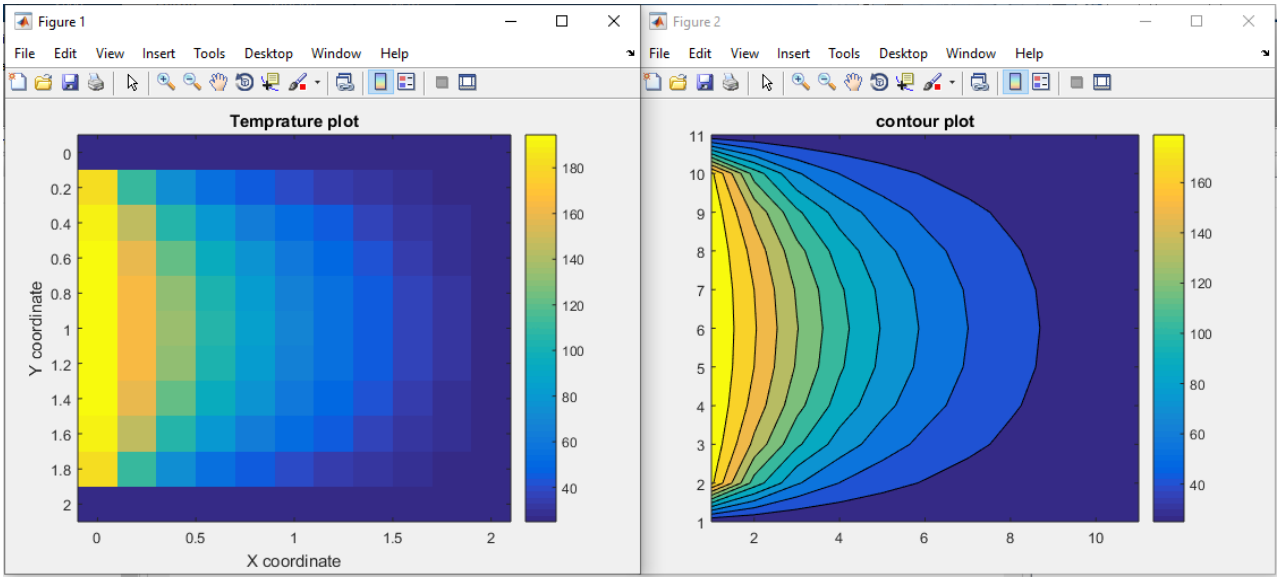

Figure 4: The temperature plot and the contour plot for thin plate

The terms in the preceding series become smaller in magnitude as n increases. Write a MATLAB program to verify this fact for n=1, …,19 for the center of the plate(x=y=1) using x=y=1 write

MATLAB program to determine how many terms are required in the series to produce a temperature calculation that is accurate to within 9% nine percent. That is for what value of n the addition of the next term in the series will produce a change in T of less than 9%). Modify the program from part be to compute the temperature in plate using the space of 0.2 for both x and y. At this stage the solution for the two-dimensional steady state heat equation is checked on MATLAB software by programming the solution equation and giving arbitrary temperature of 200 on the left edge and varying the temperature on the other three edges from 25 to 175 to verify the flow of temperature from higher temperature gradient to lower temperature gradient. And the thin plate on which exposed to the above arbitrary temperature is specified as a square.

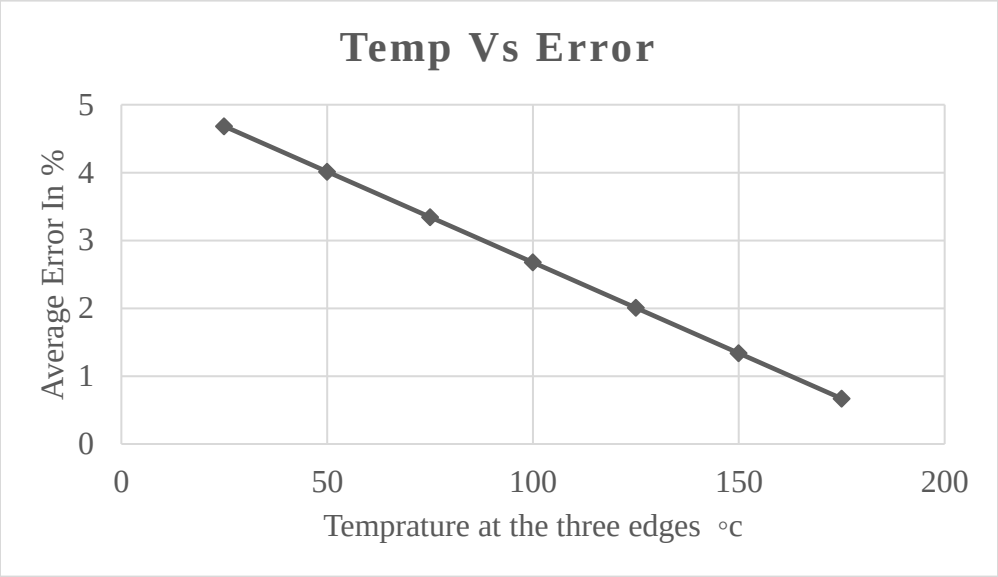

Figure 5:- The error minimization due to the increment of temperature on the three edges

Up on the variation of the temperature on the three edges the distribution of the temperature on the plate is depicted above numerically and the deviation of the temperature from the applied temperature of 200 ◦C applied on the left edge of the rectangular thin plate illustrated graphically on figure 5, therefore the error that represents the deviation is less than 9%, and the average maximum error is 4.68% and the average minimum error is 0.66%. The graph shows that the error decreases as the temperature on the three edge increases and the error increases as the temperature on the three edges decreases.

3.2. Applied mechanical stress.

3.2.1. Equation of motion

Relates the stress with body forces and balancing of forces and moments acting on any component was enforced in order to ensure that the component was in equilibrium.

Two-dimensional equations.

Consider two-dimensional infinitesimal element of width and height Δx and Δy as well as unit depth into the page.

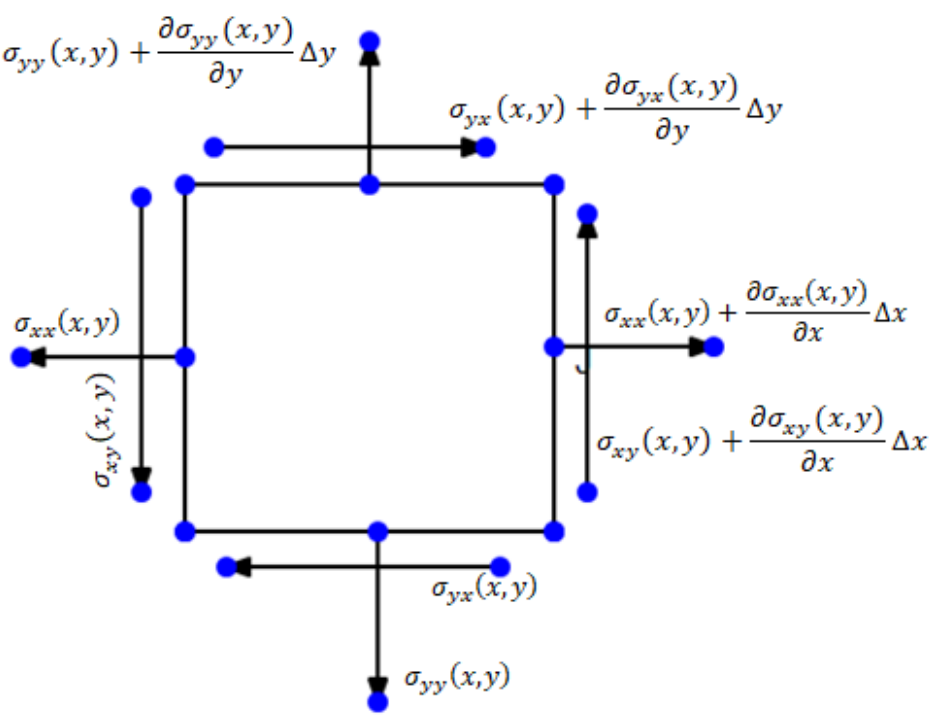

Figure 6:- Normal and shear stresses acting on differential element

Apply newton's second law.

$$\sum F = Ma \qquad [3.21]$$

$$\frac{\partial \sigma_{xx}}{\partial x} + \frac{\partial \sigma_{xy}}{\partial y} = \rho \frac{\partial^2 u}{\partial t^2}$$
$$\frac{\partial \sigma_{xy}}{\partial x} + \frac{\partial \sigma_{yy}}{\partial y} = \rho \frac{\partial^2 v}{\partial t^2} \qquad [3.22]$$

The equation of equilibrium

If the material is not moving (or is moving at a constant velocity) and is in static equilibrium, then the equation of motion reduced to the equation of equilibrium.

$$\frac{\partial \sigma_{xx}}{\partial x} + \frac{\partial \sigma_{xy}}{\partial y} = 0$$
$$\frac{\partial \sigma_{xy}}{\partial x} + \frac{\partial \sigma_{yy}}{\partial y} = 0 \qquad [3.23]$$

Strain analysis

$\varepsilon_x = \frac{\partial u}{\partial x}$ and $\varepsilon_y = \frac{\partial v}{\partial y}$, the normal strain. And the shear strain is, $\gamma_{xy} = \frac{\partial u}{\partial y} + \frac{\partial v}{\partial x}$

Constitutive equation

The strain at appoint can be completely described by the six strain components in their turns can be completely defined by the displacement components u, v and w. (MARTIN, 2005)

The constitutive equation relates stress and strain and linear elasticity we simply have $\sigma_{ij} = E_{ijk}\varepsilon_{ij}$ where E is modulus of elasticity (MARTIN, 2005).

Therefore, we may write the generalized Hooke's law as;

$$\varepsilon_x = \frac{1}{E}\left[\sigma_x - v\left(\sigma_y + \sigma_z\right)\right]$$
$$\varepsilon_y = \frac{1}{E}\left[\sigma_y - v(\sigma_x + \sigma_z)\right] \qquad [3.24]$$
$$\varepsilon_z = \frac{1}{E}\left[\sigma_z - v(\sigma_x + \sigma_y)\right]$$

It is also known that the shear stress $\tau = G\gamma$ where G is a shear stress γ is the shear stress.

From dilatation or bulk modulus analysis the change in volume of the element having original unit length and unit volume, can be represented by;

$$e = \varepsilon_x + \varepsilon_y + \varepsilon_z \qquad [3.25]$$

And e is the change in volume per unit volume, it referred to as a dislocation of the material.

$$e = \tfrac{1}{E}\left[\sigma_x - v\left(\sigma_y + \sigma_z\right)\right] + \tfrac{1}{E}\left[\sigma_y - v(\sigma_x + \sigma_z)\right] + \tfrac{1}{E}\left[\sigma_z - v(\sigma_x + \sigma_y)\right]$$
$$e = \frac{(1-2v)}{E}(\sigma_x + \sigma_y + \sigma_z) \qquad [3.26]$$

A case of special interest is that a body subjected to a uniform hydrostatic pressure P each of the stress component is the equal to –P. (FERDINAND P.BEER, E.RUSSELL JOHANSTON, JR., 2006).

Therefore,

$$\sigma_x + \sigma_y + \sigma_z = -3P \qquad [3.27]$$

Then after substitution

$$e = \frac{(1-2v)}{E}(-3P) \quad [3.28]$$

Introducing the constant $k = \frac{E}{3(1-2v)}$ and we can say$e = -\frac{P}{K}$, the constant k is known as the bulk modulus of compression of material, is expressed in the same units as the modulus of elasticity that is in Pascal.

From elementary thermos elasticity, change in temperature may also cause stresses if thermal gradient or some external constraints exists. Provided that the materials remain linearly elastic, stress pattern due to thermal effect may be superimposed upon that due to applied forces and we may write as, (MARTIN, 2005), where αT is deformation due to thermal stress.

$$\varepsilon_x = \frac{1}{E}\left[\sigma_x - v(\sigma_y + \sigma_z)\right] + \alpha T$$
$$\varepsilon_y = \frac{1}{E}\left[\sigma_y - v(\sigma_x + \sigma_z)\right] + \alpha T \quad [3.29]$$
$$\varepsilon_z = \frac{1}{E}\left[\sigma_z - v(\sigma_x + \sigma_y)\right] + \alpha T$$

It is sometimes convenient to express stress in terms of strain this may be done using the solution $e = \varepsilon_x + \varepsilon_y + \varepsilon_z$, substitute the for, $\varepsilon_x,\ \varepsilon_y,\ \varepsilon_z$

$$e = \frac{1}{E}\left[\sigma_x - v(\sigma_y + \sigma_z)\right] + \alpha T + \frac{1}{E}\left[\sigma_y - v(\sigma_x + \sigma_z)\right] + \alpha T + \frac{1}{E}\left[\sigma_z - v(\sigma_x + \sigma_y)\right] + \alpha T$$

$$e = \frac{1}{E}(1-2v)(\sigma_x + \sigma_y + \sigma_z) + 3\alpha T$$

$$e = \frac{1}{3k}(\sigma_x + \sigma_y + \sigma_z) + 3\alpha T \quad [3.30]$$

Combine this with $\varepsilon_x = \frac{1}{E}\left[\sigma_x - v(\sigma_y + \sigma_z)\right] + \alpha T$ we get;

$$\sigma_x = \frac{E\varepsilon_x}{1+v} + \frac{3vk(e-3\alpha T)}{1+v} - \frac{E\alpha T}{1+v}$$

Substituting $G = \frac{E}{2(1+v)}$ and $\lambda = \frac{3kv}{1+v}$

The normal and shear stress can be written as;

$$\sigma_x = 2G\varepsilon_x + \lambda e - 3k\alpha T \quad [3.31]$$
$$\sigma_y = 2G\varepsilon_y + \lambda e - 3k\alpha T \quad [3.32]$$

Where, $G = \mu$, $v = \frac{\lambda}{2(\lambda+\mu)}$ and $k = \frac{3\lambda+2\mu}{3}$ as well as, $e = \varepsilon_x + \varepsilon_y + \varepsilon_z$

Then,

$$\sigma_x = (2\mu + \lambda)\varepsilon_x + \lambda\varepsilon_y - \alpha(2\mu + 3\lambda)T$$
$$\sigma_y = (2\mu + \lambda)\varepsilon_y + \lambda\varepsilon_x - \alpha(2\mu + 3\lambda)T \quad [3.33]$$
$$\tau_{xy} = \mu\gamma_{xy}$$

Displacement potentials

Displacement potentials are defined as the energy or potential that exhibits the resistance for the displacement of the particle or differential element from the entire material caused by the applied load. And the Quantities ϕ and ψ are called the scalar potential and the vector potential, respectively. The sum of the gradient of a scalar potential plus the curl of a vector potential." Mathematically the displacement field is depicted as in the textbook of theory of elasticity theory , application and numeric's (MARTIN, 2005).

$$u = \frac{\partial\phi}{\partial x} + \frac{\partial\psi}{\partial y}$$
$$v = \frac{\partial\phi}{\partial y} - \frac{\partial\psi}{\partial x} \quad [3.34]$$

Then,

$$\varepsilon_x = \frac{\partial u}{\partial x} = \frac{\partial}{\partial x}\left[\frac{\partial\phi}{\partial x} + \frac{\partial\psi}{\partial y}\right]$$
$$\varepsilon_x = \frac{\partial^2\phi}{\partial x^2} + \frac{\partial^2\psi}{\partial x\partial y} \quad [3.35]$$

$$\varepsilon_y = \frac{\partial v}{\partial y} = \frac{\partial}{\partial y}\left[\frac{\partial\phi}{\partial y} - \frac{\partial\psi}{\partial x}\right]$$
$$\varepsilon_y = \frac{\partial^2\phi}{\partial y^2} - \frac{\partial^2\psi}{\partial x\partial y} \quad [3.36]$$

$$\gamma_{xy} = \frac{\partial u}{\partial y} + \frac{\partial v}{\partial x} = \frac{\partial}{\partial y}\left[\frac{\partial\phi}{\partial x} + \frac{\partial\psi}{\partial y}\right] + \frac{\partial}{\partial x}\left[\frac{\partial\phi}{\partial y} - \frac{\partial\psi}{\partial x}\right]$$
$$\gamma_{xy} = \frac{\partial^2\psi}{\partial y^2} + 2\frac{\partial^2\phi}{\partial x\partial y} - \frac{\partial^2\psi}{\partial x^2} \quad [3.37]$$

3.2.2. Equation of motion as a function displacement potential.

The thermos-mechanical stress and displacement fields associated with the propagating crack tip in isentropic homogeneous material will derived from the generalized Hooke's law associated with the equation of the motion and finally the equation of motion will have expressed as a function of displacement potentials.

Since the material is isentropic homogeneous, it has similar properties throughout the materials therefore, $\mu = \mu_0,\ \rho = \rho_0,\ \alpha = \alpha_0,\ k = k_0$.

Rewriting Hooke's law (plain-stress-strain) u(x,y), v(x,y) but w=0.

$$\sigma_x = \lambda\left(\frac{\partial u}{\partial x} + \frac{\partial v}{\partial y}\right) + 2\mu\frac{\partial u}{\partial x} - \alpha(3\lambda + 2\mu)T \quad [3.38]$$

$$\sigma_y = \lambda\left(\frac{\partial u}{\partial x} + \frac{\partial v}{\partial y}\right) + 2\mu\frac{\partial v}{\partial y} - \alpha(3\lambda + 2\mu)T \quad [3.39]$$

$$\tau_{xy} = \mu\left(\frac{\partial u}{\partial y} + \frac{\partial v}{\partial x}\right) \quad [3.40]$$

Hooke's law in terms of displacement potentials.

$$\sigma_x = (2\mu_0 + \lambda_0)\left[\frac{\partial^2\phi}{\partial x^2} + \frac{\partial^2\psi}{\partial x\partial y}\right] + \lambda_0\left[\frac{\partial^2\phi}{\partial y^2} - \frac{\partial^2\psi}{\partial x\partial y}\right] - \alpha(3\lambda_0 + 2\mu_0)T \quad [3.41]$$

$$\sigma_y = (2\mu_0 + \lambda_0)\left[\frac{\partial^2\phi}{\partial y^2} - \frac{\partial^2\psi}{\partial x\partial y}\right] + \lambda_0\left[\frac{\partial^2\phi}{\partial x^2} + \frac{\partial^2\psi}{\partial x\partial y}\right] - \alpha(3\lambda_0 + 2\mu_0)T \quad [3.42]$$

$$\tau_{xy} = \mu\left[\frac{\partial^2\psi}{\partial y^2} + 2\frac{\partial^2\phi}{\partial x\partial y} - \frac{\partial^2\psi}{\partial x^2}\right] \quad [3.43]$$

Recalling equation of motion. Where; $\sigma_{xx} = \sigma_x,\ \sigma_{yy} = \sigma_y\ and\ \sigma_{xy} = \tau_{xy}$.

$$\frac{\partial\sigma_{xx}}{\partial x} = \frac{\partial}{\partial x}\left[(2\mu_0 + \lambda_0)\left[\frac{\partial^2\phi}{\partial x^2} + \frac{\partial^2\psi}{\partial x\partial y}\right] + \lambda_0\left[\frac{\partial^2\phi}{\partial y^2} - \frac{\partial^2\psi}{\partial x\partial y}\right] - \alpha(3\lambda_0 + 2\mu_0)T\right]$$

$$\frac{\partial\sigma_{xx}}{\partial x} = (2\mu_0 + \lambda_0)\left[\frac{\partial^3\phi}{\partial x^3} + \frac{\partial^3\psi}{\partial x^2\partial y}\right] + \lambda_0\left[\frac{\partial^3\phi}{\partial x\partial y^2} - \frac{\partial^3\psi}{\partial x^2\partial y}\right] - \alpha(3\lambda_0 + 2\mu_0)\frac{\partial T}{\partial x} \quad [3.44]$$

$$\frac{\partial\sigma_{yy}}{\partial y} = \frac{\partial}{\partial y}\left[(2\mu_0 + \lambda_0)\left[\frac{\partial^2\phi}{\partial y^2} - \frac{\partial^2\psi}{\partial x\partial y}\right] + \lambda_0\left[\frac{\partial^2\phi}{\partial x^2} + \frac{\partial^2\psi}{\partial x\partial y}\right] - \alpha(3\lambda_0 + 2\mu_0)T\right]$$

$$\frac{\partial\sigma_{yy}}{\partial y} = (2\mu_0 + \lambda_0)\left[\frac{\partial^3\phi}{\partial y^3} - \frac{\partial^3\psi}{\partial x\partial y^2}\right] + \lambda_0\left[\frac{\partial^3\phi}{\partial x^2\partial y} + \frac{\partial^3\psi}{\partial x\partial y^2}\right] - \alpha(3\lambda_0 + 2\mu_0)\frac{\partial T}{\partial y} \quad [3.45]$$

$$\frac{\partial\sigma_{xy}}{\partial x} = \frac{\partial}{\partial x}\left[\mu_0\left[\frac{\partial^2\psi}{\partial y^2} + 2\frac{\partial^2\phi}{\partial x\partial y} - \frac{\partial^2\psi}{\partial x^2}\right]\right]$$

$$\frac{\partial\sigma_{xy}}{\partial x} = \mu_0\left[\frac{\partial^3\psi}{\partial x\partial y^2} + 2\frac{\partial^3\phi}{\partial x^2\partial y} - \frac{\partial^3\psi}{\partial x^3}\right] \quad [3.46]$$

$$\frac{\partial\sigma_{xy}}{\partial y} = \frac{\partial}{\partial y}\left[\mu_0\left[\frac{\partial^2\psi}{\partial y^2} + 2\frac{\partial^2\phi}{\partial x\partial y} - \frac{\partial^2\psi}{\partial x^2}\right]\right]$$

$$\frac{\partial \sigma_{xy}}{\partial y} = \mu_0 \left[\frac{\partial^3 \psi}{\partial y^3} + 2\frac{\partial^3 \phi}{\partial x \partial y^2} - \frac{\partial^3 \psi}{\partial x^2 \partial y}\right] \quad [3.47]$$

Then substitute equation[3.44], [3.45], [3.46] and [3.47] in equation of motion along x axis and y axis.

$$\lambda_0\left(\frac{\partial^3 \phi}{\partial x^3} + \frac{\partial^3 \phi}{\partial x \partial y^2}\right) + \mu_0\left(2\frac{\partial^3 \phi}{\partial x^3} + 2\frac{\partial^3 \phi}{\partial x \partial y^2} + \frac{\partial^3 \psi}{\partial x^2 \partial y} + \frac{\partial^3 \psi}{\partial y^3}\right) - \alpha_0(3\lambda_0 + 2\mu_0)\frac{\partial T}{\partial x} = \rho_0 \frac{\partial^2 u}{\partial t^2} \quad [3.48]$$

Now let's introduce the notation of Laplace operator.

$\nabla^2 = \frac{\partial^2}{\partial x^2} + \frac{\partial^2}{\partial y^2}$……..……2D Laplace operator

$$\lambda_0\left(\frac{\partial}{\partial x}\frac{\partial^2 \phi}{\partial x^2} + \frac{\partial}{\partial x}\frac{\partial^2 \phi}{\partial y^2}\right) + \mu_0\left(2\frac{\partial}{\partial x}\frac{\partial^2 \phi}{\partial x^2} + 2\frac{\partial}{\partial x}\frac{\partial^2 \phi}{\partial y^2} + \frac{\partial}{\partial y}\frac{\partial^2 \psi}{\partial x^2} + \frac{\partial}{\partial y}\frac{\partial^2 \psi}{\partial y^2}\right) - \alpha_0(3\lambda_0 + 2\mu_0)\frac{\partial T}{\partial x} = \rho_0 \frac{\partial^2 u}{\partial t^2}$$

$$\lambda_0 \frac{\partial}{\partial x}\nabla^2 \phi + \mu_0\left(2\frac{\partial}{\partial x}\nabla^2 \phi + \frac{\partial}{\partial x}\nabla^2 \psi\right) - \alpha_0(3\lambda_0 + 2\mu_0)\frac{\partial T}{\partial x} = \rho_0 \frac{\partial^2 u}{\partial t^2}$$

$$(2\mu_0 + \lambda_0)\frac{\partial}{\partial x}\nabla^2 \phi + \mu_0 \frac{\partial}{\partial y}\nabla^2 \psi - \alpha_0(3\lambda_0 + 2\mu_0)\frac{\partial T}{\partial x} = \rho_0 \frac{\partial^2}{\partial t^2}\left[\frac{\partial \phi}{\partial x} + \frac{\partial \psi}{\partial y}\right] \quad [3.49]$$

Similarly, for the equation of motion along the y directions.

$$\mu_0\left[\frac{\partial^3 \psi}{\partial x \partial y^2} + 2\frac{\partial^3 \phi}{\partial x^2 \partial y} - \frac{\partial^3 \psi}{\partial x^3}\right] + (2\mu_0 + \lambda_0)\left[\frac{\partial^3 \phi}{\partial y^3} - \frac{\partial^3 \psi}{\partial x \partial y^2}\right] + \lambda_0\left[\frac{\partial^3 \phi}{\partial x^2 \partial y} + \frac{\partial^3 \psi}{\partial x \partial y^2}\right] - \alpha_0(3\lambda_0 +$$

$$2\mu_0)\frac{\partial T}{\partial y} = \rho_0 \frac{\partial^2 v}{\partial t^2}$$

$$\mu_0\left(2\frac{\partial^3 \phi}{\partial x^2 \partial y} + 2\frac{\partial^3 \phi}{\partial y^3} - \frac{\partial^3 \psi}{\partial x^3} - \frac{\partial^3 \psi}{\partial x \partial y^2}\right) + \lambda_0\left(\frac{\partial^3 \phi}{\partial x^2 \partial y} + \frac{\partial^3 \phi}{\partial y^3}\right) - \alpha_0(3\lambda_0 + 2\mu_0)\frac{\partial T}{\partial y} = \rho_0 \frac{\partial^2 v}{\partial t^2}$$

$$\mu_0\left(2\frac{\partial}{\partial y}\nabla^2 \phi - \frac{\partial}{\partial x}\nabla^2 \psi\right) + \lambda_0\left(\frac{\partial}{\partial y}\nabla^2 \phi\right) - \alpha_0(3\lambda_0 + 2\mu_0)\frac{\partial T}{\partial y} = \rho_0 \frac{\partial^2 v}{\partial t^2}$$

$$(2\mu_0 + \lambda_0)\frac{\partial}{\partial y}\nabla^2 \phi - \lambda_0 \frac{\partial}{\partial x}\nabla^2 \psi - \alpha_0(3\lambda_0 + 2\mu_0)\frac{\partial T}{\partial y} = \rho_0 \frac{\partial^2 v}{\partial t^2}$$

$$(2\mu_0 + \lambda_0)\frac{\partial}{\partial y}\nabla^2 \phi - \lambda_0 \frac{\partial}{\partial x}\nabla^2 \psi - \alpha_0(3\lambda_0 + 2\mu_0)\frac{\partial T}{\partial y} = \rho_0 \frac{\partial^2}{\partial t^2}\left[\frac{\partial \phi}{\partial y} - \frac{\partial \psi}{\partial x}\right] \quad [3.50]$$

Then lets derivate equation [3.49] and [3.50] with respect to x and y as well as add and subtract their derivations as follows.

Derivation of equation [3.49] with respect to x.

$$\frac{\partial}{\partial x}\left[(2\mu_0 + \lambda_0)\frac{\partial}{\partial x}\nabla^2 \phi + \mu_0 \frac{\partial}{\partial y}\nabla^2 \psi - \alpha_0(3\lambda_0 + 2\mu_0)\frac{\partial T}{\partial x} = \rho_0 \frac{\partial^2}{\partial t^2}\left[\frac{\partial \phi}{\partial x} + \frac{\partial \psi}{\partial y}\right]\right]$$

$$(2\mu_0+\lambda_0)\frac{\partial^2}{\partial x^2}\nabla^2\phi+\mu_0\frac{\partial^2}{\partial x\partial y}\nabla^2\psi-\alpha_0(3\lambda_0+2\mu_0)\frac{\partial^2 T}{\partial x^2}$$
$$=\rho_0\frac{\partial^2}{\partial t^2}\left[\frac{\partial^2\phi}{\partial x^2}+\frac{\partial^2\psi}{\partial x\partial y}\right] \quad [3.51]$$

Derivations of equation [3.50] with respect to y.

$$\frac{\partial}{\partial y}\left[(2\mu_0+\lambda_0)\frac{\partial}{\partial y}\nabla^2\phi-\lambda_0\frac{\partial}{\partial x}\nabla^2\psi-\alpha_0(3\lambda_0+2\mu_0)\frac{\partial T}{\partial y}=\rho_0\frac{\partial^2}{\partial t^2}\left[\frac{\partial\phi}{\partial y}-\frac{\partial\psi}{\partial x}\right]\right]$$

$$(2\mu_0+\lambda_0)\frac{\partial^2}{\partial y^2}\nabla^2\phi-\mu_0\frac{\partial^2}{\partial x\partial y}\nabla^2\psi-\alpha_0(3\lambda_0+2\mu_0)\frac{\partial^2 T}{\partial y^2}$$
$$=\rho_0\frac{\partial^2}{\partial t^2}\left[\frac{\partial^2\phi}{\partial y^2}-\frac{\partial^2\psi}{\partial x\partial y}\right] \quad [3.52]$$

Then let's add the derivation of equation [3.49] with respect to x and equation [3.50] with respect to y such that;

$$\left\{(2\mu_0+\lambda_0)\frac{\partial^2}{\partial x^2}\nabla^2\phi+\mu_0\frac{\partial^2}{\partial x\partial y}\nabla^2\psi-\alpha_0(3\lambda_0+2\mu_0)\frac{\partial^2 T}{\partial x^2}=\rho_0\frac{\partial^2}{\partial t^2}\left[\frac{\partial^2\phi}{\partial x^2}+\frac{\partial^2\psi}{\partial x\partial y}\right]\right\}+\left\{(2\mu_0+\right.$$

$$\left.\lambda_0)\frac{\partial^2}{\partial y^2}\nabla^2\phi-\mu_0\frac{\partial^2}{\partial x\partial y}\nabla^2\psi-\alpha_0(3\lambda_0+2\mu_0)\frac{\partial^2 T}{\partial y^2}=\rho_0\frac{\partial^2}{\partial t^2}\left[\frac{\partial^2\phi}{\partial y^2}-\frac{\partial^2\psi}{\partial x\partial y}\right]\right\}$$

$$(2\mu_0+\lambda_0)\left(\frac{\partial^2}{\partial x^2}+\frac{\partial^2}{\partial y^2}\right)\nabla^2\phi-\alpha_0(3\lambda_0+2\mu_0)\left(\frac{\partial^2 T}{\partial x^2}+\frac{\partial^2 T}{\partial y^2}\right)=\rho_0\frac{\partial^2}{\partial t^2}\left(\frac{\partial^2\phi}{\partial x^2}+\frac{\partial^2\phi}{\partial y^2}\right)$$

$$(2\mu_0+\lambda_0)\nabla^2\nabla^2\phi-\alpha_0(3\lambda_0+2\mu_0)\nabla^2 T=\rho_0\frac{\partial^2}{\partial t^2}\nabla^2\phi \quad [3.53]$$

Next let's differentiate equation [3.49] with respect to y and equation [3.50] with respect to x and subtract the later from the former.

Differentiate equation [3.49] with respect to y.

$$\frac{\partial}{\partial y}\left[(2\mu_0+\lambda_0)\frac{\partial}{\partial x}\nabla^2\phi+\mu_0\frac{\partial}{\partial y}\nabla^2\psi-\alpha_0(3\lambda_0+2\mu_0)\frac{\partial T}{\partial x}=\rho_0\frac{\partial^2}{\partial t^2}\left[\frac{\partial\phi}{\partial x}+\frac{\partial\psi}{\partial y}\right]\right]$$

$$(2\mu_0+\lambda_0)\frac{\partial^2}{\partial x\partial y}\nabla^2\phi+\mu_0\frac{\partial^2}{\partial y^2}\nabla^2\psi-\alpha_0(3\lambda_0+2\mu_0)\frac{\partial^2 T}{\partial x\partial y}$$
$$=\rho_0\frac{\partial^2}{\partial t^2}\left[\frac{\partial^2\phi}{\partial x\partial y}+\frac{\partial^2\psi}{\partial y^2}\right] \quad [3.54]$$

Differentiation of equation [3.50] with respect to x.

$$\frac{\partial}{\partial x}\left[(2\mu_0+\lambda_0)\frac{\partial}{\partial y}\nabla^2\phi-\lambda_0\frac{\partial}{\partial x}\nabla^2\psi-\alpha_0(3\lambda_0+2\mu_0)\frac{\partial T}{\partial y}=\rho_0\frac{\partial^2}{\partial t^2}\left[\frac{\partial\phi}{\partial y}-\frac{\partial\psi}{\partial x}\right]\right]$$

$$(2\mu_0+\lambda_0)\frac{\partial^2}{\partial x\partial y}\nabla^2\phi-\lambda_0\frac{\partial^2}{\partial x^2}\nabla^2\psi-\alpha_0(3\lambda_0+2\mu_0)\frac{\partial^2 T}{\partial x\partial y}=\rho_0\frac{\partial^2}{\partial t^2}\left[\frac{\partial^2\phi}{\partial x\partial y}-\frac{\partial^2\psi}{\partial x^2}\right] \quad [3.55]$$

Then lets subtract the differentiation of equation [3.50] with respect to x from the differentiation of equation [3.49] with respect to y such that;

$$\left\{(2\mu_0+\lambda_0)\frac{\partial^2}{\partial x\partial y}\nabla^2\phi+\mu_0\frac{\partial^2}{\partial y^2}\nabla^2\psi-\alpha_0(3\lambda_0+2\mu_0)\frac{\partial^2 T}{\partial x\partial y}=\rho_0\frac{\partial^2}{\partial t^2}\left[\frac{\partial^2\phi}{\partial x\partial y}+\frac{\partial^2\psi}{\partial y^2}\right]\right\}-\left\{(2\mu_0+\lambda_0)\frac{\partial^2}{\partial x\partial y}\nabla^2\phi-\mu_0\frac{\partial^2}{\partial x^2}\nabla^2\psi-\alpha_0(3\lambda_0+2\mu_0)\frac{\partial^2 T}{\partial x\partial y}=\rho_0\frac{\partial^2}{\partial t^2}\left[\frac{\partial^2\phi}{\partial x\partial y}-\frac{\partial^2\psi}{\partial x^2}\right]\right\}$$

$$\mu_0\frac{\partial^2}{\partial x^2}\nabla^2\psi+\mu_0\frac{\partial^2}{\partial y^2}\nabla^2\psi=\rho_0\frac{\partial^2}{\partial t^2}\left[\frac{\partial^2\psi}{\partial x^2}+\frac{\partial^2\psi}{\partial y^2}\right]$$

$$\mu_0\nabla^2\psi=\rho_0\frac{\partial^2}{\partial t^2}\psi \quad [3.56]$$

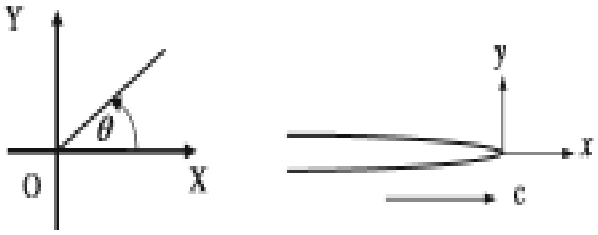

Figure 7:- Propagating crack-tip orientation with respect to reference coordinate system

Where, $\nabla^2=\frac{\partial^2}{\partial X^2}+\frac{\partial^2}{\partial Y^2}$

For a propagating crack as shown in figure 7, the reference coordinates (X and Y) can be transformed to crack-tip coordinates using the relations$x=X-ct, y=Y$, where c is the constant crack-tip speed.(Kidane, Chalivendra and Shukla, 2010)

For cracks propagating in a gradually curving path as reported in different literature displacement potentials equations developed using straight crack orientation tangent to the curved crack tip can

be considered. By transforming to crack-tip coordinates and rearranging terms, the above equations of motion can be written as (Kidane, Chalivendra and Shukla, 2010).

$$\alpha_l{}^2 \frac{\partial^2 \phi}{\partial x^2} + \frac{\partial^2 \phi}{\partial y^2} - \alpha \frac{(3\delta+2)}{\delta+2} T = 0 \qquad [3.57]$$

$$\alpha_s{}^2 \frac{\partial^2 \psi}{\partial x^2} + \frac{\partial^2 \psi}{\partial y^2} = 0 \qquad [3.58]$$

Where, $\alpha_l = \sqrt{1 - \frac{\rho}{\mu} \frac{c^2}{(k+2)}}$ $\alpha_s = \sqrt{1 - \frac{\rho}{\mu} c^2}$ and $\delta = \frac{\lambda}{\mu}$

(Parameswaran and Shukla, 1999) stated that the vitality that in the homogeneous material the parameter α_l and α_s are represented as function of crack speed and elastic property only this is applied for the crack speed less than the shear wave speed.

Then here let's explain what are the parameter α_l and α_s starting from the useful relation of the useful relation called the Helmholtz theorem states that any sufficiently continuous vector field can be represented as the sum of the gradient of a scalar potential plus the curl of a vector potential." Mathematically the displacement field is depicted as in the textbook of theory of elasticity theory , application and numeric's (MARTIN, 2005).

$$u = \nabla\phi + \nabla \times \psi \qquad [3.59]$$

Where, where ϕ is the scalar potential and ψ is the vector potential. The gradient term in the decomposition has a zero curl and is referred to as the lamellar or irrotational part, while the curl has no divergence.

Equation [3.59] is the expression for the displacement for the particles from the entire material exposed to the stress wave, so the displacement field can be analyzed separately, and the most general displacement field can be obtained by adding both solutions together. To do that lets recall the general three dimensional Navier equations as depicted (MARTIN, 2005).

$$(\lambda + 2\mu)\nabla(\nabla^2\phi) + \mu\nabla \times (\nabla^2\psi) + F = \rho\ddot{u} \qquad [3.60]$$

The Navier equation represents a hyperbolic system of partial differential equation and hence admits propagating wave solutions. By dropping the body force F and considering the two-dimensional Navier equation becomes $(\lambda + 2\mu)\nabla(\nabla\phi) + \mu\nabla \times (\nabla \times \psi) = \rho\ddot{u}$.

First looking for the scalar potential term, suppose that the displacement is given by $u = \nabla\phi$ and we are going to find ascalar ϕ such that $u = \nabla\phi$ then it follows that$\nabla \times \psi = 0$. Thus $\nabla \times \psi = 0$ or $curl\psi = 0$ can be interpreted as no rotation of the materials particles but a small element of

material can still undergo normal and shear strain, but the element will not rotate as rigid body in space. Now substitute $\nabla \times \psi = 0$ in Navier equations.

$(\lambda + 2\mu)\nabla(\nabla\phi) = \rho\ddot{u}$

$(\lambda + 2\mu)\frac{\partial^2 u_i}{\partial x_k \partial x_k} = \rho\frac{\partial^2 u_i}{\partial t^2}$ This is with the index notation of k and i.

$\frac{\partial^2 u_i}{\partial x_k \partial x_k} = \frac{1}{{C_L}^2}\frac{\partial^2 u_i}{\partial t^2}$ For $C_L = \sqrt{\frac{\lambda+2\mu}{\rho}} = \sqrt{\frac{E(1-v)}{\rho(1+v)(1-2v)}}$

This deformation seen that to obey the standard wave equation with a characteristic speed C_L such wave is called irrotational or dilatational wave speed.

$$C_L = \sqrt{\frac{\lambda+2\mu}{\rho}} = \sqrt{\frac{E(1-v)}{\rho(1+v)(1-2v)}} \qquad [3.61]$$

Moreover, C_L is called the irrotational or dilatational wave speed.

Consider now the displacement field $\nabla \times \psi = u$ or $curl\psi = u$ then it follows that$\nabla\phi = 0$. Thus, the condition that the displacement field be divergence free implies that there is no volume change. In addition, there can be normal strain only so long as their sum is zero. Then substitute $\nabla \times \psi = u$ and $\nabla\phi = 0$ in Navier equations as follows;

$\mu\nabla(\nabla\psi) = \rho\ddot{u}$

$\mu\frac{\partial^2 u_i}{\partial x_k \partial x_k} = \rho\frac{\partial^2 u_i}{\partial t^2}$

$\frac{\partial^2 u_i}{\partial x_k \partial x_k} = \frac{1}{{C_s}^2}\frac{\partial^2 u_i}{\partial t^2}$ For $C_s = \sqrt{\frac{\mu}{\rho}} = \sqrt{\frac{E}{2\rho(1+v)}}$

This displacement field thus corresponds to stress waves travelling at speed C_s causing the material to shear.

$$C_s = \sqrt{\frac{\mu}{\rho}} = \sqrt{\frac{E}{2\rho(1+v)}} \qquad [3.62]$$

These equivoluminal waves are called shear waves speed or waves of distortion speed.

Clearly, $C_L > C_s$ a material at a distance from a source of stress wave will first receive the dilatation wave speeds and then the equivoluminal wave speeds; hence, in different textbooks these waves are called primary (P) wave speed and secondary (S) wave speed respectively.

And the material the parameter α_l and α_s are expressed as a function of crack speed and displacement wave speeds such that;

$\alpha_l = \sqrt{1 - \frac{c^2}{{C_L}^2}}$ And $\alpha_s = \sqrt{1 - \frac{c^2}{{C_s}^2}}$ as well as; $\alpha_l = \sqrt{1 - \frac{\rho}{\mu}\frac{c^2}{(k+2)}}$ $\alpha_s = \sqrt{1 - \frac{\rho}{\mu}c^2}$

3.2.3. Perturbation of temperature fields

Perturbation theory comprises mathematical methods for finding an approximate solution to a problem, by starting from the exact solution of a related, simpler problem. But here we utilize perturbation theory for the superimposition of the solution of steady state temperature solutions. The smaller parameter ε that exists in the asymptotic approach for the transformation of coordinates from (x, y) to (η_1, η_2), as well as in the general solution principle. The solution of steady state temperature does not have the smaller parameter ε that makes suitable to superimpose with the mechanical stress fields solved by asymptotic approach. But after perturbing the solution of temperature field we can superimpose by separating like terms as represented in equation [3.73], [3.74], [3.75] and [3.76]. Thus, the smaller ε utilized here to get the approximate solution of steady state temperature equation that is almost similar to the solution obtained by the ordinary solution principle with acceptable deviation, and also the solution is capable to superimposed to the mechanical stress field through the solution of equation of motion. This smaller parameter will not affect the crack position as well as the quality and quantity of the temperature flow except the acceptable error from the ordinary solution that is represented by graph in figure 10.

From the solution of Dirichlet problem using separable equation of the Laplace equation depicted in equation [3.3] and [3.4] and we get the ordinary differential equations such that, $X'' + KX = 0$ and $Y'' - KY = 0$ to the rectangle on which the temperature is applied as follows.

And satisfies X(0)=1 and Y(0)=1 as well as X(a)=0 and Y(b)=0.

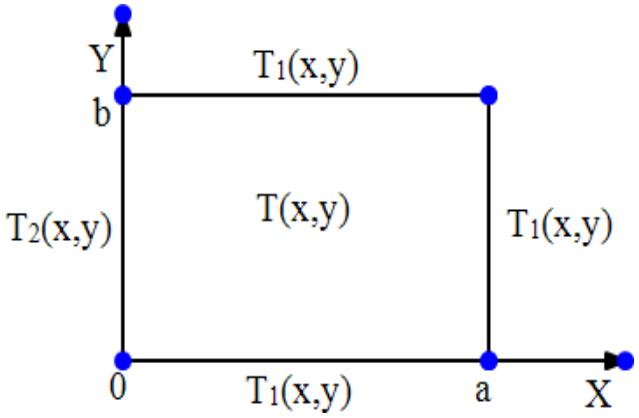

Figure 8:- The application of temperature for the perturbation principles

Then let's introduce a small parameter to perturb the ordinary differential equation when the smaller parameter ε is $0 < \varepsilon < 1$.

, $X'' + \varepsilon KX = 0$ and $Y'' - \varepsilon KY = 0$

Then, let's assume the solution for the perturbed ordinary differential equation as follows (Johnson, 2005).

$$X(x,\varepsilon) = \sum_{n=0}^{\infty} \varepsilon^n X_n(x) \quad [3.63]$$

$$Y(y,\varepsilon) = \sum_{n=0}^{\infty} \varepsilon^n Y_n(y) \quad [3.64]$$

Then let's expand the intended solution assumed by the method of perturbation.

$$X_n(x) = \varepsilon^{(0)}X_0 + \varepsilon^{(1)}X_1 + \varepsilon^{(2)}X_2 + \varepsilon^{(3)}X_3 + \cdots \quad [3.65]$$

$$Y_n(y) = \varepsilon^{(0)}Y_0 + \varepsilon^{(1)}Y_1 + \varepsilon^{(2)}Y_2 + \varepsilon^{(3)}Y_3 + \cdots \quad [3.66]$$

Which is called the perturbation series.

Then $T(x,y) = X_n(x)Y_n(y)$

$T(x,y) = \sum_{n=0}^{\infty} \varepsilon^n X_n(x) \sum_{n=0}^{\infty} \varepsilon^n Y_n(y)$

$T(x,y) = \varepsilon^0 x_0\left[\varepsilon^{(0)}Y_0 + \varepsilon^{(1)}Y_1 + \varepsilon^{(2)}Y_2 + \varepsilon^{(3)}Y_3 + \cdots\right] + \varepsilon^1 x_1\left[\varepsilon^{(0)}Y_0 + \varepsilon^{(1)}Y_1 + \varepsilon^{(2)}Y_2 + \varepsilon^{(3)}Y_3 + \cdots\right] + \varepsilon^2 x_2\left[\varepsilon^{(0)}Y_0 + \varepsilon^{(1)}Y_1 + \varepsilon^{(2)}Y_2 + \varepsilon^{(3)}Y_3 + \cdots\right] \ldots$

However, here the temperature stats from n=1 and the zero-term become zero and we get.

$T(x,y) = \varepsilon^1 x_1\left[\varepsilon^{(1)}Y_1 + \varepsilon^{(2)}Y_2 + \varepsilon^{(3)}Y_3 + \cdots\right] + \varepsilon^2 x_2\left[\varepsilon^{(1)}Y_1 + \varepsilon^{(2)}Y_2 + \varepsilon^{(3)}Y_3 + \cdots\right] \ldots$

Then let's ignore the third term and the higher order power of the epsilon after 2 exponents.

$T(x,y) = \varepsilon^2 x_1 y_1$

But from equation [3.20] let's take the first term that satisfies the boundary condition figure 8

$$T(x,y) = \varepsilon^2 A_n sin\left(\frac{n\pi}{a}x\right) sinh\left(\frac{n\pi}{a}(b-y)\right) \quad [3.67]$$

$$A_n = \frac{2}{\text{asinh}(\frac{n\pi}{a}b)} \int_0^a f_1(x)\, sin\left(\frac{n\pi}{a}x\right) dx \quad [3.68]$$

Then let's load the equation on MATLAB by keeping the three edges of at 25℃ and the one left edge to be 200℃ then the small parameter $\varepsilon = 0.8\, to\, 1.07$ then upon this values of small parameter ε we can compare the value of temperature, then we can select the value of small ε.

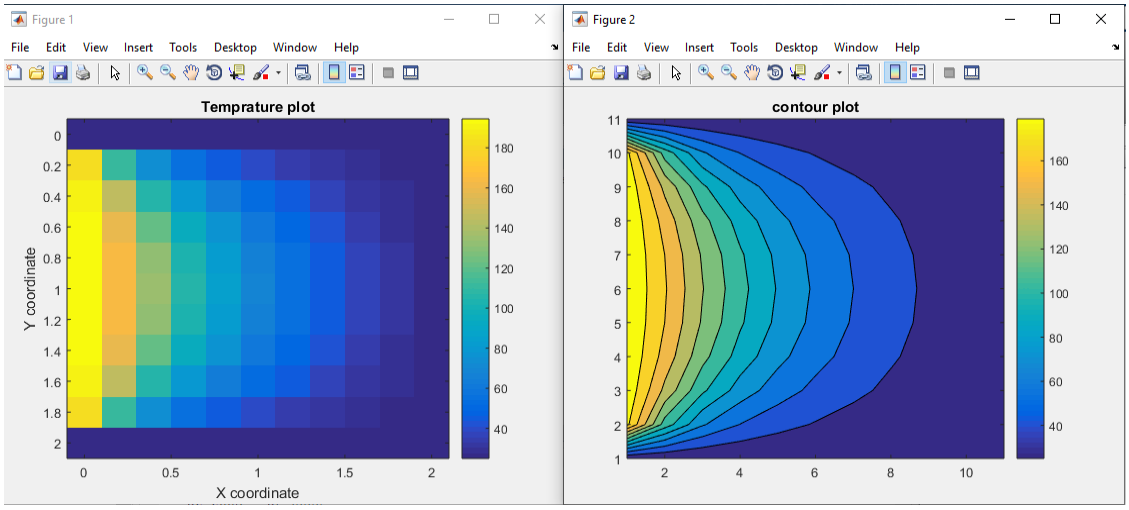

Figure 9:-The temperature distribution for the thin for the smaller parameter epsilon ε =1.00

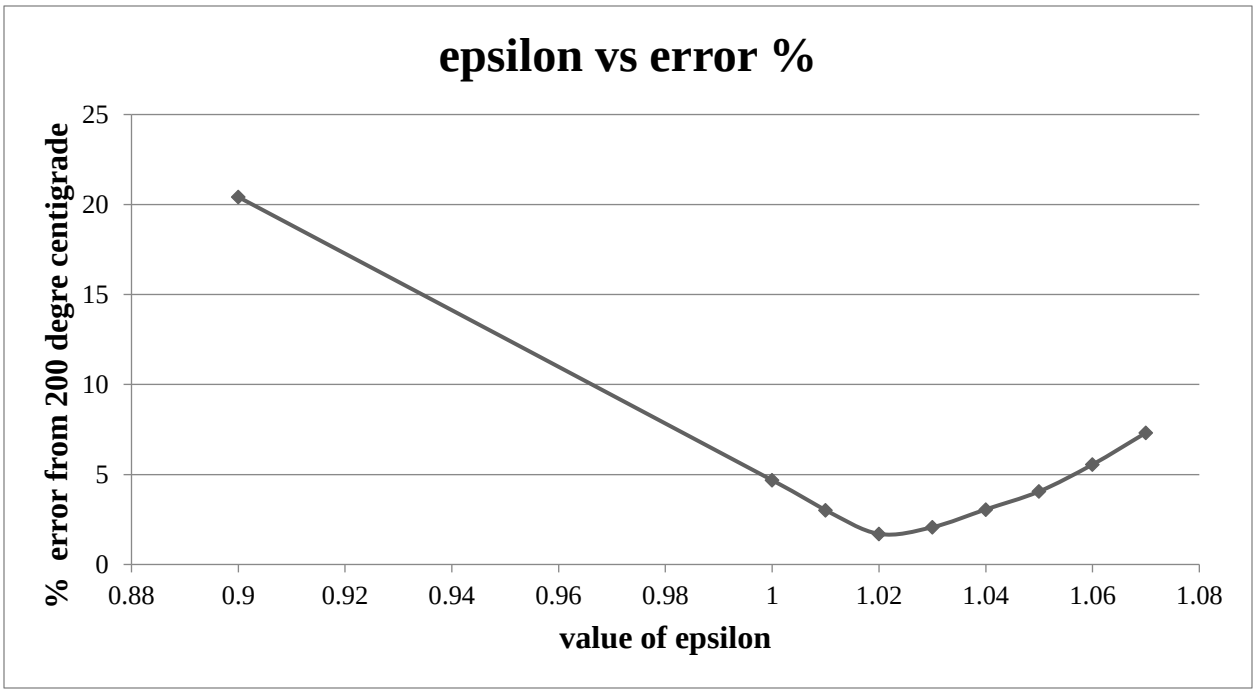

Figure 10:- The deviation of left edge temperature from 200℃

3.2.4. The solution for the equation of motion

Now the solution for the equation of motion expressed as a function of displacement potentials was depicted in literature(Kidane, Chalivendra and Shukla, 2010) which is using the asymptotic

expansion. Now let us recall the equation of motion depicted by equation [3.57] and [3.58] then the solution to get the displacement potentials was assumed as follows. And this is done by transforming to the new coordinates η_1 and η_2 in which the expression is $x = {\eta_1}/{\varepsilon}$, $y = {\eta_1}/{\varepsilon}$ for $0 < \varepsilon < 1$, (Kidane *et al.*, 2010).

$$\phi(x,y) = \phi(\varepsilon\eta_1, \varepsilon\eta_2) = \sum_{n=0}^{\infty} \varepsilon^{\frac{n+3}{2}} \phi_n(\eta_1, \eta_2) \quad [3.69]$$

$$\psi(x,y) = \psi(\varepsilon\eta_1, \varepsilon\eta_2) = \sum_{n=0}^{\infty} \varepsilon^{\frac{n+3}{2}} \psi_n(\eta_1, \eta_2) \quad [3.70]$$

Now let's substitute equation [3.71] and [3.72] into equation [3.57]and [3.58] as follows;

$$\sum_{n=0}^{\infty} \varepsilon^{\frac{n+3}{2}} \left({\alpha_l}^2 \frac{\partial^2 \phi}{\partial {\eta_1}^2} + \frac{\partial^2 \phi}{\partial {\eta_2}^2} \right) - \alpha \frac{(3\delta + 2)}{\delta + 2} \sum_{n=0}^{\infty} \varepsilon^{2n} T_n = 0 \quad [3.71]$$

$$\sum_{n=0}^{\infty} \varepsilon^{\frac{n+3}{2}} \left({\alpha_l}^2 \frac{\partial^2 \psi}{\partial {\eta_1}^2} + \frac{\partial^2 \psi}{\partial {\eta_2}^2} \right) = 0 \quad [3.72]$$

For equation [3.71] and [3.72] to be valid, the partial differential equation corresponding to each power of ε(for n=0, 1, 2, 3,...) should vanish independently. This leads to a set of partial differential equations. The solution for n=0 and n=1 will calculated as follows.

For n=0; we get, the following partial differential equation.

$$\varepsilon^{\frac{3}{2}} \left({\alpha_l}^2 \frac{\partial^2 \phi}{\partial {\eta_1}^2} + \frac{\partial^2 \phi}{\partial {\eta_2}^2} \right) - \alpha \frac{(3\delta+2)}{\delta+2} \varepsilon^0 T_0 = 0$$

$$\varepsilon^{\frac{3}{2}} \left({\alpha_l}^2 \frac{\partial^2 \phi}{\partial {\eta_1}^2} + \frac{\partial^2 \phi}{\partial {\eta_2}^2} \right) = 0 \quad [3.73]$$

$$\varepsilon^{\frac{3}{2}} \left({\alpha_l}^2 \frac{\partial^2 \psi}{\partial {\eta_1}^2} + \frac{\partial^2 \psi}{\partial {\eta_2}^2} \right) = 0 \quad [3.74]$$

For n=1, we get,

$$\varepsilon^2 \left({\alpha_l}^2 \frac{\partial^2 \phi}{\partial {\eta_1}^2} + \frac{\partial^2 \phi}{\partial {\eta_2}^2} \right) - \alpha \frac{(3\delta + 2)}{\delta + 2} \varepsilon^2 T_1 = 0 \quad [3.75]$$

$$\varepsilon^2 \left({\alpha_l}^2 \frac{\partial^2 \psi}{\partial {\eta_1}^2} + \frac{\partial^2 \psi}{\partial {\eta_2}^2} \right) = 0 \quad [3.76]$$

Now based on the first two terms we get the set of partial differential equations, but based on the types of partial differential equations the solution is also different, such that homogeneous and also non homogeneous differential equations.

Equation [3.73] [3.74] and [3.76] are homogeneous partial differential equations but equation [3.75] is non-homogeneous partial differential equation in which the general solution is the sum of complementary and particular solutions. Now, let us sort the equation within the power of epsilonε.

$\varepsilon^{\frac{3}{2}}$ Terms,

$$\left({\alpha_l}^2\frac{\partial^2\phi}{\partial{\eta_1}^2}+\frac{\partial^2\phi}{\partial{\eta_2}^2}\right)=0$$

$$\left({\alpha_l}^2\frac{\partial^2\psi}{\partial{\eta_1}^2}+\frac{\partial^2\psi}{\partial{\eta_2}^2}\right)=0$$

ε^2 Terms,

$$\left({\alpha_l}^2\frac{\partial^2\phi}{\partial{\eta_1}^2}+\frac{\partial^2\phi}{\partial{\eta_2}^2}\right)-\alpha\frac{(3\delta+2)}{\delta+2}\varepsilon^2T_1=0$$

$$\left({\alpha_l}^2\frac{\partial^2\psi}{\partial{\eta_1}^2}+\frac{\partial^2\psi}{\partial{\eta_2}^2}\right)=0$$

The general homogeneous solution as explained in literature (Kidane, Chalivendra and Shukla, 2010) was written as follows;

$$\phi_n(\rho_l\theta_l,t)=A_m{\rho_l}^{\frac{(n+3)}{2}}cos\left(\frac{1}{2}(n+3)\theta_l\right)+C_n{\rho_l}^{\frac{(n+3)}{2}}sin\left(\frac{1}{2}(n+3)\theta_l\right) \quad [3.77]$$

$$\psi_n(\rho_s,\theta_s,t)=B_n{\rho_s}^{\frac{(n+3)}{2}}sin\left(\frac{1}{2}(n+3)\theta_s\right)+D_n{\rho_s}^{\frac{(n+3)}{2}}cos\left(\frac{1}{2}(n+3)\theta_s\right) \quad [3.78]$$

Where, $\rho_s=[{\eta_1}^2+{\alpha_l}^2{\eta_2}^2]^{1/2}, and\ \theta_l=\frac{\alpha_l\eta_2}{\eta_1}\rho_l=[{\eta_1}^2+{\alpha_s}^2{\eta_2}^2]^{1/2}, tan\theta_s=\frac{\alpha_s\eta_2}{\eta_1}$ and $A_n, B_n,$ $C_n,$ and D_n are real constants.

Then for the first two terms n=0 and n=1 we have four partial differential equations but for n=1 the ϕ term is non homogeneous partial differential equation and it consists of two solutions such that classical (complementary) and particular solutions, but the other three equations are homogeneous partial differential equations consists only classical (complementary) solutions.

The homogeneous solutions for n=0 and n=1 are;

$$\phi_0(\rho_l\theta_l,t)=A_0{\rho_l}^{\frac{3}{2}}cos\left(\frac{3}{2}\theta_l\right)+C_0{\rho_l}^{\frac{3}{2}}sin\left(\frac{3}{2}\theta_l\right) \quad [3.79]$$

$$\psi_0(\rho_s,\theta_s,t) = B_0{\rho_s}^{\frac{3}{2}}sin\left(\frac{3}{2}\theta_s\right) + D_0{\rho_s}^{\frac{3}{2}}cos\left(\frac{3}{2}\theta_s\right) \quad [3.80]$$

$$\psi_1(\rho_s,\theta_s,t) = B_1{\rho_s}^2sin(2\theta_s) + D_1{\rho_s}^2cos(2\theta_s) \quad [3.81]$$

But $\left({\alpha_l}^2\frac{\partial^2\phi}{\partial{\eta_1}^2} + \frac{\partial^2\phi}{\partial{\eta_2}^2}\right) - \alpha\frac{(3\delta+2)}{\delta+2}\varepsilon^2T_1 = 0$ consists of the classical and particular solutions, such that the classical solution is calculated by setting the equation as $\left({\alpha_l}^2\frac{\partial^2\phi}{\partial{\eta_1}^2} + \frac{\partial^2\phi}{\partial{\eta_2}^2}\right) = 0$ then the solution is;

$${\phi'}_1(\rho_l\theta_l,t) = A_1{\rho_l}^2cos(2\theta_l) + C_1{\rho_l}^2sin(2\theta_l) \quad [3.82]$$

Then the homogeneous solutions are equation [3.79], [3.80], [3.81] and [3.82] but the particular solution is calculated as;

$$\left({\alpha_l}^2\frac{\partial^2\phi}{\partial{\eta_1}^2} + \frac{\partial^2\phi}{\partial{\eta_2}^2}\right) = \alpha\frac{(3\delta+2)}{\delta+2}\varepsilon^2T_1$$

But $\mathrm{T_1(x,y)} = \mathrm{A_1}\sin\left(\frac{\pi}{\mathrm{a}}\mathrm{x}\right)\sinh\left(\frac{\pi}{\mathrm{a}}(\mathrm{b}-\mathrm{y})\right)$ for, $\mathrm{A_1} = \frac{2}{\mathrm{a}\sinh(\frac{\pi}{\mathrm{a}}\mathrm{b})}\int_0^{\mathrm{a}}\mathrm{f_1(x)}\sin\left(\frac{\pi}{\mathrm{a}}\mathrm{x}\right)\mathrm{dx}$

$$\left({\alpha_l}^2\frac{\partial^2\phi}{\partial{\eta_1}^2} + \frac{\partial^2\phi}{\partial{\eta_2}^2}\right) = \alpha\frac{(3\delta+2)}{\delta+2}\mathrm{A_1}\sin\left(\frac{\pi}{\mathrm{a}}\mathrm{x}\right)\sinh\left(\frac{\pi}{\mathrm{a}}(\mathrm{b}-\mathrm{y})\right) \quad [3.83]$$

Then from calculus of mathematics when we integrate the above equation both sides by recalling $\nabla^2 = \frac{\partial^2}{\partial x^2} + \frac{\partial^2}{\partial y^2} = \frac{\partial^2}{\partial{\eta_1}^2} + \frac{\partial^2}{\partial{\eta_2}^2}$ we can replace the left hand side of the equation as;

$${\phi''}_1 = \int\int\alpha\frac{(3\delta+2)}{\delta+2}\mathrm{A_1}\sin\left(\frac{\pi}{\mathrm{a}}\mathrm{x}\right)\sinh\left(\frac{\pi}{\mathrm{a}}(\mathrm{b}-\mathrm{y})\right)dxdy \quad [3.84]$$

Then equation [3.84] is the multiple integral and by remembering, the rule of multiple integral from calculus and it is calculated as;

$${\phi''}_1 = \frac{(3\delta+2)}{\delta+2}\mathrm{A_1}\left(\int\sin\left(\frac{\pi}{\mathrm{a}}\mathrm{x}\right)dx\right)\left(\int\sinh\left(\frac{\pi}{\mathrm{a}}(\mathrm{b}-\mathrm{y})\right)dy\right)$$

Then let's recall the integration of trigonometric and hyperbolic functions we get the particular solutions such that;

$${\phi''}_1 = -\mathrm{A_1}\frac{(3\delta+2)a}{(\delta+2)\pi}cos\left(\frac{\pi}{\mathrm{a}}\mathrm{x}\right)\cosh\left(\frac{\pi}{\mathrm{a}}(\mathrm{b}-\mathrm{y})\right) \quad [3.85]$$

Then the general solution for equation $\left({\alpha_l}^2\frac{\partial^2\phi}{\partial{\eta_1}^2} + \frac{\partial^2\phi}{\partial{\eta_2}^2}\right) - \alpha\frac{(3\delta+2)}{\delta+2}\varepsilon^2T_1 = 0$ is the sum of [3.82] and equation [3.85], which are classical and particular solutions.

$$\phi_1 = {\phi'}_1 + {\phi''}_1$$

$$\phi_1(\rho_l\theta_l,t) = A_1{\rho_l}^2 cos(2\theta_l) + C_1{\rho_l}^2 sin(2\theta_l) - \mathrm{A}_1\frac{(3\delta+2)a}{(\delta+2)\pi}cos\left(\frac{\pi}{\mathrm{a}}\mathrm{x}\right)\cosh\left(\frac{\pi}{\mathrm{a}}(\mathrm{b}-\mathrm{y})\right) \quad [3.86]$$

By substituting the expressions for $\phi_0, \psi_0, \phi_1 and\ \psi_1$ into equation [3.69] and [3.70] in terms of crack-tip coordinates, the displacement potentials can be represented as.

$$\phi(x,y) = A_0{\rho_l}^{\frac{3}{2}}cos\left(\frac{3}{2}\theta_l\right) + C_0{\rho_l}^{\frac{3}{2}}sin\left(\frac{3}{2}\theta_l\right) + A_1{\rho_l}^2 cos(2\theta_l) + C_1{\rho_l}^2 sin(2\theta_l) - \mathrm{K}_1\frac{(3\delta+2)a}{(\delta+2)\pi}cos\left(\frac{\pi}{\mathrm{a}}\mathrm{x}\right)\cosh\left(\frac{\pi}{\mathrm{a}}(\mathrm{b}-\mathrm{y})\right) \quad [3.87]$$

$$\psi(x,y) = B_0{\rho_s}^{\frac{3}{2}}sin\left(\frac{3}{2}\theta_s\right) + D_0{\rho_s}^{\frac{3}{2}}cos\left(\frac{3}{2}\theta_s\right) + B_1{\rho_s}^2 sin(2\theta_s) + D_1{\rho_s}^2 cos(2\theta_s) \quad [3.88]$$

Equation [3.87] and [3.88] are the solution of equation of motion that represents the displacement potentials. Equation [3.85] is the temperature field equation which is not transformed to the new coordinate system η_1 and η_2 which is expressed as $\eta_1 = {}^{x}/_{\varepsilon}$, $\eta_2 = {}^{y}/_{\varepsilon}$ for, $0 < \varepsilon < 1$, the expression was utilized to analyze the phenomenon more closely. New equation [3.87] can be written as;

$$\phi(x,y) = A_0{\rho_l}^{\frac{3}{2}}cos\left(\frac{3}{2}\theta_l\right) + C_0{\rho_l}^{\frac{3}{2}}sin\left(\frac{3}{2}\theta_l\right) + A_1{\rho_l}^2 cos(2\theta_l) + C_1{\rho_l}^2 sin(2\theta_l) - \mathrm{K}_1\frac{(3\delta+2)a}{(\delta+2)\pi}cos\left(\frac{\pi}{\mathrm{a}}\varepsilon\eta_1\right)\cosh\left(\frac{\pi}{\mathrm{a}}(\mathrm{b}-\varepsilon\eta_2)\right)$$

From the perturbation of the temperature filed equation the smaller parameter was the coefficient as it square its self as ε^2 and as depicted in literature (Kidane, Chalivendra and Shukla, 2010) and (Kidane *et al.*, 2010) we can replace it with the parameter ρ which is expressed as;

$$\rho = ({\eta_1}^2 + {\eta_2}^2)^{\frac{1}{2}} \quad [3.89]$$

$$\theta = tan\frac{\eta_2}{\eta_1} \quad [3.90]$$

Therefore with the constant q_0 that will introduced in the literature (Kidane, Chalivendra and Shukla, 2010).

$$\phi(x,y) = A_0{\rho_l}^{\frac{3}{2}}cos\left(\frac{3}{2}\theta_l\right) + C_0{\rho_l}^{\frac{3}{2}}sin\left(\frac{3}{2}\theta_l\right) + A_1{\rho_l}^2 cos(2\theta_l) + C_1{\rho_l}^2 sin(2\theta_l) - \mathrm{K}_1\frac{(3\delta+2)a}{(\delta+2)\pi}q_0\rho^2 cos\left(\frac{\pi}{\mathrm{a}}\varepsilon\eta_1\right)\cosh\left(\frac{\pi}{\mathrm{a}}(\mathrm{b}-\varepsilon\eta_2)\right)$$

Then after insertion of the coordinates η_1 and η_2 as a function of ρ and θ by rearranging equation [3.89] and [3.90] we can write equations as follows;

$$\phi(x,y) = A_0\rho_l^{\frac{3}{2}}cos\left(\frac{3}{2}\theta_l\right) + C_0\rho_l^{\frac{3}{2}}sin\left(\frac{3}{2}\theta_l\right) + A_1{\rho_l}^2cos(2\theta_l) + C_1{\rho_l}^2sin(2\theta_l) -$$

$$\mathrm{K}_1\frac{(3\delta+2)a}{(\delta+2)\pi}q_0\rho^2cos\left(\frac{\pi}{\mathrm{a}}\varepsilon\sin\theta\right)\cosh\left(\frac{\pi}{\mathrm{a}}(\mathrm{b}-\varepsilon\rho\,\sin\theta)\right)$$

Then after all, the smaller parameter introduced in the coordinate plane will be ignored since the constant q_n will recover some uncertainty as well we can write the final displacement potentials as;

$$\begin{aligned}\phi(\rho_l,\theta_l,\theta) = {} & A_0\rho_l^{\frac{3}{2}}cos\left(\frac{3}{2}\theta_l\right) + C_0\rho_l^{\frac{3}{2}}sin\left(\frac{3}{2}\theta_l\right) + A_1{\rho_l}^2cos(2\theta_l) \\ & + C_1{\rho_l}^2sin(2\theta_l) \\ & - \mathrm{K}_1\frac{(3\delta+2)a}{(\delta+2)\pi}q_0\rho^2cos\left(\frac{\pi}{\mathrm{a}}\rho\,\sin\theta\right)\cosh\left(\frac{\pi}{\mathrm{a}}(\mathrm{b}-\rho\,\sin\theta)\right)\end{aligned} \qquad [3.91]$$

$$\begin{aligned}\psi(\rho_s,\theta_s) = {} & B_0\rho_s^{\frac{3}{2}}sin\left(\frac{3}{2}\theta_s\right) + D_0\rho_s^{\frac{3}{2}}cos\left(\frac{3}{2}\theta_s\right) + B_1{\rho_s}^2sin(2\theta_s) \\ & + D_1{\rho_s}^2cos(2\theta_s)\end{aligned} \qquad [3.92]$$

In the nutshell, equation [3.91] and [3.92] are the displacement potentials that are needed for the next progress of the modeling of the strain and stress fields.

"If f(z) is differentiable at z_0 and throughout a neighborhood of z_0, then f(z) is described as analytic (or regular or holomorphic) at z_0. If f(z) is analytic everywhere in the finite complex plane, it is described as entire. Examples of entire functions include Exp, Sin, Cos, Sinh, and Cosh. Functions which are analytic except on branch cuts include Log, ArcSin, ArcCos, ArcSinh, and ArcCosh." (James J. Kelly, 2006).

(FREUND, 1990) stated that by considering the function $f(\varsigma)$ of complex variable $\varsigma = \eta_1 + i\eta_2 = \rho e^{i\theta}$ defined in a neighborhood of a particular point. If $f(\varsigma)$ is differentiable with respect to ς at that point, then it is an analytic function at that point. If $f(\varsigma)$ is analytic at every point in a region, it is said to be analytic in the region. Analyticity of $f(\varsigma)$ in turn implies that derivatives of all orders exist. If $f(\varsigma)$ is analytic then, with $f(\varsigma)$ = u(η_1, η_2) + iv (η_1, η_2) it follows that;

$\frac{\partial u}{\partial \eta_1} = \frac{\partial v}{\partial \eta_2}$ And $\frac{\partial u}{\partial \eta_2} = -\frac{\partial v}{\partial \eta_1}$ where ς =Greek letter stigma

These relations are called the Cauchy-Riemann equations. If $f(\varsigma)$ is analytic in a region, then the Cauchy-Riemann relations imply that (FREUND, 1990);

$\nabla^2 u = 0$ and $\nabla^2 v = 0$

in that region. Real functions that satisfy Laplace's equation are said to be harmonic functions. A general solution of the partial differential equation $\nabla^2 u = 0$ over some region is $u = Re\{F(\varsigma)\}$ or $u = Im\{G(\varsigma)\}$. Where $F(\varsigma)$ or $G(\varsigma)$ is an analytic function in the region that must be determined from the boundary conditions (FREUND, 1990).

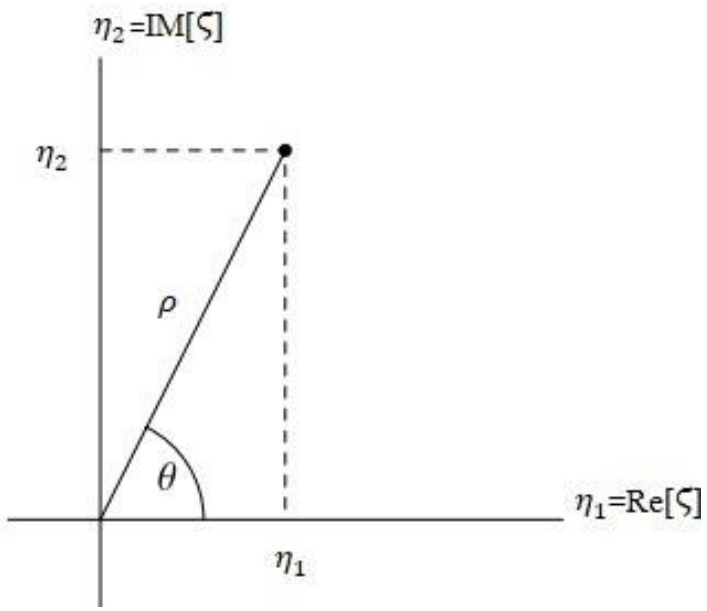

Figure 11:- Cartesian and polar representations of complex numbers

Up on using Figure 11, which is the complex plane of $\eta_1, and\ \eta_2$ coordinates the cosine term is the real part and the sine term is the complex part the magnitude of the complex variable ς is given by the expression.

$$|\varsigma| = \rho = \sqrt{\eta_1{}^2 + \eta_2{}^2} = \sqrt{(\rho cos\theta)^2 + (\rho sin\theta)^2} \qquad [3.93]$$

Therefore, equation [3.91] and [3.92] has a set of imaginary and set of real parts of the complex number notation, so let's substitute Re [] in place of cosine and IM [] in place of sine terms such that;

$$\phi(\rho_l, \theta_l) = A_0 Re[\varsigma_l^{\frac{3}{2}}] + C_0 IM[\varsigma_l^{\frac{3}{2}}] + A_1 Re[\varsigma_l{}^2] + C_1 IM[\varsigma_l{}^2] - \mathrm{K}_1 \frac{(3\delta + 2)a}{(\delta + 2)\pi} \cosh\left(\frac{\pi}{\mathrm{a}}(\mathrm{b} - \rho \sin\theta)\right) q_0 Re[\varsigma^2] \qquad [3.94]$$

$$\psi(\rho_s,\theta_s) = B_0 IM[\varsigma_s^{\frac{3}{2}}] + D_0 Re[\varsigma_s^{\frac{3}{2}}] + B_1 IM[\varsigma_s{}^2] + D_1 Re[\varsigma_s{}^2] \quad [3.95]$$

Therefore from equation [3.34] the expression for the displacements from the displacement potential is give as a function of x and y such that; $u = \frac{\partial\phi}{\partial x} + \frac{\partial\psi}{\partial y}$ and, $v = \frac{\partial\phi}{\partial y} - \frac{\partial\psi}{\partial x}$, therefore let's transform equation [3.91] and [3.92] back to x, y plane.

$$\phi(x,y) = A_0 r_l^{\frac{3}{2}} cos\left(\frac{3}{2}\theta_l\right) + C_0 r_l^{\frac{3}{2}} sin\left(\frac{3}{2}\theta_l\right) + A_1 r_l{}^2 cos(2\theta_l) + C_1 r_l{}^2 sin(2\theta_l) - \mathrm{K}_1 \frac{(3\delta+2)a}{(\delta+2)\pi} q_0 r^2 cos\left(\frac{\pi}{\mathrm{a}}x\right) \cosh\left(\frac{\pi}{\mathrm{a}}(\mathrm{b}-y)\right) \quad [3.96]$$

$$\psi(x,y) = B_0 r_s^{\frac{3}{2}} sin\left(\frac{3}{2}\theta_s\right) + D_0 r_s^{\frac{3}{2}} cos\left(\frac{3}{2}\theta_s\right) + B_1 r_s{}^2 sin(2\theta_s) + D_1 r_s{}^2 cos(2\theta_s) \quad [3.71]$$

Where, $r_l = (x^2 + \alpha_l y^2)^{\frac{1}{2}}$, $tan\theta_l = \frac{\alpha_l y}{x}$, $r_s = (x^2 + \alpha_s y^2)^{\frac{1}{2}}$ and $tan\theta_s = \frac{\alpha_s y}{x}$

Like equation [3.94] and [3.95] let's substitute Re [] in place of cosine and IM [] in place of sine terms by noting the expression $|\varsigma| = r = \sqrt{x^2 + x^2} = \sqrt{(rcos\theta)^2 + (rsin\theta)^2}$ such that;

$$\phi(x,y) = A_0 Re[\varsigma_l^{\frac{3}{2}}] + C_0 IM[\varsigma_l^{\frac{3}{2}}] + A_1 Re[\varsigma_l{}^2] + C_1 IM[\varsigma_l{}^2] - \mathrm{K}_1 \frac{(3\delta+2)a}{(\delta+2)\pi} \cosh\left(\frac{\pi}{\mathrm{a}}(\mathrm{b}-y)\right) q_0 Re[\varsigma^2] \quad [3.98]$$

$$\psi(x,y) = B_0 IM[\varsigma_s^{\frac{3}{2}}] + D_0 Re[\varsigma_s^{\frac{3}{2}}] + B_1 IM[\varsigma_s{}^2] + D_1 Re[\varsigma_s{}^2] \quad [3.99]$$

The displacements field in the x-direction is given by $u = \frac{\partial\phi}{\partial x} + \frac{\partial\psi}{\partial y}$ therefore; let's find the differentiation of ϕ as a function of x and ψ as a function of y as follows;

$$\frac{\partial\phi}{\partial x} = \frac{\partial}{\partial x}\left\{A_0 Re[\varsigma_l^{\frac{3}{2}}] + C_0 IM[\varsigma_l^{\frac{3}{2}}] + A_1 Re[\varsigma_l{}^2] + C_1 IM[\varsigma_l{}^2] - \mathrm{K}_1 \frac{(3\delta+2)a}{(\delta+2)\pi} \cosh\left(\frac{\pi}{\mathrm{a}}(\mathrm{b}-y)\right) q_0 Re[\varsigma^2]\right\}$$

$$\frac{\partial\phi}{\partial x} = A_0 \frac{3}{2} Re[\varsigma_l^{\frac{1}{2}}] + C_0 \frac{3}{2} IM[\varsigma_l^{\frac{1}{2}}] + A_1 2Re[\varsigma_l] + C_1 2IM[\varsigma_l] - \mathrm{K}_1 \frac{(3\delta+2)a}{(\delta+2)\pi} \cosh\left(\frac{\pi}{\mathrm{a}}(\mathrm{b}-y)\right) q_0 2Re[\varsigma]$$

$$\frac{\partial\phi}{\partial x} = A_0\frac{3}{2}\zeta_l^{\frac{1}{2}}cos\frac{1}{2}\theta_l + C_0\frac{3}{2}\zeta_l^{\frac{1}{2}}sin\frac{1}{2}\theta_l + A_1 2\zeta_l cos\theta_l + C_1 2sin\theta_l - \mathrm{K}_1\frac{(3\delta+2)a}{(\delta+2)\pi}\cosh\left(\frac{\pi}{\mathrm{a}}(\mathrm{b}-y)\right)q_0 2\zeta cos\theta \quad [3.100]$$

$$\frac{\partial\psi}{\partial y} = \frac{\partial}{\partial y}\left\{B_0 IM[\zeta_s^{\frac{3}{2}}] + D_0 Re[\zeta_s^{\frac{3}{2}}] + B_1 IM[\zeta_s{}^2] + D_1 Re[\zeta_s{}^2]\right\}$$

$$\frac{\partial\psi}{\partial y} = B_0\frac{3}{2}\alpha_s IM[\zeta_s^{\frac{1}{2}}] + D_0\frac{3}{2}\alpha_s Re[\zeta_s^{\frac{1}{2}}] + B_1 2\alpha_s IM[\zeta_s] + D_1 2\alpha_s Re[\zeta_s]$$

$$\frac{\partial\psi}{\partial y} = B_0\frac{3}{2}\alpha_s\zeta_s^{\frac{1}{2}}sin\frac{1}{2}\theta_s + D_0\frac{3}{2}\alpha_s\zeta_s^{\frac{1}{2}}cos\frac{1}{2}\theta_s + B_1 2\alpha_s\zeta_s sin\theta_s + D_1 2\alpha_s\zeta_s cos\theta_s \quad [3.101]$$

Now let's substitute equation [3.100] and [3.101] in equation [3.34] to get the displacement field in the x direction of equation $u = \frac{\partial\phi}{\partial x} + \frac{\partial\psi}{\partial y}$ such that;

$$u = \left\{A_0\frac{3}{2}\zeta_l^{\frac{1}{2}}cos\frac{1}{2}\theta_l + C_0\frac{3}{2}\zeta_l^{\frac{1}{2}}sin\frac{1}{2}\theta_l + A_1 2\zeta_l cos\theta_l + C_1 2sin\theta_l - \mathrm{K}_1\frac{(3\delta+2)a}{(\delta+2)\pi}\cosh\left(\frac{\pi}{\mathrm{a}}(\mathrm{b}-y)\right)q_0 2\zeta cos\theta_l\right\} + \left\{B_0\frac{3}{2}\alpha_s\zeta_s^{\frac{1}{2}}sin\frac{1}{2}\theta_s + D_0\frac{3}{2}\alpha_s\zeta_s^{\frac{1}{2}}cos\frac{1}{2}\theta_s + B_1 2\alpha_s\zeta_s sin\theta_s + D_1 2\alpha_s\zeta_s cos\theta_s\right\}$$

$$u = A_0\frac{3}{2}\zeta_l^{\frac{1}{2}}cos\frac{1}{2}\theta_l + C_0\frac{3}{2}\zeta_l^{\frac{1}{2}}sin\frac{1}{2}\theta_l + A_1 2\zeta_l cos\theta_l + C_1 2\zeta_l sin\theta_l - \mathrm{K}_1\frac{(3\delta+2)a}{(\delta+2)\pi}\cosh\left(\frac{\pi}{\mathrm{a}}(\mathrm{b}-y)\right)q_0 2\zeta cos\theta + B_0\frac{3}{2}\alpha_s\zeta_s^{\frac{1}{2}}sin\frac{1}{2}\theta_s + D_0\frac{3}{2}\alpha_s\zeta_s^{\frac{1}{2}}cos\frac{1}{2}\theta_s + B_1 2\alpha_s\zeta_s sin\theta_s + D_1 2\alpha_s\zeta_s cos\theta_s \quad [3.102]$$

Equation [3.102] is equation of displacement fields in x direction and to get the displacement field in the y direction lets differentiate ϕ with respect to y and ψ with respect to x and substitute in $v = \frac{\partial\phi}{\partial y} - \frac{\partial\psi}{\partial x}$ such that;

$$\frac{\partial\phi}{\partial y} = \frac{\partial}{\partial y}\left\{A_0 Re[\zeta_l^{\frac{3}{2}}] + C_0 IM[\zeta_l^{\frac{3}{2}}] + A_1 Re[\zeta_l{}^2] + C_1 IM[\zeta_l{}^2] - \mathrm{K}_1\frac{(3\delta+2)a}{(\delta+2)\pi}\cosh\left(\frac{\pi}{\mathrm{a}}(\mathrm{b}-y)\right)q_0 Re[\zeta^2]\right\}$$

$$\frac{\partial\phi}{\partial y} = A_0\frac{3}{2}\alpha_l(-IM[\zeta_l^{\frac{1}{2}}]) + C_0\alpha_l\frac{3}{2}Re[\zeta_l^{\frac{1}{2}}] + A_1 2\alpha_l(-IM[\zeta_l]) + C_1 2\alpha_l Re[\zeta_l] -$$

$$\mathrm{K}_1\frac{(3\delta+2)a}{(\delta+2)\pi}\cosh\left(\frac{\pi}{\mathrm{a}}(\mathrm{b}-y)\right)q_0 2Re[\zeta] - \mathrm{K}_1\frac{(3\delta+2)a^2}{(\delta+2)\pi^2}\sinh\left(\frac{\pi}{\mathrm{a}}(\mathrm{b}-y)\right)q_0 Re[\zeta^2]$$

$$\frac{\partial\phi}{\partial y} = -A_0\frac{3}{2}\alpha_l IM[\zeta_l^{\frac{1}{2}}] + C_0\alpha_l\frac{3}{2}Re[\zeta_l^{\frac{1}{2}}] - A_1 2\alpha_l IM[\zeta_l] + C_1 2\alpha_l Re[\zeta_l] -$$

$$\mathrm{K}_1\frac{(3\delta+2)a}{(\delta+2)\pi}\cosh\left(\frac{\pi}{\mathrm{a}}(\mathrm{b}-y)\right)q_0 2Re[\zeta] - \mathrm{K}_1\frac{(3\delta+2)a^2}{(\delta+2)\pi^2}\sinh\left(\frac{\pi}{\mathrm{a}}(\mathrm{b}-y)\right)q_0 Re[\zeta^2]$$

$$\frac{\partial\phi}{\partial y} = -A_0\frac{3}{2}\alpha_l\zeta_l^{\frac{1}{2}}sin\frac{1}{2}\theta_l + C_0\alpha_l\frac{3}{2}\zeta_l^{\frac{1}{2}}cos\frac{1}{2}\theta_l - A_1 2\alpha_l\zeta_l sin\theta_l + C_1 2\alpha_l\zeta_l cos\theta_l -$$

$$\mathrm{K}_1\frac{(3\delta+2)a}{(\delta+2)\pi}\cosh\left(\frac{\pi}{\mathrm{a}}(\mathrm{b}-y)\right)q_0 2\zeta_l cos\theta - \mathrm{K}_1\frac{(3\delta+2)a^2}{(\delta+2)\pi^2}\sinh\left(\frac{\pi}{\mathrm{a}}(\mathrm{b}-y)\right)q_0\zeta^2 cos2\theta \quad [3.103]$$

$$\frac{\partial\psi}{\partial x} = \frac{\partial}{\partial x}\left\{B_0 IM[\zeta_s^{\frac{3}{2}}] + D_0 Re[\zeta_s^{\frac{3}{2}}] + B_1 IM[\zeta_s{}^2] + D_1 Re[\zeta_s{}^2]\right\}$$

$$\frac{\partial\psi}{\partial x} = B_0\frac{3}{2}IM[\zeta_s^{\frac{1}{2}}] + D_0\frac{3}{2}Re[\zeta_s^{\frac{1}{2}}] + B_1 2IM[\zeta_s] + D_1 2Re[\zeta_s]$$

$$\frac{\partial\psi}{\partial x} = B_0\frac{3}{2}\zeta_s^{\frac{1}{2}}sin\frac{1}{2}\theta_s + D_0\frac{3}{2}\zeta_s^{\frac{1}{2}}cos\frac{1}{2}\theta_s + B_1 2\zeta_s sin\theta_s + D_1 2\zeta_s cos\theta_s \quad [3.104]$$

Now let**'s** substitute equation [3.103] and [3.104] in equation [3.34] to get the displacement field in the y direction of equation$v = \frac{\partial\phi}{\partial y} - \frac{\partial\psi}{\partial x}$ such that;

$$v = \left\{-A_0\frac{3}{2}\alpha_l\zeta_l^{\frac{1}{2}}sin\frac{1}{2}\theta_l + C_0\alpha_l\frac{3}{2}\zeta_l^{\frac{1}{2}}cos\frac{1}{2}\theta_l - A_1 2\alpha_l\zeta_l sin\theta_l + C_1 2\alpha_l\zeta_l cos\theta_l -\right.$$

$$\left.\mathrm{K}_1\frac{(3\delta+2)a}{(\delta+2)\pi}\cosh\left(\frac{\pi}{\mathrm{a}}(\mathrm{b}-y)\right)q_0 2\zeta_l cos\theta - \mathrm{K}_1\frac{(3\delta+2)a^2}{(\delta+2)\pi^2}\sinh\left(\frac{\pi}{\mathrm{a}}(\mathrm{b}-y)\right)q_0\zeta^2 cos2\theta\right\} -$$

$$\left\{B_0\frac{3}{2}\zeta_s^{\frac{1}{2}}sin\frac{1}{2}\theta_s + D_0\frac{3}{2}\zeta_s^{\frac{1}{2}}cos\frac{1}{2}\theta_s + B_1 2\zeta_s sin\theta_s + D_1 2\zeta_s cos\theta_s\right\}$$

$$v = -A_0\frac{3}{2}\alpha_l\zeta_l^{\frac{1}{2}}sin\frac{1}{2}\theta_l + C_0\alpha_l\frac{3}{2}\zeta_l^{\frac{1}{2}}cos\frac{1}{2}\theta_l - A_1 2\alpha_l\zeta_l sin\theta_l +$$

$$C_1 2\alpha_l\zeta_l cos\theta_l - \mathrm{K}_1\frac{(3\delta+2)a}{(\delta+2)\pi}\cosh\left(\frac{\pi}{\mathrm{a}}(\mathrm{b}-y)\right)q_0 2\zeta_l cos\theta - \quad [3.105]$$

$$\mathrm{K}_1\frac{(3\delta+2)a^2}{(\delta+2)\pi^2}\sinh\left(\frac{\pi}{\mathrm{a}}(\mathrm{b}-y)\right)q_0\zeta^2 cos2\theta - B_0\frac{3}{2}\zeta_s^{\frac{1}{2}}sin\frac{1}{2}\theta_s - D_0\frac{3}{2}\zeta_s^{\frac{1}{2}}cos\frac{1}{2}\theta_s - B_1 2\zeta_s sin\theta_s - D_1 2\zeta_s cos\theta_s$$

Equation [3.102] and [3.105] are the displacement fields along x and y axis respectively, and in order to get the strains let's differentiate further u with respect to x to get ε_x and v with respect to y to get ε_y as well as add the derivation of u with respect to y and the derivation of v with respect to x to get γ_{xy}. Where ε_x=strain in x direction, ε_y=strain in y direction and γ_{xy}=shear strain in xy plane and expressed by $\varepsilon_x = \frac{\partial u}{\partial x}$, $\varepsilon_y = \frac{\partial v}{\partial y}$, And $\gamma_{xy} = \frac{\partial u}{\partial y} + \frac{\partial v}{\partial x}$.

The in-plane strain field in the x direction is $\varepsilon_x = \frac{\partial u}{\partial x}$

$$\frac{\partial u}{\partial x} = \frac{\partial}{\partial x}\Big\{A_0\frac{3}{2}\zeta_l^{\frac{1}{2}}cos\frac{1}{2}\theta_l + C_0\frac{3}{2}\zeta_l^{\frac{1}{2}}sin\frac{1}{2}\theta_l + A_1 2\zeta_l cos\theta_l + C_1 2\zeta_l sin\theta_l - \mathrm{K}_1\frac{(3\delta+2)a}{(\delta+2)\pi}\cosh\left(\frac{\pi}{\mathrm{a}}(\mathrm{b}-y)\right)q_0 2\zeta cos\theta + B_0\frac{3}{2}\alpha_s\zeta_s^{\frac{1}{2}}sin\frac{1}{2}\theta_s + D_0\frac{3}{2}\alpha_s\zeta_s^{\frac{1}{2}}cos\frac{1}{2}\theta_s + B_1 2\alpha_s\zeta_s sin\theta_s + D_1 2\alpha_s\zeta_s cos\theta_s\Big\}$$

$$\frac{\partial u}{\partial x} = A_0\frac{1}{2}\times\frac{3}{2}\zeta_l^{-\frac{1}{2}}cos\frac{1}{2}\theta_l - C_0\frac{1}{2}\times\frac{3}{2}\zeta_l^{-\frac{1}{2}}sin\frac{1}{2}\theta_l + 2A_1 - 2\mathrm{K}_1\frac{(3\delta+2)a}{(\delta+2)\pi}\cosh\left(\frac{\pi}{\mathrm{a}}(\mathrm{b}-y)\right)q_0 + B_0\frac{1}{2}\times\frac{3}{2}\alpha_s\zeta_s^{-\frac{1}{2}}sin\frac{1}{2}\theta_s + D_0\frac{1}{2}\times\frac{3}{2}\alpha_s\zeta_s^{-\frac{1}{2}}cos\frac{1}{2}\theta_s + 2\alpha_s D_1$$

$$\varepsilon_x = \frac{\partial u}{\partial x} = A_0\frac{3}{4}\zeta_l^{-\frac{1}{2}}cos\frac{1}{2}\theta_l - C_0\frac{3}{4}\zeta_l^{-\frac{1}{2}}sin\frac{1}{2}\theta_l - 2\mathrm{K}_1\frac{(3\delta+2)a}{(\delta+2)\pi}\cosh\left(\frac{\pi}{\mathrm{a}}(\mathrm{b}-y)\right)q_0 + B_0\frac{3}{4}\alpha_s\zeta_s^{-\frac{1}{2}}sin\frac{1}{2}\theta_s + D_0\frac{3}{4}\alpha_s\zeta_s^{-\frac{1}{2}}cos\frac{1}{2}\theta_s + 2A_1 + 2D_1\alpha_s \quad [3.106]$$

The in-plane strain field in the y direction is $\varepsilon_y = \frac{\partial v}{\partial y}$

$$\frac{\partial v}{\partial y} = \Big\{-A_0\frac{3}{2}\alpha_l\zeta_l^{\frac{1}{2}}sin\frac{1}{2}\theta_l + C_0\alpha_l\frac{3}{2}\zeta_l^{\frac{1}{2}}cos\frac{1}{2}\theta_l - A_1 2\alpha_l\zeta_l sin\theta_l + C_1 2\alpha_l\zeta_l cos\theta_l - \mathrm{K}_1\frac{(3\delta+2)a}{(\delta+2)\pi}\cosh\left(\frac{\pi}{\mathrm{a}}(\mathrm{b}-y)\right)q_0 2\zeta cos\theta - \mathrm{K}_1\frac{(3\delta+2)a^2}{(\delta+2)\pi^2}\sinh\left(\frac{\pi}{\mathrm{a}}(\mathrm{b}-y)\right)q_0\zeta^2 cos2\theta - B_0\frac{3}{2}\zeta_s^{\frac{1}{2}}sin\frac{1}{2}\theta_s - D_0\frac{3}{2}\zeta_s^{\frac{1}{2}}cos\frac{1}{2}\theta_s - B_1 2\zeta_s sin\theta_s - D_1 2\zeta_s cos\theta_s\Big\}$$

$$\frac{\partial v}{\partial y} = -A_0\frac{1}{2}\times\frac{3}{2}\alpha_l{}^2\zeta_l{}^{-\frac{1}{2}}sin\frac{1}{2}\theta_l - C_0\frac{1}{2}\times\frac{3}{2}\alpha_l{}^2\zeta_l{}^{-\frac{1}{2}}sin\frac{1}{2}\theta_l - 2A_1\alpha_l{}^2 - 2\mathrm{K}_1\frac{(3\delta+2)a}{(\delta+2)\pi}\cosh\left(\frac{\pi}{\mathrm{a}}(\mathrm{b}-y)\right)q_0 + \mathrm{K}_1\frac{(3\delta+2)a^2}{(\delta+2)\pi^2}\sinh\left(\frac{\pi}{\mathrm{a}}(\mathrm{b}-y)\right)2q_0\zeta sin\theta + B_0\frac{1}{2}\times\frac{3}{2}\alpha_s\zeta_s{}^{-\frac{1}{2}}cos\frac{1}{2}\theta_s - D_0\frac{1}{2}\times\frac{3}{2}\alpha_s\zeta_s{}^{-\frac{1}{2}}sin\frac{1}{2}\theta_s - 2B_1\alpha_s$$

$$\varepsilon_y = \frac{\partial v}{\partial y} = -A_0\frac{3}{4}\alpha_l{}^2\zeta_l{}^{-\frac{1}{2}}sin\frac{1}{2}\theta_l - C_0\frac{3}{4}\alpha_l{}^2\zeta_l{}^{-\frac{1}{2}}sin\frac{1}{2}\theta_l - 2\mathrm{K}_1\frac{(3\delta+2)a}{(\delta+2)\pi}\cosh\left(\frac{\pi}{\mathrm{a}}(\mathrm{b}-y)\right)q_0 + \mathrm{K}_1\frac{(3\delta+2)a^2}{(\delta+2)\pi^2}\sinh\left(\frac{\pi}{\mathrm{a}}(\mathrm{b}-y)\right)2q_0\zeta sin\theta + B_0\frac{3}{4}\alpha_s\zeta_s{}^{-\frac{1}{2}}cos\frac{1}{2}\theta_s - D_0\frac{3}{4}\alpha_s\zeta_s{}^{-\frac{1}{2}}sin\frac{1}{2}\theta_s - 2A_1\alpha_l{}^2 - 2B_1\alpha_s \quad [3.107]$$

To get the shear stress in the xy plane lets differentiate v with respect to x and u with respect to y and substitute the derivatives in equation $\gamma_{xy} = \frac{\partial u}{\partial y} + \frac{\partial v}{\partial x}$ such that;

$$\frac{\partial v}{\partial x} = \frac{\partial}{\partial x}\left\{-A_0\frac{3}{2}\alpha_l\zeta_l{}^{\frac{1}{2}}sin\frac{1}{2}\theta_l + C_0\alpha_l\frac{3}{2}\zeta_l{}^{\frac{1}{2}}cos\frac{1}{2}\theta_l - A_1 2\alpha_l\zeta_l sin\theta_l + C_1 2\alpha_l\zeta_l cos\theta_l - \mathrm{K}_1\frac{(3\delta+2)a}{(\delta+2)\pi}\cosh\left(\frac{\pi}{\mathrm{a}}(\mathrm{b}-y)\right)q_0 2\zeta_l cos\theta - \mathrm{K}_1\frac{(3\delta+2)a^2}{(\delta+2)\pi^2}\sinh\left(\frac{\pi}{\mathrm{a}}(\mathrm{b}-y)\right)q_0\zeta^2 cos2\theta - B_0\frac{3}{2}\zeta_s{}^{\frac{1}{2}}sin\frac{1}{2}\theta_s - D_0\frac{3}{2}\zeta_s{}^{\frac{1}{2}}cos\frac{1}{2}\theta_s - B_1 2\zeta_s sin\theta_s - D_1 2\zeta_s cos\theta_s\right\}$$

$$\frac{\partial v}{\partial x} = A_0\frac{1}{2}\times\frac{3}{2}\alpha_l\zeta_l{}^{-\frac{1}{2}}sin\frac{1}{2}\theta_l + C_0\alpha_l\frac{1}{2}\times\frac{3}{2}\zeta_l{}^{-\frac{1}{2}}cos\frac{1}{2}\theta_l + 2C_1\alpha_l - \mathrm{K}_1\frac{(3\delta+2)a}{(\delta+2)\pi}\cosh\left(\frac{\pi}{\mathrm{a}}(\mathrm{b}-y)\right)2q_0 - \mathrm{K}_1\frac{(3\delta+2)a^2}{(\delta+2)\pi^2}\sinh\left(\frac{\pi}{\mathrm{a}}(\mathrm{b}-y)\right)2q_0\zeta cos\theta + B_0\frac{1}{2}\times\frac{3}{2}\zeta_s{}^{-\frac{1}{2}}sin\frac{1}{2}\theta_s - D_0\frac{1}{2}\times\frac{3}{2}\zeta_s{}^{-\frac{1}{2}}cos\frac{1}{2}\theta_s - 2D_1$$

$$\frac{\partial v}{\partial x} = A_0\frac{3}{4}\alpha_l\zeta_l{}^{-\frac{1}{2}}sin\frac{1}{2}\theta_l + C_0\alpha_l\frac{3}{4}\zeta_l{}^{-\frac{1}{2}}cos\frac{1}{2}\theta_l - \mathrm{K}_1\frac{(3\delta+2)a}{(\delta+2)\pi}\cosh\left(\frac{\pi}{\mathrm{a}}(\mathrm{b}-y)\right)2q_0 - \mathrm{K}_1\frac{(3\delta+2)a^2}{(\delta+2)\pi^2}\sinh\left(\frac{\pi}{\mathrm{a}}(\mathrm{b}-y)\right)2q_0\zeta cos\theta + B_0\frac{3}{4}\zeta_s{}^{-\frac{1}{2}}sin\frac{1}{2}\theta_s - D_0\frac{3}{4}\zeta_s{}^{-\frac{1}{2}}cos\frac{1}{2}\theta_s + 2C_1\alpha_l - 2D_1 \quad [3.108]$$

$$\frac{\partial u}{\partial y}=\frac{\partial}{\partial y}\Big\{A_0\frac{3}{2}\varsigma_l^{\frac{1}{2}}cos\frac{1}{2}\theta_l+C_0\frac{3}{2}\varsigma_l^{\frac{1}{2}}sin\frac{1}{2}\theta_l+A_1 2\varsigma_l cos\theta_l+C_1 2\varsigma_l sin\theta_l-$$

$$\mathrm{K}_1\frac{(3\delta+2)a}{(\delta+2)\pi}\cosh\left(\frac{\pi}{\mathrm{a}}(\mathrm{b}-y)\right)q_0 2\varsigma cos\theta+B_0\frac{3}{2}\alpha_s\varsigma_s^{\frac{1}{2}}sin\frac{1}{2}\theta_s+D_0\frac{3}{2}\alpha_s\varsigma_s^{\frac{1}{2}}cos\frac{1}{2}\theta_s+$$

$$B_1 2\alpha_s\varsigma_s sin\theta_s+D_1 2\alpha_s\varsigma_s cos\theta_s\Big\}$$

$$\frac{\partial u}{\partial y}=A_0\alpha_l\frac{1}{2}\times\frac{3}{2}\varsigma_l^{-\frac{1}{2}}sin\frac{1}{2}\theta_l+C_0\alpha_l\frac{1}{2}\times\frac{3}{2}\varsigma_l^{-\frac{1}{2}}cos\frac{1}{2}\theta_l+2\alpha_l C_1-\mathrm{K}_1\frac{(3\delta+2)a}{(\delta+2)\pi}\cosh\left(\frac{\pi}{\mathrm{a}}(\mathrm{b}-\right.$$

$$\left.y)\right)2q_0-\mathrm{K}_1\frac{(3\delta+2)a^2}{(\delta+2)\pi^2}\cosh\left(\frac{\pi}{\mathrm{a}}(\mathrm{b}-y)\right)2q_0\varsigma cos\theta+B_0\frac{1}{2}\times\frac{3}{2}{\alpha_s}^2\varsigma_s^{-\frac{1}{2}}cos\frac{1}{2}\theta_s+D_0\frac{1}{2}\times$$

$$\frac{3}{2}{\alpha_s}^2\varsigma_s^{-\frac{1}{2}}sin\frac{1}{2}\theta_s+2{\alpha_s}^2B_1$$

$$\frac{\partial u}{\partial y}=A_0\alpha_l\frac{3}{4}\varsigma_l^{-\frac{1}{2}}sin\frac{1}{2}\theta_l+C_0\alpha_l\frac{3}{4}\varsigma_l^{-\frac{1}{2}}cos\frac{1}{2}\theta_l-\mathrm{K}_1\frac{(3\delta+2)a}{(\delta+2)\pi}\cosh\left(\frac{\pi}{\mathrm{a}}(\mathrm{b}-\right.$$

$$\left.y)\right)2q_0-\mathrm{K}_1\frac{(3\delta+2)a^2}{(\delta+2)\pi^2}\cosh\left(\frac{\pi}{\mathrm{a}}(\mathrm{b}-y)\right)2q_0\varsigma cos\theta+B_0\frac{3}{4}{\alpha_s}^2\varsigma_s^{-\frac{1}{2}}cos\frac{1}{2}\theta_s+ \qquad [3.109]$$

$$D_0\frac{3}{4}{\alpha_s}^2\varsigma_s^{-\frac{1}{2}}sin\frac{1}{2}\theta_s+2{\alpha_s}^2B_1+2\alpha_l C_1$$

Then the shear strain in the xy plane expressed as $\gamma_{xy}=\frac{\partial u}{\partial y}+\frac{\partial v}{\partial x}$ in which the sum of equation [3.108] and equation [3.109] and the summation depicted as follows;

$$\gamma_{xy}=\Big\{A_0\alpha_l\frac{3}{4}\varsigma_l^{-\frac{1}{2}}sin\frac{1}{2}\theta_l+C_0\alpha_l\frac{3}{4}\varsigma_l^{-\frac{1}{2}}cos\frac{1}{2}\theta_l-\mathrm{K}_1\frac{(3\delta+2)a}{(\delta+2)\pi}\cosh\left(\frac{\pi}{\mathrm{a}}(\mathrm{b}-y)\right)2q_0-$$

$$\mathrm{K}_1\frac{(3\delta+2)a^2}{(\delta+2)\pi^2}\cosh\left(\frac{\pi}{\mathrm{a}}(\mathrm{b}-y)\right)2q_0\varsigma cos\theta+B_0\frac{3}{4}{\alpha_s}^2\varsigma_s^{-\frac{1}{2}}cos\frac{1}{2}\theta_s+D_0\frac{3}{4}{\alpha_s}^2\varsigma_s^{-\frac{1}{2}}sin\frac{1}{2}\theta_s+$$

$$2{\alpha_s}^2B_1+2\alpha_l C_1\Big\}+\Big\{A_0\frac{3}{4}\alpha_l\varsigma_l^{-\frac{1}{2}}sin\frac{1}{2}\theta_l+C_0\alpha_l\frac{3}{4}\varsigma_l^{-\frac{1}{2}}cos\frac{1}{2}\theta_l-\mathrm{K}_1\frac{(3\delta+2)a}{(\delta+2)\pi}\cosh\left(\frac{\pi}{\mathrm{a}}(\mathrm{b}-\right.$$

$$\left.y)\right)2q_0-\mathrm{K}_1\frac{(3\delta+2)a^2}{(\delta+2)\pi^2}\sinh\left(\frac{\pi}{\mathrm{a}}(\mathrm{b}-y)\right)2q_0\varsigma cos\theta+B_0\frac{3}{4}\varsigma_s^{-\frac{1}{2}}sin\frac{1}{2}\theta_s-D_0\frac{3}{4}\varsigma_s^{-\frac{1}{2}}cos\frac{1}{2}\theta_s+$$

$$2C_1\alpha_l-2D_1\Big\}$$

$$\gamma_{xy} = 2\times\frac{3}{4}A_0\alpha_l\varsigma_l^{-\frac{1}{2}}sin\frac{1}{2}\theta_l + 2\times\frac{3}{4}C_0\alpha_l\varsigma_l^{-\frac{1}{2}}cos\frac{1}{2}\theta_l - 2\times \mathrm{K}_1\frac{(3\delta+2)a}{(\delta+2)\pi}\cosh\left(\frac{\pi}{\mathrm{a}}(\mathrm{b}-y)\right)2q_0 - 2\times \mathrm{K}_1\frac{(3\delta+2)a^2}{(\delta+2)\pi^2}\cosh\left(\frac{\pi}{\mathrm{a}}(\mathrm{b}-y)\right)2q_0\varsigma cos\theta + \frac{3}{4}B_0\varsigma_s^{-\frac{1}{2}}\left(\alpha_s{}^2cos\frac{1}{2}\theta_s + sin\frac{1}{2}\theta_s\right) + \frac{3}{4}D_0\varsigma_s^{-\frac{1}{2}}\left(\alpha_s{}^2sin\frac{1}{2}\theta_s - cos\frac{1}{2}\theta_s\right) + 2(\alpha_s{}^2B_1 - D_1) + 4C_1\alpha_l$$

$$\gamma_{xy} = \frac{3}{2}A_0\alpha_l\varsigma_l^{-\frac{1}{2}}sin\frac{1}{2}\theta_l + \frac{3}{2}C_0\alpha_l\varsigma_l^{-\frac{1}{2}}cos\frac{1}{2}\theta_l - 4\mathrm{K}_1\frac{(3\delta+2)a}{(\delta+2)\pi}\cosh\left(\frac{\pi}{\mathrm{a}}(\mathrm{b}-y)\right)q_0(1+\frac{a}{\pi}\varsigma cos\theta) + \frac{3}{4}B_0\varsigma_s^{-\frac{1}{2}}\left(\alpha_s{}^2cos\frac{1}{2}\theta_s + sin\frac{1}{2}\theta_s\right) + \frac{3}{4}D_0\varsigma_s^{-\frac{1}{2}}\left(\alpha_s{}^2sin\frac{1}{2}\theta_s - cos\frac{1}{2}\theta_s\right) + 2(\alpha_s{}^2B_1 - D_1) + 4C_1\alpha_l \qquad [3.110]$$

Now we derived the in plane strain fields as presented in equation[3.106], [3.107] and [3.110] and the next step is developing stress field equation exposed to thermo-mechanical load by utilizing equation [3.33] and substituting the in plane strain fields in place of ε_x, ε_y and γ_{xy}.

$$\sigma_x = (2\mu+\lambda)\left\{A_0\frac{3}{4}\varsigma_l^{-\frac{1}{2}}cos\frac{1}{2}\theta_l - C_0\frac{3}{4}\varsigma_l^{-\frac{1}{2}}sin\frac{1}{2}\theta_l - 2\mathrm{K}_1\frac{(3\delta+2)a}{(\delta+2)\pi}\cosh\left(\frac{\pi}{\mathrm{a}}(\mathrm{b}-y)\right)q_0 + B_0\frac{3}{4}\alpha_s\varsigma_s^{-\frac{1}{2}}sin\frac{1}{2}\theta_s + D_0\frac{3}{4}\alpha_s\varsigma_s^{-\frac{1}{2}}cos\frac{1}{2}\theta_s + 2A_1 + 2D_1\alpha_s\right\} + \lambda\left\{-A_0\frac{3}{4}\alpha_l{}^2\varsigma_l^{-\frac{1}{2}}sin\frac{1}{2}\theta_l - C_0\frac{3}{4}\alpha_l{}^2\varsigma_l^{-\frac{1}{2}}sin\frac{1}{2}\theta_l - 2\mathrm{K}_1\frac{(3\delta+2)a}{(\delta+2)\pi}\cosh\left(\frac{\pi}{\mathrm{a}}(\mathrm{b}-y)\right)q_0 + \mathrm{K}_1\frac{(3\delta+2)a^2}{(\delta+2)\pi^2}\sinh\left(\frac{\pi}{\mathrm{a}}(\mathrm{b}-y)\right)2q_0\varsigma sin\theta + B_0\frac{3}{4}\alpha_s\varsigma_s^{-\frac{1}{2}}cos\frac{1}{2}\theta_s - D_0\frac{3}{4}\alpha_s\varsigma_s^{-\frac{1}{2}}sin\frac{1}{2}\theta_s - 2A_1\alpha_l{}^2 - 2B_1\alpha_s\right\} - \alpha(2\mu+3\lambda)T$$

$$\sigma_y = (2\mu+\lambda)\left\{-A_0\frac{3}{4}\alpha_l{}^2\varsigma_l^{-\frac{1}{2}}sin\frac{1}{2}\theta_l - C_0\frac{3}{4}\alpha_l{}^2\varsigma_l^{-\frac{1}{2}}sin\frac{1}{2}\theta_l - 2\mathrm{K}_1\frac{(3\delta+2)a}{(\delta+2)\pi}\cosh\left(\frac{\pi}{\mathrm{a}}(\mathrm{b}-y)\right)q_0 + \mathrm{K}_1\frac{(3\delta+2)a^2}{(\delta+2)\pi^2}\sinh\left(\frac{\pi}{\mathrm{a}}(\mathrm{b}-y)\right)2q_0\varsigma sin\theta + B_0\frac{3}{4}\alpha_s\varsigma_s^{-\frac{1}{2}}cos\frac{1}{2}\theta_s - D_0\frac{3}{4}\alpha_s\varsigma_s^{-\frac{1}{2}}sin\frac{1}{2}\theta_s - 2A_1\alpha_l{}^2 - 2B_1\alpha_s\right\} + \lambda\left\{A_0\frac{3}{4}\varsigma_l^{-\frac{1}{2}}cos\frac{1}{2}\theta_l - C_0\frac{3}{4}\varsigma_l^{-\frac{1}{2}}sin\frac{1}{2}\theta_l - 2\mathrm{K}_1\frac{(3\delta+2)a}{(\delta+2)\pi}\cosh\left(\frac{\pi}{\mathrm{a}}(\mathrm{b}-y)\right)q_0 + B_0\frac{3}{4}\alpha_s\varsigma_s^{-\frac{1}{2}}sin\frac{1}{2}\theta_s + D_0\frac{3}{4}\alpha_s\varsigma_s^{-\frac{1}{2}}cos\frac{1}{2}\theta_s + 2A_1 + 2D_1\alpha_s\right\} - \alpha(2\mu+3\lambda)T$$

$$\tau_{xy} = \mu\left\{\frac{3}{2}A_0\alpha_l\zeta_l^{-\frac{1}{2}}sin\frac{1}{2}\theta_l + \frac{3}{2}C_0\alpha_l\zeta_l^{-\frac{1}{2}}cos\frac{1}{2}\theta_l - 4K_1\frac{(3\delta+2)a}{(\delta+2)\pi}\cosh\left(\frac{\pi}{a}(b-y)\right)q_0(1 + \frac{a}{\pi}\zeta cos\theta) + \frac{3}{4}B_0\zeta_s^{-\frac{1}{2}}\left(\alpha_s{}^2cos\frac{1}{2}\theta_s + sin\frac{1}{2}\theta_s\right) + \frac{3}{4}D_0\zeta_s^{-\frac{1}{2}}\left(\alpha_s{}^2sin\frac{1}{2}\theta_s - cos\frac{1}{2}\theta_s\right) + 2(\alpha_s{}^2B_1 - D_1) + 4C_1\alpha_l\right\}$$

$$\sigma_x = 2\mu\left\{\frac{3}{4}A_0\zeta_l^{-\frac{1}{2}}\cos\frac{1}{2}\theta_l - \frac{3}{4}C_0\zeta_l^{-\frac{1}{2}}\sin\frac{1}{2}\theta_l - 2K_1\frac{(3\delta+2)a}{(\delta+2)\pi}\cosh\left(\frac{\pi}{a}(b-y)\right)q_0 + \frac{3}{4}B_0\alpha_s\zeta_s^{-\frac{1}{2}}\sin\frac{1}{2}\theta_s + \frac{3}{4}D_0\alpha_s\zeta_s^{-\frac{1}{2}}\cos\frac{1}{2}\theta_s + 2A_1 + 2D_1\alpha_s\right\} + \lambda\left\{\frac{3}{4}A_0\zeta_l^{-\frac{1}{2}}\left(\cos\frac{1}{2}\theta_l - \alpha_l{}^2\sin\frac{1}{2}\theta_l\right) - \frac{3}{4}C_0\zeta_l^{-\frac{1}{2}}\sin\frac{1}{2}\theta_l(1+\alpha_l{}^2) + 2K_1\frac{(3\delta+2)a}{(\delta+2)\pi}q_0\left(2\cosh\left(\frac{\pi}{a}(b-y)\right) - \frac{\pi}{a}\sinh\left(\frac{\pi}{a}(b-y)\right)\zeta\sin\theta\right) + \frac{3}{4}B_0\alpha_s\zeta_s^{-\frac{1}{2}}\left(\cos\frac{1}{2}\theta_s + \sin\frac{1}{2}\theta_s\right) + \frac{3}{4}D_0\alpha_s\zeta_s^{-\frac{1}{2}}\left(\cos\frac{1}{2}\theta_s - \sin\frac{1}{2}\theta_s\right) + 2A_1(1-\alpha_l{}^2) + 2\alpha_s(D_1 - B_1)\right\} - \alpha(2\mu+3\lambda)T \quad [3.111]$$

$$\sigma_y = 2\mu\left\{-\frac{3}{4}A_0\alpha_l{}^2\zeta_l^{-\frac{1}{2}}\sin\frac{1}{2}\theta_l - \frac{3}{4}C_0\alpha_l{}^2\zeta_l^{-\frac{1}{2}}\sin\frac{1}{2}\theta_l - 2K_1\frac{(3\delta+2)a}{(\delta+2)\pi}q_0\left(\cosh\left(\frac{\pi}{a}(b-y)\right) + \frac{\pi}{a}\sinh\left(\frac{\pi}{a}(b-y)\right)\zeta\sin\theta\right) + \frac{3}{4}B_0\alpha_s\zeta_s^{-\frac{1}{2}}\cos\frac{1}{2}\theta_s - \frac{3}{4}D_0\alpha_s\zeta_s^{-\frac{1}{2}}\sin\frac{1}{2}\theta_s - 2A_1\alpha_l{}^2 - 2B_1\alpha_s\right\} + \lambda\left\{\frac{3}{4}A_0\zeta_l^{-\frac{1}{2}}\left(\cos\frac{1}{2}\theta_l - \alpha_l{}^2\sin\frac{1}{2}\theta_l\right) - \frac{3}{4}C_0\zeta_l^{-\frac{1}{2}}\sin\frac{1}{2}\theta_l(1+\alpha_l{}^2) + 2K_1\frac{(3\delta+2)a}{(\delta+2)\pi}q_0\left(2\cosh\left(\frac{\pi}{a}(b-y)\right) - \frac{\pi}{a}\sinh\left(\frac{\pi}{a}(b-y)\right)\zeta\sin\theta\right) + \frac{3}{4}B_0\alpha_s\zeta_s^{-\frac{1}{2}}\left(\cos\frac{1}{2}\theta_s + \sin\frac{1}{2}\theta_s\right) + \frac{3}{4}D_0\alpha_s\zeta_s^{-\frac{1}{2}}\left(\cos\frac{1}{2}\theta_s - \sin\frac{1}{2}\theta_s\right) + 2A_1(1-\alpha_l{}^2) + 2\alpha_s(D_1 - B_1)\right\} - \alpha(2\mu+3\lambda)T \quad [3.112]$$

$$\tau_{xy} = \mu\left\{\frac{3}{2}A_0\alpha_l\zeta_l^{-\frac{1}{2}}\sin\frac{1}{2}\theta_l + \frac{3}{2}C_0\alpha_l\zeta_l^{-\frac{1}{2}}\cos\frac{1}{2}\theta_l - 4K_1\frac{(3\delta+2)a}{(\delta+2)\pi}\cosh\left(\frac{\pi}{a}(b - y)\right)q_0(1 + \frac{a}{\pi}\zeta\cos\theta) + \frac{3}{4}B_0\zeta_s^{-\frac{1}{2}}\left(\alpha_s{}^2\cos\frac{1}{2}\theta_s + \sin\frac{1}{2}\theta_s\right) + \frac{3}{4}D_0\zeta_s^{-\frac{1}{2}}\left(\alpha_s{}^2\sin\frac{1}{2}\theta_s - \cos\frac{1}{2}\theta_s\right) + 2(\alpha_s{}^2B_1 - D_1) + 4C_1\alpha_l\right\} \quad [3.113]$$

Equation [3.111], [3.112] and equation [3.113] are in plane stress or the thermo-mechanical stress fields that is exposed to the thermo-mechanical loading condition and namely these are thermo-mechanical normal stress in x direction, thermo-mechanical normal stress in y direction and thermo-mechanical shear stress in xy plane respectively.

Up on further simplification of the above thermo-mechanical stress field equation by letting the notation of sigma

$$\delta = \frac{\lambda}{\mu} \quad [3.114]$$

Then substitute equation [3.114] in place of λ and some rearrangment we can get the following equations of thermo-mechanical stress fields.

$$\frac{\sigma_x}{\mu} = \left(\frac{3}{4}(2+\delta)\zeta_l^{-\frac{1}{2}}\cos\frac{1}{2}\theta_l - \frac{3}{4}\delta\alpha_l{}^2\zeta_l^{-\frac{1}{2}}\sin\frac{1}{2}\theta_l\right)A_0 - C_0\left(\frac{3}{4}(2+\delta(1+\alpha_l{}^2))\right)\zeta_l^{-\frac{1}{2}}\sin\frac{1}{2}\theta_l + \left(\frac{3}{4}(2+\delta)\alpha_s\zeta_s^{-\frac{1}{2}}\sin\frac{1}{2}\theta_s + \frac{3}{4}\delta\alpha_s\zeta_s^{-\frac{1}{2}}\cos\frac{1}{2}\theta_s\right)B_0 + \left(\frac{3}{4}(2+\delta)\alpha_s\zeta_s^{-\frac{1}{2}}\cos\frac{1}{2}\theta_s - \frac{3}{4}\delta\alpha_s\zeta_s^{-\frac{1}{2}}\sin\frac{1}{2}\theta_s\right)D_0 + \left(4+2\delta(1-\alpha_l{}^2)\right)A_1 + 4D_1\alpha_s + 2\delta\alpha_s(D_1 - B_1) + 4K_1\frac{(3\delta+2)a}{(\delta+2)\pi}q_0\left[\cosh\left(\frac{\pi}{a}(b-y)\right)(1-\frac{\delta\pi}{a}) - \frac{\pi}{a}\sinh\left(\frac{\pi}{a}(b-y)\right)\right]\zeta\sin\theta - (2+3\delta)\alpha T \quad [3.115]$$

$$\frac{\sigma_y}{\mu} = \frac{3}{4}\left[\left(\delta\varsigma_l^{-\frac{1}{2}}\cos\frac{1}{2}\theta_l - (2\alpha_l{}^2 + \delta\alpha_l{}^2)\varsigma_l^{-\frac{1}{2}}\sin\frac{1}{2}\theta_l\right)A_0 - \left((2\alpha_l{}^2 + \delta(1 + \alpha_l{}^2))\varsigma_l^{-\frac{1}{2}}\sin\frac{1}{2}\theta_l\right)C_0 + \left((2\alpha_s + \delta\alpha_s)\varsigma_s^{-\frac{1}{2}}\cos\frac{1}{2}\theta_s + \delta\alpha_s\varsigma_s^{-\frac{1}{2}}\sin\frac{1}{2}\theta_s\right)B_0 - \left((2\alpha_s + \delta\alpha_s)\varsigma_s^{-\frac{1}{2}}\sin\frac{1}{2}\theta_s + \delta\alpha_s\varsigma_s^{-\frac{1}{2}}\cos\frac{1}{2}\theta_s\right)D_0\right] + (2\delta(1 - \alpha_l{}^2) - 4\alpha_l{}^2)A_1 - 4B_1\alpha_s + 2\delta\alpha_s(D_1 - B_1) + 4K_1\frac{(3\delta+2)a}{(\delta+2)\pi}q_0\left[\cosh\left(\frac{\pi}{a}(b-y)\right)(1 - \frac{\delta\pi}{a}) - \frac{\pi}{a}\sinh\left(\frac{\pi}{a}(b-y)\right)\right]\varsigma\sin\theta - (2 + 3\delta)\alpha T \quad [3.116]$$

$$\frac{\tau_{xy}}{\mu} = \frac{3}{2}A_0\alpha_l\varsigma_l^{-\frac{1}{2}}\sin\frac{1}{2}\theta_l + \frac{3}{4}B_0\varsigma_s^{-\frac{1}{2}}\left(\alpha_s{}^2\cos\frac{1}{2}\theta_s + \sin\frac{1}{2}\theta_s\right) + \frac{3}{2}C_0\alpha_l\varsigma_l^{-\frac{1}{2}}\cos\frac{1}{2}\theta_l + \frac{3}{4}D_0\varsigma_s^{-\frac{1}{2}}\left(\alpha_s{}^2\sin\frac{1}{2}\theta_s - \cos\frac{1}{2}\theta_s\right) + 2(\alpha_s{}^2B_1 - D_1) + 4C_1\alpha_l - 4K_1\frac{(3\delta+2)a}{(\delta+2)\pi}\cosh\left(\frac{\pi}{a}(b-y)\right)q_0\left(1 + \frac{a}{\pi}\varsigma\cos\theta\right) \quad [3.117]$$

Constants

At this stage lets calculate the values of the constants K_1, A_0, A_1, B_0, B_1 C_0 C_1 D_0 and D_1 by recalling the dynamic stress intensity factor relation K_{ID} which is the dynamic stress intensity factor for opening and K_{IID} the dynamic stress intensity factor for shear mode and the relation with these stress intensity factors with corresponding inplane stress are presented in (Chalivendra, 2007) as;

$$K_{ID} = \lim_{\substack{x\to 0\\ y=0}} \sqrt{2\pi}\,\sigma_y \qquad [3.118]$$

$$K_{IID} = \lim_{\substack{x\to 0\\ y=0}} \sqrt{2\pi}\,\tau_{xy} \qquad [3.119]$$

$$K_{ID} = \mu \lim_{\substack{x\to 0\\ y=0}} \sqrt{2\pi}\left\{\frac{3}{4}\left[\left(\delta\varsigma_l^{-\frac{1}{2}}\cos\frac{1}{2}\theta_l - (2\alpha_l{}^2 + \delta\alpha_l{}^2)\varsigma_l^{-\frac{1}{2}}\sin\frac{1}{2}\theta_l\right)A_0 - \left(\left(2\alpha_l{}^2 + \delta(1+\alpha_l{}^2)\right)\varsigma_l^{-\frac{1}{2}}\sin\frac{1}{2}\theta_l\right)C_0 + \left((2\alpha_s + \delta\alpha_s)\varsigma_s^{-\frac{1}{2}}\cos\frac{1}{2}\theta_s + \delta\alpha_s\varsigma_s^{-\frac{1}{2}}\sin\frac{1}{2}\theta_s\right)B_0 - \left((2\alpha_s + \delta\alpha_s)\varsigma_s^{-\frac{1}{2}}\sin\frac{1}{2}\theta_s + \delta\alpha_s\varsigma_s^{-\frac{1}{2}}\cos\frac{1}{2}\theta_s\right)D_0\right] + (2\delta(1-\alpha_l{}^2) - 4\alpha_l{}^2)A_1 - 4B_1\alpha_s + 2\delta\alpha_s(D_1 - B_1) + 4K_1\frac{(3\delta+2)a}{(\delta+2)\pi}q_0\left[\cosh\left(\frac{\pi}{a}(b-y)\right)\left(1-\frac{\delta\pi}{a}\right) - \frac{\pi}{a}\sinh\left(\frac{\pi}{a}(b-y)\right)\right]\varsigma\sin\theta - (2+3\delta)\alpha T\right\}$$

$$K_{IID} = \lim_{\substack{x\to 0\\ y=0}} \sqrt{2\pi}\left\{\frac{3}{2}A_0\alpha_l\varsigma_l^{-\frac{1}{2}}\sin\frac{1}{2}\theta_l + \frac{3}{4}B_0\varsigma_s^{-\frac{1}{2}}\left(\alpha_s{}^2\cos\frac{1}{2}\theta_s + \sin\frac{1}{2}\theta_s\right) + \frac{3}{2}C_0\alpha_l\varsigma_l^{-\frac{1}{2}}\cos\frac{1}{2}\theta_l + \frac{3}{4}D_0\varsigma_s^{-\frac{1}{2}}\left(\alpha_s{}^2\sin\frac{1}{2}\theta_s - \cos\frac{1}{2}\theta_s\right) + 2(\alpha_s{}^2B_1 - D_1) + 4C_1\alpha_l - 4K_1\frac{(3\delta+2)a}{(\delta+2)\pi}\cosh\left(\frac{\pi}{a}(b-y)\right)q_0\left(1+\frac{a}{\pi}\varsigma\cos\theta\right)\right\}$$

Thus at $y = 0$, $x \to 0$ then $r = 0$

Then by analyzing the limit of the boundary condition give we can get, the relations between A_0, $K_{ID}$and C_0, K_{IID} are obtained respectively.

$$A_0(t) = \frac{(1+\alpha_s{}^2)(1-\alpha_1{}^2)}{4\alpha_l\alpha_s - (1+\alpha_s{}^2)^2}\frac{K_{ID}(t)}{\mu\sqrt{2\pi}} \qquad [3.120]$$

$$C_0(t) = \frac{2\alpha_s(1-\alpha_l{}^2)}{4\alpha_l\alpha_s - (1+\alpha_s{}^2)^2}\frac{K_{IID}(t)}{\mu\sqrt{2\pi}} \quad [3.121]$$

Now let's consider the boundary conditon of $y = 0, \theta = \pi, \tau_{xy} = 0$ and $\sigma_y = 0$ to get the relation between A_0 and B_0 as well as C_0 and D_0

Inplies that $0 = \frac{3}{2}\alpha_l A_0 + \frac{3}{4}(1+\alpha_s{}^2)B_0$ and $0 = \frac{3}{2}\alpha_l D_0 - \frac{3}{4}(1+\alpha_s{}^2)C_0$

$$B_0(t) = \frac{-2\alpha_l}{1+\alpha_s{}^2}A_0(t) \quad [3.122]$$

$$D_0(t) = \frac{1+\alpha_s{}^2}{2\alpha_s}C_0(t) \quad [3.123]$$

Now for the rest of the constants lets proceed by separation of like terms and apply, $\tau_{xy} = 0$ $\sigma_x = 0$ and $\sigma_y = 0$ we get,

$0 = 2\delta\alpha_s(D_1 - B_1)$

$0 = 4 + 2\delta(1-\alpha_l{}^2)A_1 + 4D_1\alpha_s + 2\delta\alpha_s(D_1 - B_1)$

$0 = (2\delta(1-\alpha_l{}^2) - 4\alpha_l{}^2)A_1 - 4B_1\alpha_s + 2\delta\alpha_s(D_1 - B_1)$

Then $D_1 = B_1$

$$A_1 = \frac{1}{4\delta(2\alpha_l{}^2 - 1)} \quad [3.124]$$

$$B_1 = \frac{2\delta(1-\alpha_l{}^2) - 4\alpha_l{}^2}{4\alpha_s\delta(2\alpha_l{}^2 - 1)} \quad [3.125]$$

The relationship beteween the instantanious stress intensity factor and dynamic stress intensity factor is given by the expresssion $K_{ID} = R_{(C)}K_I$ and $K_{IID} = R_{(C)}K_{II}$ where K_I and K_{II} are the instantanius stress intensity factors as well K_{ID} and K_{IID} are the material resisitance or the stress intensity factor associated with the crack propagation speed. $R_{(C)}$ universal function of crack speed and its value is 1 when c=o the crack speed is zero, and matimaticall expressed as (T.L. Anderson, 2005);

$$R_{(C)} = \left(1 - \frac{C}{C_r}\right)\sqrt{(1 - hc)} \quad [3.126]$$

$$h = \frac{2}{C_L}\left(\frac{C_s}{C_r}\right)^2 \left[1 - \left(\frac{C_s}{C_L}\right)\right]^2 \quad [3.127]$$

$$C_o = \sqrt{\frac{E}{\rho}} \quad [3.128]$$

$\mathrm{C} = \mathrm{C_r}\left(1 - \frac{\mathrm{a_o}}{\mathrm{a}}\right)$ and the $\mathrm{C_r}$ is raleight (surface) wave speed for v=0.3 poission's ratio, the ratio of $\mathrm{C_r}$to $\mathrm{C_o}$ is 0.57 (T.L. Anderson, 2005). The stress at the singularity zon is given by

$$\sigma_{ij} = \frac{K_{ID}}{\sqrt{2\pi r}} f_{ij}(\theta, c) \quad [3.129]$$

$$\sigma_{ij} = \frac{K_{IID}}{\sqrt{2\pi r}} f_{ij}(\theta, c) \quad [3.130]$$

Chapter Four

4. Results and discussion

By utilizing the methods of asymptotic approach, perturbation theory with the ordinary differential and partial differential equation, the intended thermo-mechanical stress fields were developed as σ_{xx}, σ_{yy} and τ_{xy} and these are the superimposition of mechanical and thermal stress fields. For the stress field x direction the mechanical stress field is; $\frac{\sigma_x}{\mu} = \left(\frac{3}{4}(2+\delta)\varsigma_l^{-\frac{1}{2}}\cos\frac{1}{2}\theta_l - \frac{3}{4}\delta{\alpha_l}^2\varsigma_l^{-\frac{1}{2}}\sin\frac{1}{2}\theta_l\right)A_0 - C_0\left(\frac{3}{4}(2+\delta(1+{\alpha_l}^2))\right)\varsigma_l^{-\frac{1}{2}}\sin\frac{1}{2}\theta_l + \left(\frac{3}{4}(2+\delta)\alpha_s\varsigma_s^{-\frac{1}{2}}\sin\frac{1}{2}\theta_s + \frac{3}{4}\delta\alpha_s\varsigma_s^{-\frac{1}{2}}\cos\frac{1}{2}\theta_s\right)B_0 + \left(\frac{3}{4}(2+\delta)\alpha_s\varsigma_s^{-\frac{1}{2}}\cos\frac{1}{2}\theta_s - \frac{3}{4}\delta\alpha_s\varsigma_s^{-\frac{1}{2}}\sin\frac{1}{2}\theta_s\right)D_0 + \left(4+2\delta(1-{\alpha_l}^2)\right)A_1 + 4D_1\alpha_s + 2\delta\alpha_s(D_1 - B_1)$ and the thermal stress repented by $4K_1\frac{(3\delta+2)a}{(\delta+2)\pi}q_0\left[\cosh\left(\frac{\pi}{a}(b-y)\right)(1-\frac{\delta\pi}{a}) - \frac{\pi}{a}\sinh\left(\frac{\pi}{a}(b-y)\right)\right]\varsigma\sin\theta - (2+3\delta)\alpha T.$

Likely for the thermo-mechanical stress field in the y direction σ_{yy} the mechanical stress field is $\frac{\sigma_y}{\mu} = \frac{3}{4}\left[\left(\delta\varsigma_l^{-\frac{1}{2}}\cos\frac{1}{2}\theta_l - (2{\alpha_l}^2+\delta{\alpha_l}^2)\varsigma_l^{-\frac{1}{2}}\sin\frac{1}{2}\theta_l\right)A_0 - \left(\left(2{\alpha_l}^2+\delta(1+{\alpha_l}^2)\right)\varsigma_l^{-\frac{1}{2}}\sin\frac{1}{2}\theta_l\right)C_0 + \left((2\alpha_s+\delta\alpha_s)\varsigma_s^{-\frac{1}{2}}\cos\frac{1}{2}\theta_s + \delta\alpha_s\varsigma_s^{-\frac{1}{2}}\sin\frac{1}{2}\theta_s\right)B_0 - \left((2\alpha_s+\delta\alpha_s)\varsigma_s^{-\frac{1}{2}}\sin\frac{1}{2}\theta_s + \delta\alpha_s\varsigma_s^{-\frac{1}{2}}\cos\frac{1}{2}\theta_s\right)D_0\right] + (2\delta(1-{\alpha_l}^2) - 4{\alpha_l}^2)A_1 - 4B_1\alpha_s + 2\delta\alpha_s(D_1 - B_1)$ as well the thermal stress field is $4K_1\frac{(3\delta+2)a}{(\delta+2)\pi}q_0\left[\cosh\left(\frac{\pi}{a}(b-y)\right)(1-\frac{\delta\pi}{a}) - \frac{\pi}{a}\sinh\left(\frac{\pi}{a}(b-y)\right)\right]\varsigma\sin\theta - (2+3\delta)\alpha T.$

For the in-plane shear stress τ_{xy} the mechanical stress field represented by the formula of $\frac{\tau_{xy}}{\mu} = \frac{3}{2}A_0\alpha_l\varsigma_l^{-\frac{1}{2}}\sin\frac{1}{2}\theta_l + \frac{3}{4}B_0\varsigma_s^{-\frac{1}{2}}\left({\alpha_s}^2\cos\frac{1}{2}\theta_s + \sin\frac{1}{2}\theta_s\right) + \frac{3}{2}C_0\alpha_l\varsigma_l^{-\frac{1}{2}}\cos\frac{1}{2}\theta_l + \frac{3}{4}D_0\varsigma_s^{-\frac{1}{2}}\left({\alpha_s}^2\sin\frac{1}{2}\theta_s - \cos\frac{1}{2}\theta_s\right) + 2({\alpha_s}^2B_1 - D_1) + 4C_1\alpha_l$ and the thermal stress depicted by the formula $4K_1\frac{(3\delta+2)a}{(\delta+2)\pi}\cosh\left(\frac{\pi}{a}(b-y)\right)q_0\left(1+\frac{a}{\pi}\varsigma\cos\theta\right).$

The variation of the stress components near the crack tip is depicted in figure 12, 13 and 14 below and this graph plotted for the visualization of the effect of the temperature on the propagation of the crack that is the thermo-mechanical stress field effects. The coefficient of thermal expansion (α) of titanium (which is of primary interest in our experimental research of (Kidane, Chalivendra and Shukla, 2010)) 8.9 × 10−6/◦C is used with the values of Poisson's ratio v=0.21,modulus of elasticity, E=110GPa, the density $\rho = 4420\,{}^{kg}/_{m^3}$ and r=0.002meter.

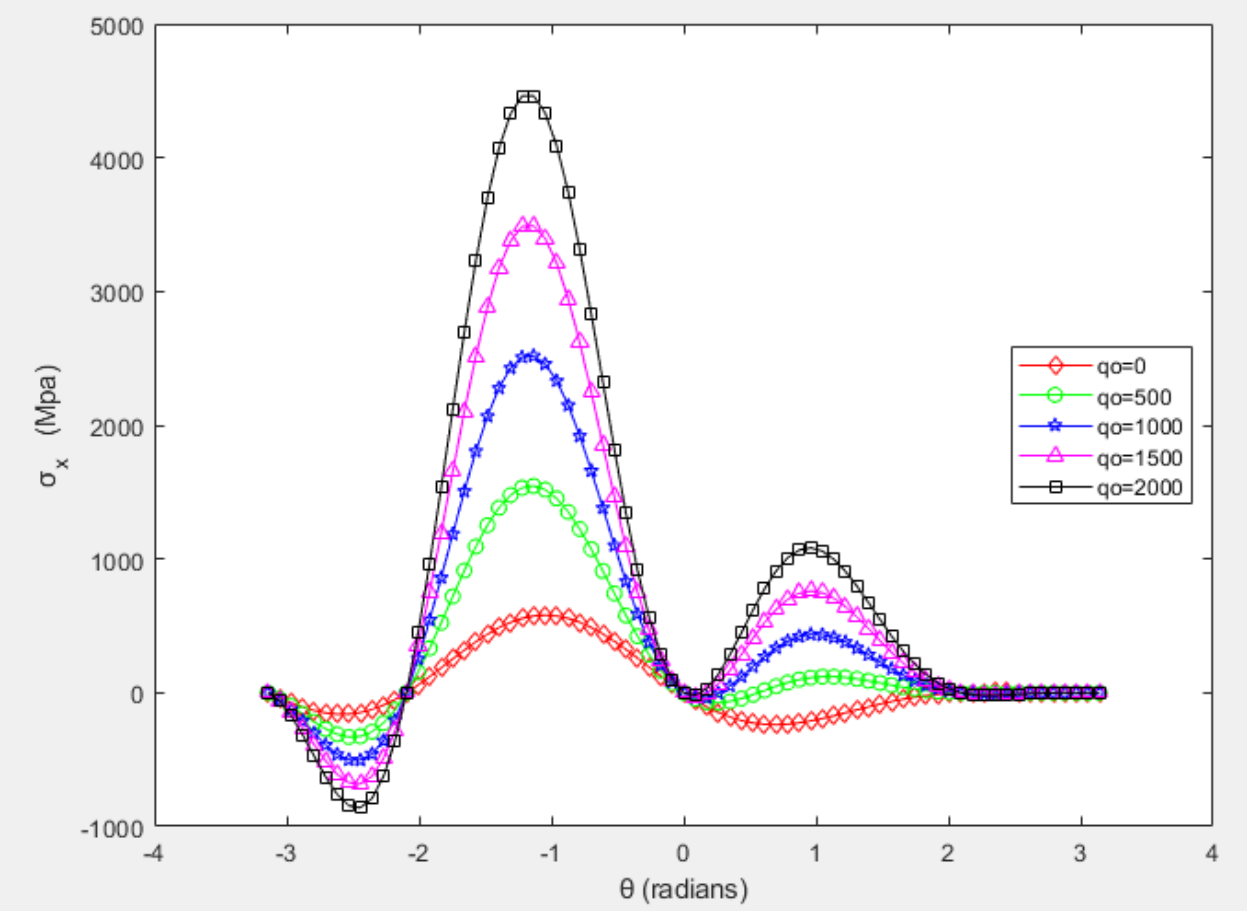

Figure 12:- the in-plane stress in x direction up on the variation of temperature

Most of the input data are taken from literature (Kidane *et al.*, 2010) and (Kidane, Chalivendra and Shukla, 2010) and the $K_{ID} = 11MPa - m^{1/2}$ and $K_{IID} = 0.2K_{ID}$ as well as $K_{eff} = \sqrt{{K_{ID}}^2 + {K_{IID}}^2}$. The temperature is 22℃ for the heat flow value of $q_o = 0$ which is isothermal stress filed which is kept at room temperature and at this for the constant speed c the propagation of crack become at a constant rate and from the graph it shows that the ratio of σ_{xx} to $\frac{K_{ID}}{\sqrt{2\pi r}}$ counted as 0.05 and

there is no variation in the weighting function or the geometrical function since it is isothermal. Up on the developed thermo-mechanical stress field the effect of the temperature by varying the value of heat flux q_o the effect of temperature specified. As well to observe the stress distribution at the crack at the crack tip, the thin plate with the dimension of 16cm square with the initial crack length of 2mm introduced at the left center edge horizontally developed as depicted in figure below and the distribution of the stress detected.

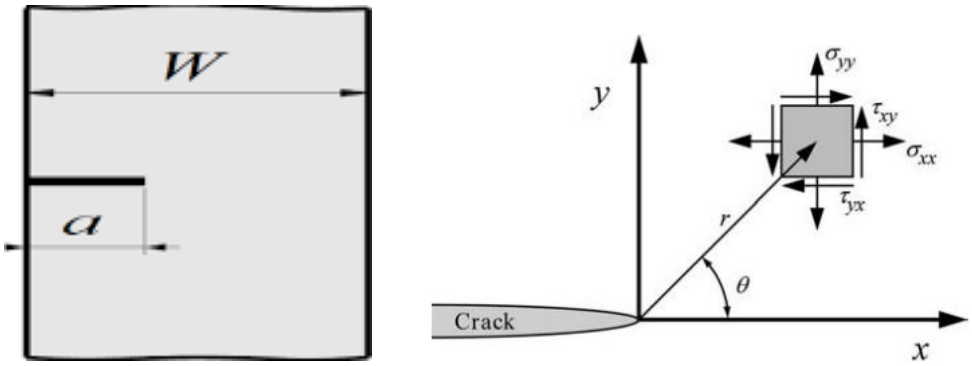

Figure 13:- Definition of the coordinate axis ahead of a crack tip

(Kidane, Chalivendra and Shukla, 2010) stated that the superimposition of the stress caused by the temperature with the mechanical stress field results imposing normal stress on the traction free crack faces and also these stresses are produced by thermal stresses that are exposed to temperature. As the normal stresses on the crack face violates on of the boundary conditions and therefore the stress need to be removed and accomplished by superimposing an equal and opposite stress fields on the crack face, particularly each point on the crack face.

Then when we come to the graph of stress, we analyzed the stress around the tip for r=0.002m, at $\theta = 0°$, the value of $\sigma_{xx} = 0$, this is due to the removal of the stress by the application of the opposite stress, as θ increased to $\pi/2$ the stress in x direction increases gradually to the maximum value. And when the value of θ increased beyond $\pi/2$ to π or when we analyzed the stress at the open space (the gap created by the crack) the stress decreases and the isothermal stress becomes approximately similar or approaches to the thermo-mechanical stress field in the x direction. This will happen due to the presence of the gap in the plate created by the crack, and the temperature will not transmit or flow, rather than convection, but convection is not considered in this research. Therefore, for the anti-clockwise directional variation of θ the stress σ_{xx} increase for θ is in between 0 and $\pi/2$ and decrease for the θ value of $\pi/2$ and π.

For the clockwise directional observation as the value of θ varies from 0 to $-\pi/2$ the value of stress σ_{xx} increases from 0 to the maximum value as well the scale also larger than the anticlockwise direction, and as the value of θ varies from $-\pi/2$ to $-\pi$ the stress σ_{xx} decreases and it becomes below the iso thermal for θ value of -2 to -3.14 radians.

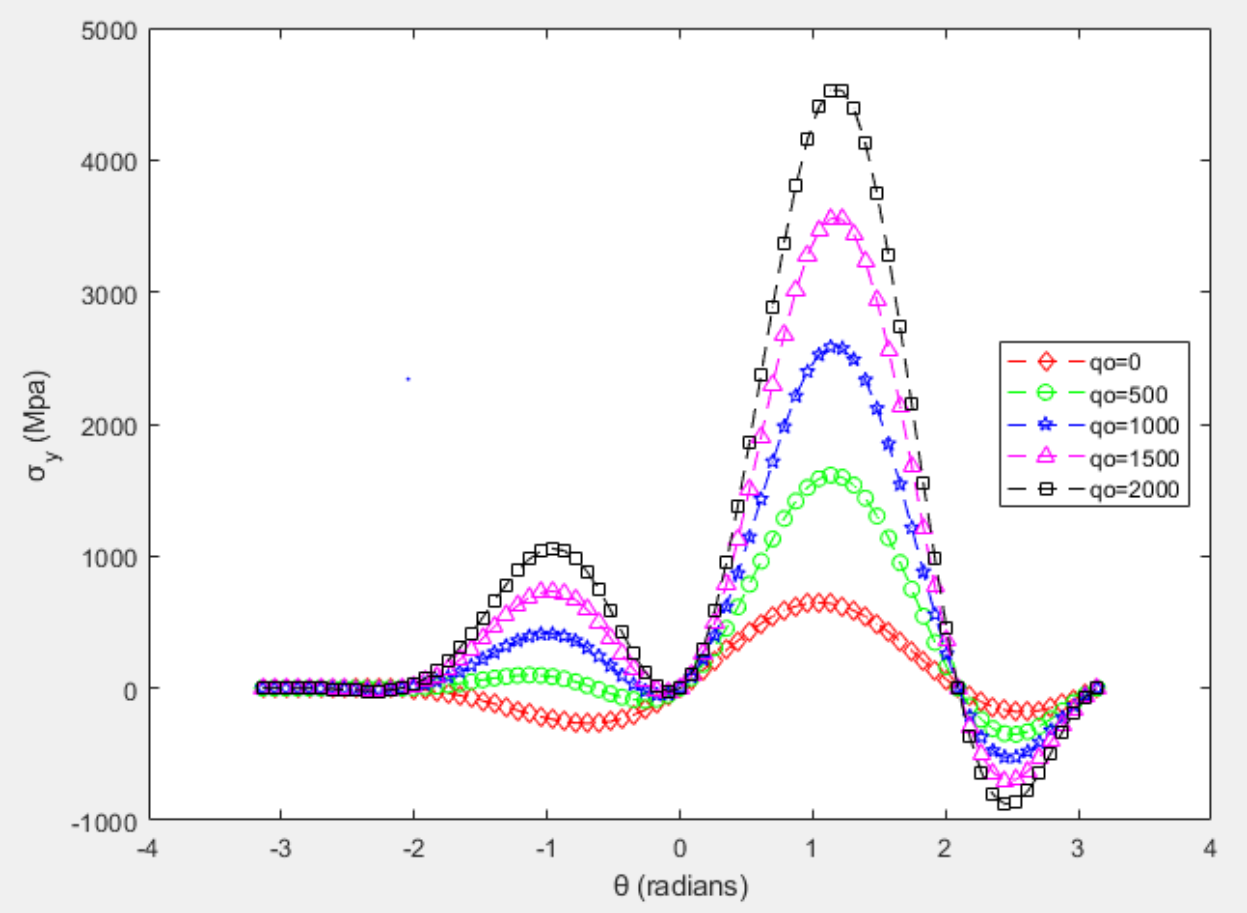

Figure 14:- the in-plane stress in y direction up on the variation of temperature

Also in Figure 14 for the isothermal for $q_o = 0$ means no temperature field around the crack tip and at the load is pure mechanical and the graph shows that the crack propagation at a constant speed and mechanical load is also constant. Moreover, for the shear stress depicted in figure 14 the effect of isothermal stress at $q_o = 0$ gives the same result as like as the stress in x direction and y direction. The observation for the distribution of the thermo-mechanical stress field in the y direction is also similar to thermo-mechanical stress field in x direction except the direction. The directional differences resulted from the application of σ_{xx} applied horizontally and σ_{yy} vertically. Then as the value of $\theta = 0°$, the value of σ_{yy} approaches to zero and exactly zero, but the value

of θ increases to $\pi/2$ the stress in y direction increases gradually to the maximum value. As the value of θ increases beyond $\pi/2$ to π or distribution of thermo-mechanical stress σ_{yy} near the open space (the gap created by the crack) decreases and it becomes below the isothermal for the θ in between -2 and -3.14 rad.

Then from this observation for the anticlockwise direction stress σ_{yy} increases for θ is in between 0 and $\pi/2$ as well as decreases for θ value of $\pi/2$ to π. For the clockwise analysis as the value of θ varies from 0 to $-\pi/2$ the value of thermo-mechanical stress, σ_{yy} decreases, as well as the thermo-mechanical stress σ_{yy} and isothermal stress approaches each other and becomes similar. This is happened at the open space, since there is no thermal conduction appear.

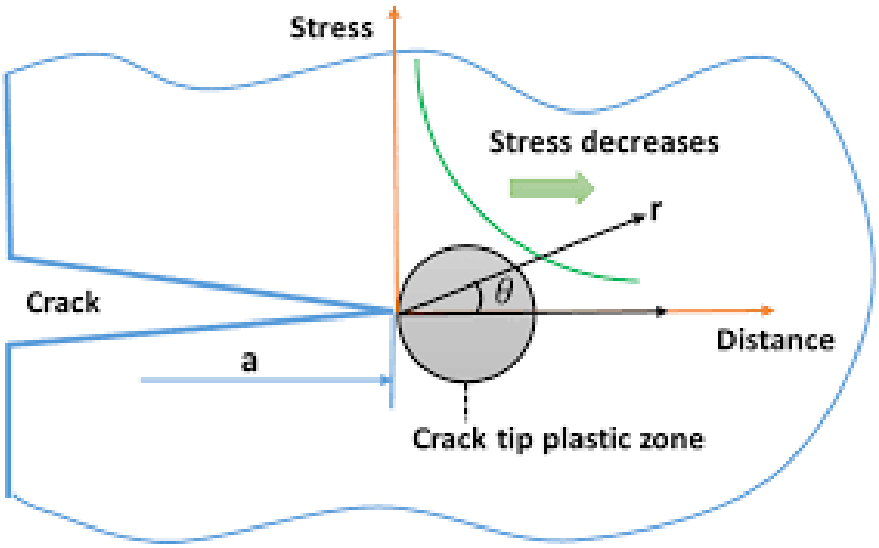

Figure 15:- Crack tip plastic zone model

As depicted in (Nestor Perez, 2004) from the IRWIN'S approximation of plastic zone at the crack tip, the effect of plastic zone at the effect of plastic zone, is artificially extended to r that is plastic zone correction. From the figure 15 the stress σ_{xx} and σ_{yy} become zero for $\theta = 0$ and this depends on the value of r. as $r \to 0$ the thermo-mechanical σ_{xx} and $\sigma_{yy} \to \infty$ which occurs mathematically, not physically. As $r \to \infty$ the value of thermo-mechanical stress σ_{xx} and $\sigma_{yy} \to 0$ and in our case r=0.002m makes σ_{xx} and σ_{yy} become zero at $\theta = 0$.

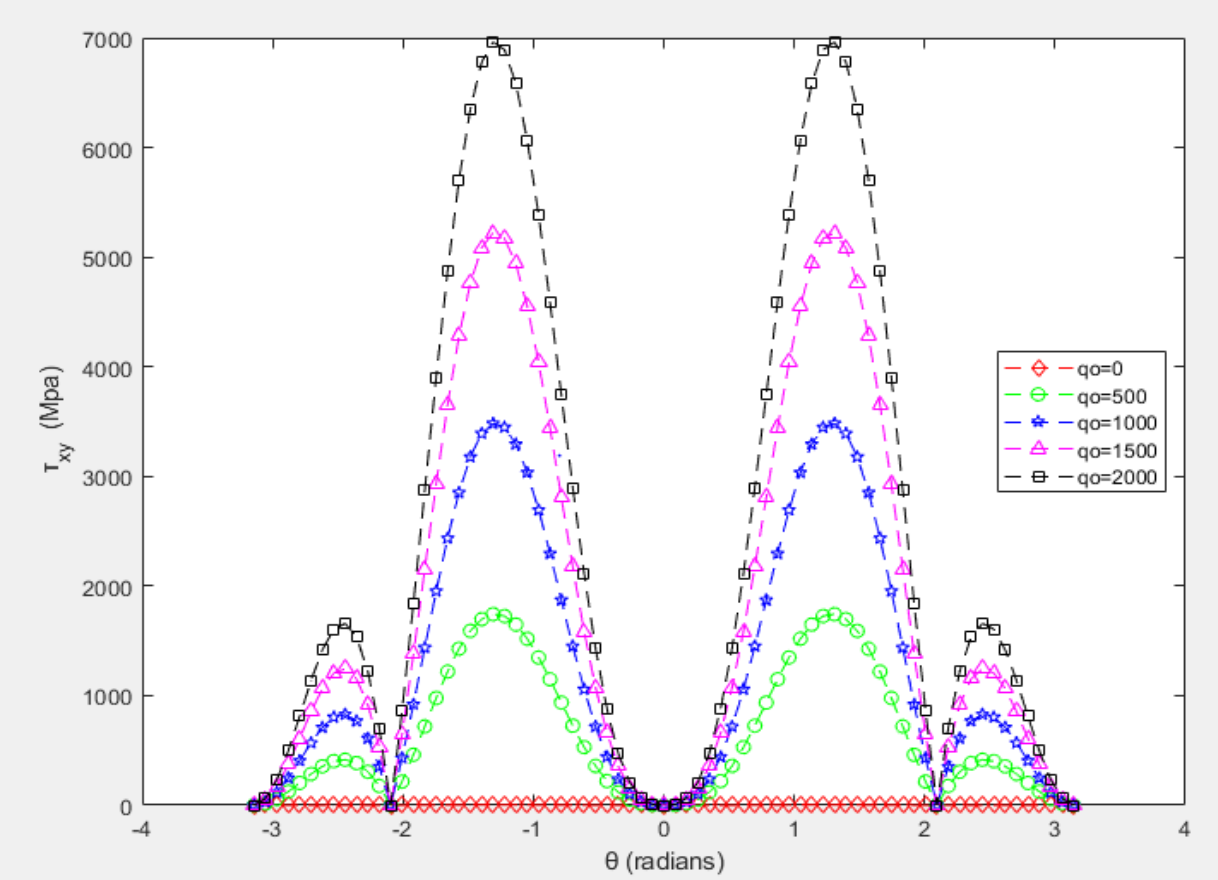

Figure 16:- the shear stress in xy direction up on the variation of temperature

For the shear stress τ_{xy} is also zero at $\theta = 0$ and maximum when the value of θ increase to $\pm\pi/2$ then decreases to zero when θ approaches to $\pm\pi$. This happened when r approaches to the open space the value of τ_{xy} decreases and becomes zero at $\theta = \pm\pi$. And also, from crack tip plasticity as the value of $r \to \infty$ the stress $\tau_{xy} \to 0$, therefore, at $\theta = 0$ and r=0.002m will make the shear stress zero.

For the temprature increase beyond $22℃$ as well as the value of q_o varies beyond zero and it means there is the temprature field at the crack tip generated from the expossure of the material to temprature at the edge of the material not at the crack tip, and the stress applied is thermo-mechanical and it affects the value of the stress components, σ_{xx} σ_{yy} and τ_{xy}. The effect of the temperature on the in plane stress components will also affect the stress intensity factor or the material resisitance since there relation is expressed by $\sigma_{ij} = \frac{K_{ID}}{\sqrt{2\pi r}} f_{ij}(\theta, c)$ and $\sigma_{ij} = \frac{K_{IID}}{\sqrt{2\pi r}} f_{ij}(\theta, c)$. And from the expression the stress intensity factors and the stress components have

direct relationship. And the effect of the temepratue field on the stress intensity factor have similar result and lets plot the for the K_{ID} by rearranging $\sigma_{ij} = \frac{K_{ID}}{\sqrt{2\pi r}} f_{ij}(\theta, c)$ by taking $f_{ij}(\theta, c)$ from the mechanical loading condition from (T.L. Anderson, 2005) of appendix 4: dynamic fracture analysis such that ;

$$f_{xx}(\theta, c) = \frac{1+\alpha_s{}^2}{4\alpha_S\alpha_l - (1+\alpha_s{}^2)^2}\left[(1 + 2\alpha_l{}^2 - \alpha_s{}^2)cos\left(\frac{\theta_l}{2}\right)\sqrt{\frac{r}{\varsigma_l}} - \frac{4\alpha_l\alpha_s}{1+\alpha_s{}^2}cos\left(\frac{\theta_s}{2}\right)\sqrt{\frac{r}{\varsigma_s}}\right] \quad [4.1]$$

$$f_{yy}(\theta, c) = \frac{1+\alpha_s{}^2}{4\alpha_s\alpha_l - (1+\alpha_s{}^2)^2}\left[-(1 + \alpha_s{}^2)cos\left(\frac{\theta_l}{2}\right)\sqrt{\frac{r}{\varsigma_l}} + \frac{4\alpha_l\alpha_s}{1+\alpha_s{}^2}cos\left(\frac{\theta_s}{2}\right)\sqrt{\frac{r}{\varsigma_s}}\right] \quad [4.2]$$

$$f_{xy}(\theta, c) = \frac{2\alpha_l(1+\alpha_s{}^2)}{4\alpha_s\alpha_l - (1+\alpha_s{}^2)^2}\left[sin\left(\frac{\theta_l}{2}\right)\sqrt{\frac{r}{\varsigma_l}} - sin\left(\frac{\theta_s}{2}\right)\sqrt{\frac{r}{\varsigma_s}}\right] \quad [4.3]$$

Know we can calulate the value of the K_{ID} such that $K_{ID} = \sigma_{ij}\sqrt{2\pi r}/f_{ij}(\theta, c)$ where σ_{ij} is the thermo-mechanical stress fields that are getterd from the analysis.

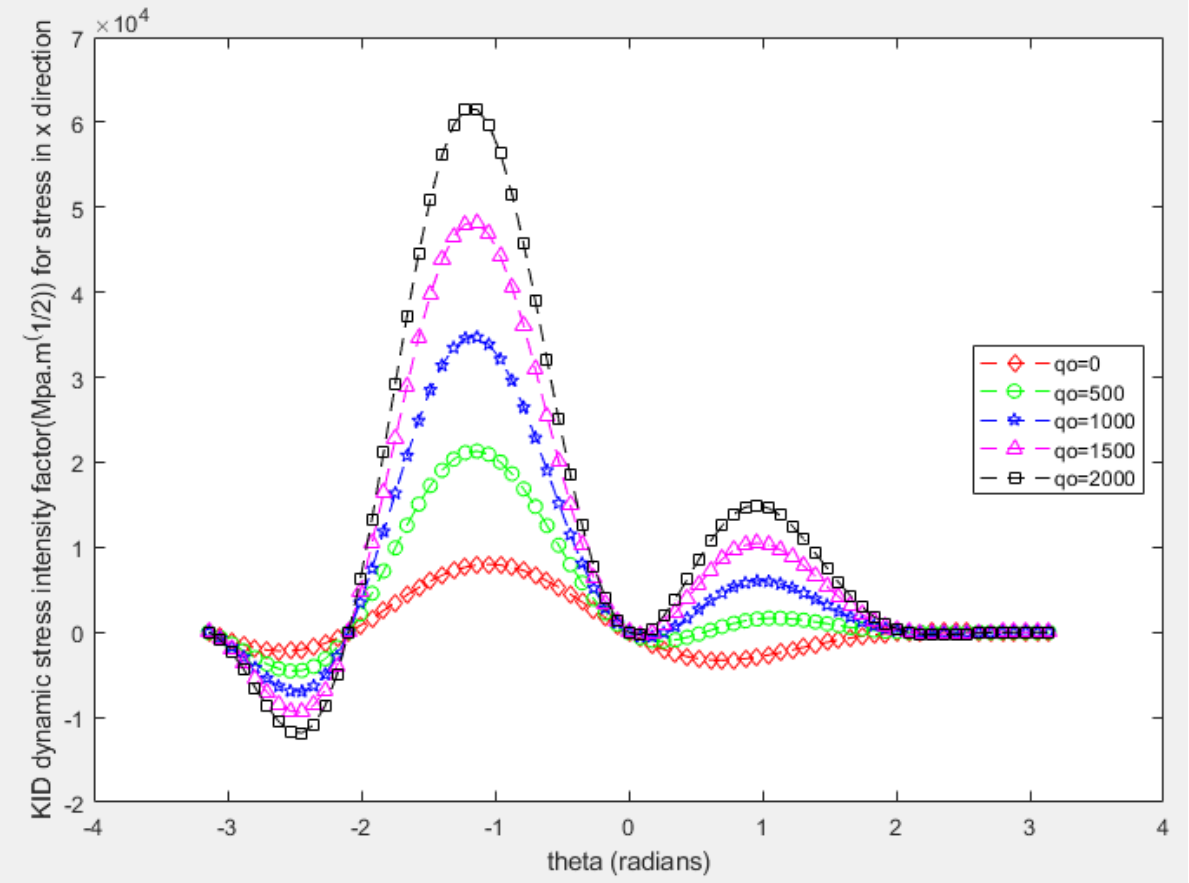

Figure 17:- The dynamic stress intensity factor that is calculated from the thermo-mechanical stress field in x direction

It is seen that the dynamic stress intensity factor K_{ID} calculated from the thermo-mechanical stress field in the x direction or σ_{xx} and $f_{xx}(\theta, c)$ plotted in figure 17 by varying the value of q_o from 0 to 2000. In addition, as it depicted in the graph at the value of $q_o = 0$ it is isothermal and it have a constant value to resist the cracking force at a constant speed of the crack c. As the value of the q_o increase beyond the value 0, the material will overstress to propagate the crack and the material will need high resistance to overcome the crack propagation, therefore the dynamic stress intensity factor will increase. This effect is similar to the stress in x direction.

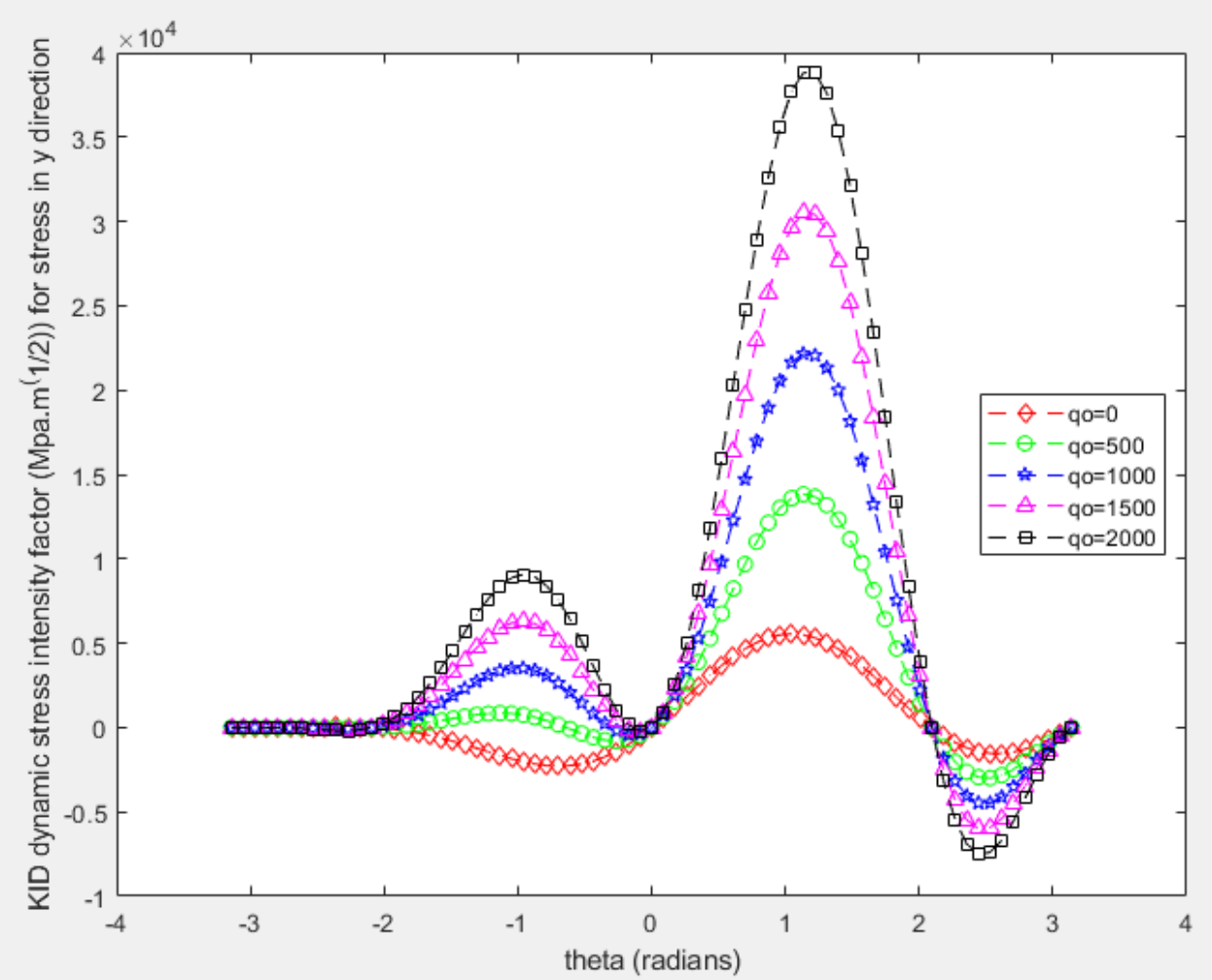

Figure 18:- The dynamic stress intensity factor that is calculated from the thermo-mechanical stress field in y direction

In figure 18 the dynamic stress intensity factor K_{ID} evaluated from the thermo-mechanical stress field in the y direction plotted and the effect of temperature is similar to the stress including at the value of θ = -2π to -0.5 π and 0.5 π to 2π it drops below the isothermal stress field equation.

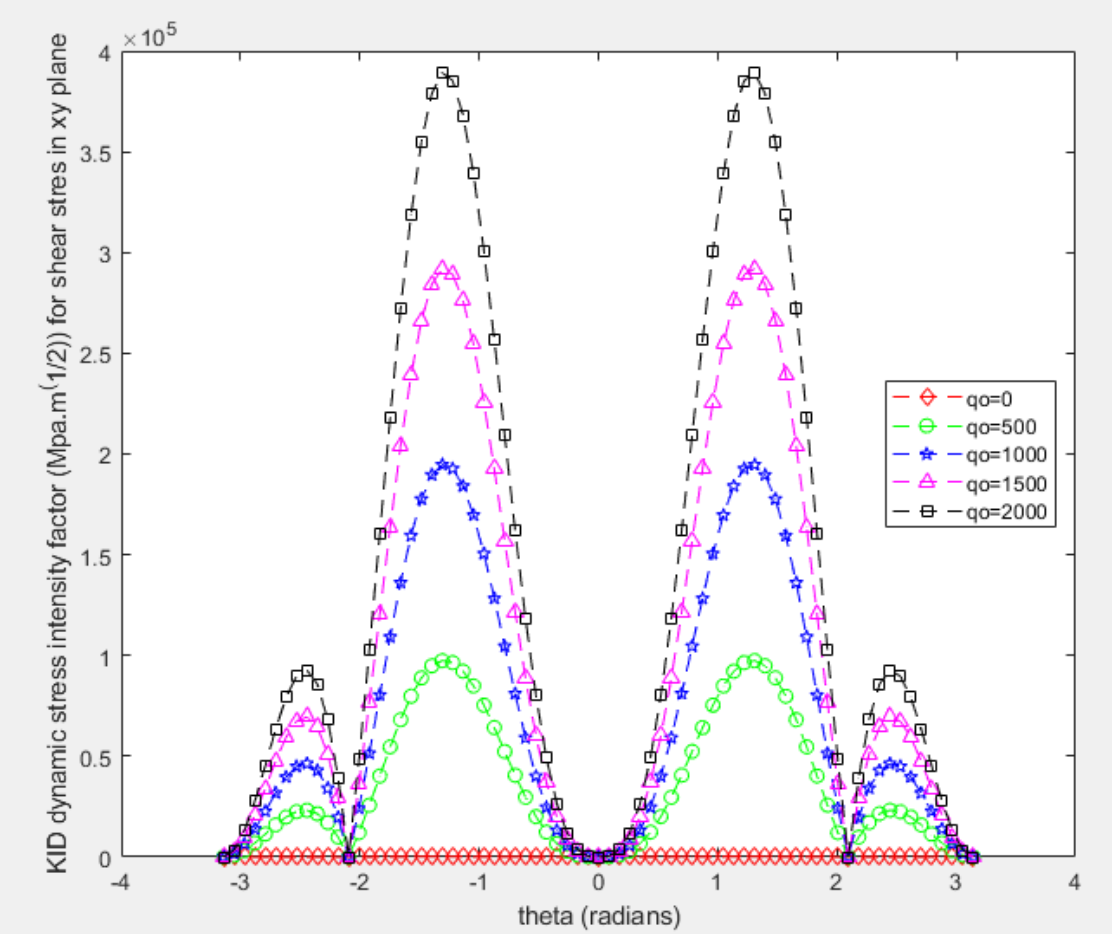

Figure 19:- The dynamic stress intensity factor that is calculated from the thermo-mechanical stress field in xy direction or from the shear stress

For the dynamic stress, intensification factor evaluated from the thermo-mechanical shear stress plotted in figure 19 and the effect is similar to the shear stress illustrated in figure 17. The value of the shear stress as well as the dynamic stress intensification factor meets periodically at some points for all values of q_o. As the stress intensity factors are directly proportional to the stress the effects or temperature and the values of each stress intensity factors at each values of the angular displacement θ are similar to the stress σ_{xx}, σ_{yy} and τ_{xy} as depicted in figure 17, 18 and 19.

Chapter Five

5. Conclusion, Recommendation and Future work

5.1. Conclusion

The main objective of this research was achieved; the thermo-mechanical stress field equations near the crack tip for the mixed mode thermo-mechanical stress field developed using ordinary solution of steady state two-dimensional temperature field. For the ordinary temperature field solution, the perturbation theory is introduced to cooperate and superimpose the solution of temperature obtained from ordinary solution principle with the asymptotic solution for the equation of motion expressed as a function of displacement potentials ϕ and ψ. Up on utilization of MATLAB programs to check the satisfaction of boundary condition for the solution of the temperature field both perturbed and unperturbed satisfies the boundary condition and realizes that the best solution that is done instead of using asymptotic solution principles. Moreover, based on the plot programmed on MATLAB it leads to the following two observations.

The temperature field changes the magnitude of the in-plane stress components (σ_{xx}, σ_{yy} and τ_{xy}) such that the magnitude of the stress increase as the value of temperature increased. This tells us the material will overstressed due to the temperature applied at the edge of the material that is with initial crack.

The dynamic stress intensity factor also increased as the value of temperature increased, this tells that as the material with initial crack overstressed to propagate the crack the material will resist the stress to overcome the propagation. Therefore, the dynamic stress intensity factor will be increased with the value of temperature and in plane stress to work safely by withstanding the thermo-mechanical stress field developed.

5.2. Recommendation

The scope of this thesis has proven to be the utilization of mathematical models and formulas of ordinary differential equations, partial differential equations and the solution principles of those equations. Up on the solution principle the steady state 2D partial differential equation solved and verified numerically by MATLAB for the boundary conditions. The scope of this research is limited to the mathematical models, and in the next phase of the interested researchers can expand

to the experimental analysis for the thermo-mechanical loading. Up on this research 2D plate considered and steady state temperature flow analysis performed, then the stress fields from mechanical loading utilized to express equation of motion as a function of displacement potentials and superimposing with the temperature field equation. To do this the perturbation of the temperature field and the asymptotic approach for the solution of the equation of motion was the main methods used. And after a series of the derivation and manipulation of these equation the thermo-mechanical stress fields developed.

5.3. Future work

This reserch was invetigated on the development of the thermo-mechanical stress field equation based on the perturbation principles and assymptotic approch, and the intended stress field equation ad developed. As the scope is limited to the mathematical models, in the future the researcher interested in this are can take the experimental investigation and compare with this results for the effect of the temperature or heat flux on the crack propagation rate.

References

Abotula, S. *et al.* (2012) 'Dynamic curving cracks in functionally graded materials under thermo-mechanical loading', *International Journal of Solids and Structures*, 49(13), pp. 1637–1655. doi: 10.1016/j.ijsolstr.2012.03.010.

Achenbach, J. D. (1975) 'Bifurcation of a running crack in antiplane strain', *International Journal of Solids and Structures*, 11(12), pp. 1301–1314. doi: 10.1016/0020-7683(75)90059-1.

ANIFANTIS', D. E. K. A. N. K. (1995) 'SHOCK STRESS INTENSITY FACTORS USING A BOUNDARY-ONLY ELEMENT METHOD', 38(August 1994), pp. 4157–4169.

Bouhala, L., Makradi, A. and Belouettar, S. (2015) 'Thermo-anisotropic crack propagation by XFEM', *International Journal of Mechanical Sciences*, 103, pp. 235–246. doi: 10.1016/j.ijmecsci.2015.09.014.

Chalivendra, V. B. (2007) 'Asymptotic analysis of transient curved crack in functionally graded materials', *International Journal of Solids and Structures*, 44(2), pp. 465–479. doi: 10.1016/j.ijsolstr.2006.04.033.

Chen, Z. *et al.* (2018) 'Stress intensity factor-based prediction of solidification crack growth during welding of high strength steel', *Journal of Materials Processing Technology*, 252, pp. 270–278. doi: 10.1016/j.jmatprotec.2017.09.031.

Citarella, R. *et al.* (2013) 'Thermo-mechanical crack propagation in aircraft engine vane by coupled FEM-DBEM approach', *Advances in Engineering Software*, 67, pp. 57–69. doi: 10.1016/j.advengsoft.2013.07.006.

FERDINAND P.BEER, E.RUSSELL JOHANSTON, JR., J. T. D. (2006) 'Beer Mechanics_of_Materials 4th Ed.pdf'. Mc Graw Hill, Higher Education.

FREUND, L. B. (1990) *Dynamic fructure mechanics*. First. Edited by F. R. S. C. W. J. R. G. K. BATCHELOR. Cambridge, New York, Melbourne, Madrid, Cape Town, Singapore, São Paulo Cambridge: CAMBRIDGE UNIVERSITY PRESS.

Georgiadis, H. G. and Theocaris, P. S. (1985) 'On the solution of steady-state elastodynamic crack problems by using complex variable methods', *ZAMP Zeitschrift für angewandte Mathematik und Physik*, 36(1), pp. 146–165. doi: 10.1007/BF00949039.

James J. Kelly (2006) *1 Analytic Functions*.

Johnson, R. S. (2005) *Singular Perturbation Theory_ Mathematical and Analytical Techniques with Applications to Engineering (2005)*. Edited by Alan Jeffrey. Springer. Available at: http://ebooks.springerlink.com.

Kidane, A. *et al.* (2010) 'Mixed-mode dynamic crack propagation in graded materials under thermo-mechanical loading', *Engineering Fracture Mechanics*, 77(14), pp. 2864–2880. doi: 10.1016/j.engfracmech.2010.07.004.

Kidane, A., Chalivendra, V. B. and Shukla, A. (2010) 'Thermo-mechanical stress fields and strain energy associated with a mixed-mode propagating crack', *Acta Mechanica*, 215(1–4), pp. 57–69. doi: 10.1007/s00707-010-0305-x.

Kreyszig, E. (2012) 'Advanced engineering', *Geodrilling International*, (181), pp. 24–25.

Liu, C. and Rosakis, A. J. (1994) 'On the higher order asymptotic analysis of a non-uniformly propagating dynamic crack along an arbitrary path', *Journal of Elasticity*, 35(1–3), pp. 27–60. doi: 10.1007/BF00115538.

MARTIN, H. S. (2005) *Theory of elasticity Theory, Applications, and Numerics*. 200 Wheeler Road, Burlington, MA 01803, USA: Elsevier Inc. All rights reserved.

Memari, A. and Khoshravan Azar, M. R. (2019) 'Thermo-mechanical shock fracture analysis by meshless method', *Theoretical and Applied Fracture Mechanics*, 102, pp. 171–192. doi: 10.1016/j.tafmec.2019.04.013.

Nestor Perez (2004) *FRACTURE MECHANICS, Journal of Chemical Information and Modeling*. Boston: Kluwer Academic Publishers. doi: 10.1017/CBO9781107415324.004.

Parameswaran, V. and Shukla, A. (1999) 'Crack-tip stress fields for dynamic fracture in functionally gradient materials', *Mechanics of Materials*, 31(9), pp. 579–596. doi: 10.1016/S0167-6636(99)00025-3.

Pathak, H., Singh, A. and Singh, I. V. (2016) 'Three-dimensional quasi-static interfacial crack growth simulations in thermo-mechanical environment by coupled FE-EFG approach', *Theoretical and Applied Fracture Mechanics*, 86, pp. 267–283. doi: 10.1016/j.tafmec.2016.08.001.

T.L. Anderson (2005) *Fracture mechanics, Fundamentals and Applications*. third. CRC Press.

Tei-Chen, C. and Cheng-I, W. (1991) 'Coupled transient thermoelastic response in an edge-cracked plate', *Engineering Fracture Mechanics*, 39(5), pp. 915–925. doi: 10.1016/0013-

7944(91)90197-9.

Vshivkov, A. *et al.* (2019) 'Experimental and theoretical analysis of heat flux at fatigue crack tip under mixed mode loading', *Procedia Structural Integrity*, 18, pp. 608–615. doi: 10.1016/j.prostr.2019.08.206.

Wilson, W. K. and Yu, I. W. (1979) 'The use of the J-integral in thermal stress crack problems', *International Journal of Fracture*, 15(4), pp. 377–387. doi: 10.1007/BF00033062.

Appendix

A. The MATLAB program for temperature plot and the contour plot

```
%The MATLAB program for temperature plot and the contour plot of steady
%state temperature solution to check the satisfaction of boundary conditions.
%%(a)
clc
clear all
T1=175; %[degree centigrad]
T2=200; %[degree centigrad]
T=[T1 T2];
L=2; %[cm]
w=L;
x=1;
y=1;
ws=0;
i=0;
for  n=1:2:19
    i=i+1;
      ws=ws+(2/n)*sin(n*pi*x/L)*(sinh(n*pi*(w-y)/L)/sinh(n*pi*w/L));
      wss(i)=ws;
      wf=(2/pi)*ws;
end
T=(T(2)-T(1))*wf+T(1);
wss
T
%%(b)
clear T wss wf
T=[T1 T2];
ws=0;
i=0;
j=2;
for  n=1:2:19
    i=i+1;
      ws=ws+(2/n)*sin(n*pi*x/L)*(sinh(n*pi*(w-y)/L)/sinh(n*pi*w/L));
      wss(i)=ws;
      wf=(2/pi)*ws;
   j=j+1;
     T(j)=(T(2)-T(1))*wf+T(1);
     Er=T(j)-T(j-1);
     if abs(Er) < 0.1
         n
         Er
         T(j)
         break
     end
end
%%(c)
clear T wss wf Er n x y
T=[T1 T2];
ws=zeros(11,11);kx=0; i=0;
for x=0:0.2:L
    kx=kx+1; ky=0; i=i+1;
    for y=0:0.2:w
        ky=ky+1;
```

```
          for  n=1:2:19
          ws(kx,ky)=ws(kx,ky)+(2/pi)*(2/n)*sin(n*pi*x/L)*(sinh(n*pi*(w-
y)/L)/sinh(n*pi*w/L))
          T(kx,ky)=(T2-T1)*ws(kx,ky)+T1
%           Er=T(kx,ky,i)-T(kx,ky,i-1);
%             if abs(Er) <= 0.1
%               n
%               Er
%               T(j)
%             break
%             end
        end
    end
end
figure(1)
Lx=L;
Ly=w;
imagesc([0 Lx], [0 Ly],T);  title('Temprature plot')
colorbar
xlabel('X coordinate')
ylabel('Y coordinate')
figure(2)
contourf(T,10); title('contour plot')
colorbar
```

B. The MATLAB program for temperature plot and the contour plot perturbed solution.

```
%The MATLAB program for temperature plot and the contour plot  of perturbed
%temprature solution for steady state
%%(a)
clc
clear all
T1=25; %[degree centigrad]
T2=200; %[degree centigrad]
T=[T1 T2];
L=2; %[cm]
w=L;
x=1;
y=1;
e=1.07;
ws=0;
i=0;
for  n=1:2:19
    i=i+1;
      ws=ws+e^2*(2/n)*sin(n*pi*x/L)*(sinh(n*pi*(w-y)/L)/sinh(n*pi*w/L));
      wss(i)=ws;
      wf=(2/pi)*ws;
end
T=(T(2)-T(1))*wf+T(1);
wss
T
%%(b)
clear T wss wf
T=[T1 T2];
ws=0;
```

```
i=0;
j=2;
for  n=1:2:19
    i=i+1;
      ws=ws+e^2*(2/n)*sin(n*pi*x/L)*(sinh(n*pi*(w-y)/L)/sinh(n*pi*w/L));
      wss(i)=ws;
      wf=(2/pi)*ws;
   j=j+1;
     T(j)=(T(2)-T(1))*wf+T(1);
     Er=T(j)-T(j-1);
     if abs(Er) < 0.1
         n
         Er
         T(j)
         break
     end
end
%%(c)
clear T wss wf Er n x y
T=[T1 T2];
ws=zeros(11,11);kx=0; i=0;
for x=0:0.2:L
    kx=kx+1; ky=0; i=i+1;
    for y=0:0.2:w
        ky=ky+1;
         for  n=1:2:19
         ws(kx,ky)=ws(kx,ky)+e^2*(2/pi)*(2/n)*sin(n*pi*x/L)*(sinh(n*pi*(w-
y)/L)/sinh(n*pi*w/L))
         T(kx,ky)=(T2-T1)*ws(kx,ky)+T1
%          Er=T(kx,ky,i)-T(kx,ky,i-1);
%            if abs(Er) <= 0.1
%              n
%              Er
%              T(j)
%            break
%            end
        end
    end
end
figure(1)
Lx=L;
Ly=w;
imagesc([0 Lx], [0 Ly],T);  title('Temprature plot')
colorbar
xlabel('X coordinate')
ylabel('Y coordinate')
figure(2)
contourf(T,10); title('contour plot')
colorbar
```

C. MATLAB program for the plot of the stress fields and dynamic stress intensity factor.

```
%% MATLAB program for the plot of the stress fields and dynamic stress
v=0.3;                      %unitless
Ro=4.4200e-06;               %kilogram per cubic millimeter
```

```
E=110000;                   %in mega pascal
alpha=0.0000089;            %per degree centigrade
KID=100;                    %megapascal per square root of meter
KIID=0.2*KID;               %megapascal per square root of meter
Keff=sqrt(KID^2+KIID^2);    %megapascal per square root of meter
r=0.002;                    %meters
a=10;                       %centimeters
b=a;                        %centimeters
x=15;                       %cemtimeters
y=x;                        %centimeters
lambda=E/(2*(1+v));         %megapascal
mu=(E*v)/((1+v)*(1-2*v));   %megapascal
sigma=lambda/mu;
CL=sqrt((lambda+2*mu)/Ro);
CS=sqrt(mu/Ro);
C=0.5*CS;
Co=sqrt(E/Ro);
Cr=0.57*Co;
h=(2/CL)*(CS/Cr)^2*(1-(CS/CL))^2;
Rc=(1-(C/Cr))*sqrt(1-h*C);
theta=-180*pi/180:5*pi/180:180*pi/180;
T1=22;
T2=38.75;
T3=55.5;
T4=72.75;
T5=89;
qo=0;
qo1=50;
qo2=100;
qo3=150;
qo4=200;
alphaL=sqrt(1-(C^2)/(CL^2));
alphaS=sqrt(1-(C^2)/(CS^2));
rL=sqrt(x^2+alphaL^2*y^2);
rS=sqrt(x^2+alphaS^2*y^2);
thetaL=atan((alphaL*y)/x);
thetaS=atan((alphaS*y)/x);
K1=(4/pi)*(1/sinh(pi*b/a));
a1=cos(theta/2);
b1=1-sin(theta/2);
b2=1+sin(theta/2);
b3=sin(theta/2);
c1=sin(1.5*theta);
sigx=(KID/(Rc*sqrt(2*pi*r)))*a1.*b1.*c1;
sigy=(KID/(Rc*sqrt(2*pi*r)))*a1.*b2.*c1;
sigxy=(KID/(Rc*sqrt(2*pi*r)))*a1.*b3.*c1;
Ao=((1+alphaS^2)*(1-alphaL^2))/(4*alphaS*alphaL-
(1+alphaS^2)^2)*((KID)/mu*sqrt(2*pi));
Bo=((-2*alphaL)/(1+alphaS^2))*Ao;
Co=((2*alphaS)*(1-alphaL^2))/(4*alphaS*alphaL-
(1+alphaS^2)^2)*((KIID)/mu*sqrt(2*pi));
Do=((1+alphaS^2)/(2*alphaS))*Co;
A1=1/(4*sigma*(2*alphaL^2-1));
B1=(2*sigma*(1-alphaL^2)-4*alphaL^2)/(4*alphaS*(2*alphaL^2-1));
D1=B1;
```

```
C1=B1;
Fxx=((1+alphaS^2)/(4*alphaS*alphaL-(1+alphaS^2)^2))*((1+2*alphaL^2-
alphaS^2)*cos(0.5*thetaL)*sqrt(r/rL)-
((4*alphaL*alphaS)/(1+alphaS^2))*cos(0.5*thetaS)*sqrt(r/rS));
Fyy=((1+alphaS^2)/(4*alphaS*alphaL-(1+alphaS^2)^2))*(-
(1+alphaS^2)*cos(0.5*thetaL)*sqrt(r/rL)+((4*alphaL*alphaS)/(1+alphaS^2))*cos(
0.5*thetaS)*sqrt(r/rS));
Fxy=((2*alphaL*(1+alphaS^2))/(4*alphaS*alphaL-
(1+alphaS^2)^2))*(sin(0.5*thetaL)*sqrt(r/rL)-sin(0.5*thetaS)*sqrt(r/rS));
K=Keff/sqrt(2*pi*r);
SIGMAX1=(mu*((3/4)*(((2+sigma)*(1/sqrt(rL))*cos(1/2*thetaL)-
sigma*alphaS^2*(1/sqrt(rL)*sin(0.5*thetaL)))*Ao-
((2+sigma*(1+alphaL^2))*(1/sqrt(rL)*sin(0.5*thetaL)))*Co+((2+sigma)*alphaS*(1
/sqrt(rS))*sin(0.5*thetaS)+sigma*alphaS*(1/sqrt(rS))*cos(0.5*thetaS))*Bo+((2+
sigma)*alphaS*(1/sqrt(rS))*cos(0.5*thetaS)-
sigma*alphaS*(1/sqrt(rS))*sin(0.5*thetaS))*Do)+(4+2*sigma*(1-
alphaL^2))*A1+(4*D1*alphaS)+(2*sigma*alphaS*(D1-
B1))+4*K1*((2*sigma+2)*a/(sigma+2)*pi)*qo*(cosh(pi/a*(b-y)*(1-(sigma*pi/a)))-
pi/a*sinh(pi/a*(b-y)))*r*sin(theta)-(2+3*sigma)*alpha*T1))/1000000;
SIGMAY1=(mu*((3/4)*((sigma*(1/sqrt(rL))*cos(1/2*thetaL)-
(2*alphaL^2+sigma*alphaL^2)*(1/sqrt(rL))*sin(1/2*thetaL))*Ao-
((2*alphaL^2+sigma*(1+alphaL^2))*(1/sqrt(rL))*sin(1/2*thetaL))*Co+((2*alphaS+
sigma*alphaS)*(1/sqrt(rS))*cos(1/2*thetaS)+sigma*alphaS*(1/sqrt(rS))*sin(1/2*
thetaS))*Bo-
((2*alphaS+sigma*alphaS)*(1/sqrt(rS))*sin(1/2*thetaS)+sigma*alphaS*(1/sqrt(rS
))*cos(1/2*thetaS))*Do)+(2*sigma*(1-alphaL^2)-4*alphaL^2)*A1-
4*B1*alphaS+2*sigma*alphaS*(D1-
B1)+4*K1*((2*sigma+2)*a/(sigma+2)*pi)*qo*(cosh(pi/a*(b-y)*(1-(sigma*pi/a)))-
pi/a*sinh(pi/a*(b-y)))*r*sin(theta)-(2+3*sigma)*alpha*T1))/1000000;
TAUXY1=mu*(1.5*Ao*alphaL*(1/sqrt(rL))*sin(1/2*thetaL)+(3/4)*Bo*(1/sqrt(rS))*(
alphaS^2*cos(1/2*thetaS)+sin(1/2*thetaS))+1.5*Co*alphaL*(1/sqrt(rL))*cos(1/2*
thetaL)+(3/4)*Do*(1/sqrt(rS))*(alphaS^2*cos(1/2*thetaS)+sin(1/2*thetaS))+2*(a
lphaS^2*B1-D1)+4*C1*alphaL-
4*K1*((2*sigma+2)*a/(sigma+2)*pi)*qo*(cosh(pi/a*(b-
y)))*((a/pi)*r*cos(theta))).*sin(theta)/10^8;
%%
SIGMAX2=(mu*((3/4)*(((2+sigma)*(1/sqrt(rL))*cos(1/2*thetaL)-
sigma*alphaS^2*(1/sqrt(rL)*sin(0.5*thetaL)))*Ao-
((2+sigma*(1+alphaL^2))*(1/sqrt(rL)*sin(0.5*thetaL)))*Co+((2+sigma)*alphaS*(1
/sqrt(rS))*sin(0.5*thetaS)+sigma*alphaS*(1/sqrt(rS))*cos(0.5*thetaS))*Bo+((2+
sigma)*alphaS*(1/sqrt(rS))*cos(0.5*thetaS)-
sigma*alphaS*(1/sqrt(rS))*sin(0.5*thetaS))*Do)+(4+2*sigma*(1-
alphaL^2))*A1+(4*D1*alphaS)+(2*sigma*alphaS*(D1-
B1))+4*K1*((2*sigma+2)*a/(sigma+2)*pi)*qo1*(cosh(pi/a*(b-y)*(1-
(sigma*pi/a)))-pi/a*sinh(pi/a*(b-y)))*r*sin(theta)-
(2+3*sigma)*alpha*T2))/1000000;
SIGMAY2=(mu*((3/4)*((sigma*(1/sqrt(rL))*cos(1/2*thetaL)-
(2*alphaL^2+sigma*alphaL^2)*(1/sqrt(rL))*sin(1/2*thetaL))*Ao-
((2*alphaL^2+sigma*(1+alphaL^2))*(1/sqrt(rL))*sin(1/2*thetaL))*Co+((2*alphaS+
sigma*alphaS)*(1/sqrt(rS))*cos(1/2*thetaS)+sigma*alphaS*(1/sqrt(rS))*sin(1/2*
thetaS))*Bo-
((2*alphaS+sigma*alphaS)*(1/sqrt(rS))*sin(1/2*thetaS)+sigma*alphaS*(1/sqrt(rS
))*cos(1/2*thetaS))*Do)+(2*sigma*(1-alphaL^2)-4*alphaL^2)*A1-
4*B1*alphaS+2*sigma*alphaS*(D1-
```

```
B1)+4*K1*((2*sigma+2)*a/(sigma+2)*pi)*qo1*(cosh(pi/a*(b-y)*(1-(sigma*pi/a)))-
pi/a*sinh(pi/a*(b-y)))*r*sin(theta)-(2+3*sigma)*alpha*T2))/1000000;
TAUXY2=mu*(1.5*Ao*alphaL*(1/sqrt(rL))*sin(1/2*thetaL)+(3/4)*Bo*(1/sqrt(rS))*(
alphaS^2*cos(1/2*thetaS)+sin(1/2*thetaS))+1.5*Co*alphaL*(1/sqrt(rL))*cos(1/2*
thetaL)+(3/4)*Do*(1/sqrt(rS))*(alphaS^2*cos(1/2*thetaS)+sin(1/2*thetaS))+2*(a
lphaS^2*B1-D1)+4*C1*alphaL-
4*K1*((2*sigma+2)*a/(sigma+2)*pi)*qo1*(cosh(pi/a*(b-
y)))*(1+(a/pi)*r*cos(theta))).*sin(theta)/10^8;
%%
SIGMAX3=(mu*((3/4)*(((2+sigma)*(1/sqrt(rL))*cos(1/2*thetaL)-
sigma*alphaS^2*(1/sqrt(rL)*sin(0.5*thetaL)))*Ao-
((2+sigma*(1+alphaL^2))*(1/sqrt(rL)*sin(0.5*thetaL)))*Co+((2+sigma)*alphaS*(1
/sqrt(rS))*sin(0.5*thetaS)+sigma*alphaS*(1/sqrt(rS))*cos(0.5*thetaS))*Bo+((2+
sigma)*alphaS*(1/sqrt(rS))*cos(0.5*thetaS)-
sigma*alphaS*(1/sqrt(rS))*sin(0.5*thetaS))*Do)+(4+2*sigma*(1-
alphaL^2))*A1+(4*D1*alphaS)+(2*sigma*alphaS*(D1-
B1))+4*K1*((2*sigma+2)*a/(sigma+2)*pi)*qo2*(cosh(pi/a*(b-y)*(1-
(sigma*pi/a)))-pi/a*sinh(pi/a*(b-y)))*r*sin(theta)-
(2+3*sigma)*alpha*T3))/1000000;
SIGMAY3=(mu*((3/4)*((sigma*(1/sqrt(rL))*cos(1/2*thetaL)-
(2*alphaL^2+sigma*alphaL^2)*(1/sqrt(rL))*sin(1/2*thetaL))*Ao-
((2*alphaL^2+sigma*(1+alphaL^2))*(1/sqrt(rL))*sin(1/2*thetaL))*Co+((2*alphaS+
sigma*alphaS)*(1/sqrt(rS))*cos(1/2*thetaS)+sigma*alphaS*(1/sqrt(rS))*sin(1/2*
thetaS))*Bo-
((2*alphaS+sigma*alphaS)*(1/sqrt(rS))*sin(1/2*thetaS)+sigma*alphaS*(1/sqrt(rS
))*cos(1/2*thetaS))*Do)+(2*sigma*(1-alphaL^2)-4*alphaL^2)*A1-
4*B1*alphaS+2*sigma*alphaS*(D1-
B1)+4*K1*((2*sigma+2)*a/(sigma+2)*pi)*qo2*(cosh(pi/a*(b-y)*(1-(sigma*pi/a)))-
pi/a*sinh(pi/a*(b-y)))*r*sin(theta)-(2+3*sigma)*alpha*T3))/1000000;
TAUXY3=mu*(1.5*Ao*alphaL*(1/sqrt(rL))*sin(1/2*thetaL)+(3/4)*Bo*(1/sqrt(rS))*(
alphaS^2*cos(1/2*thetaS)+sin(1/2*thetaS))+1.5*Co*alphaL*(1/sqrt(rL))*cos(1/2*
thetaL)+(3/4)*Do*(1/sqrt(rS))*(alphaS^2*cos(1/2*thetaS)+sin(1/2*thetaS))+2*(a
lphaS^2*B1-D1)+4*C1*alphaL-
4*K1*((2*sigma+2)*a/(sigma+2)*pi)*qo2*(cosh(pi/a*(b-
y)))*(1+(a/pi)*r*cos(theta))).*sin(theta)/10^8;
%%
SIGMAX4=(mu*((3/4)*(((2+sigma)*(1/sqrt(rL))*cos(1/2*thetaL)-
sigma*alphaS^2*(1/sqrt(rL)*sin(0.5*thetaL)))*Ao-
((2+sigma*(1+alphaL^2))*(1/sqrt(rL)*sin(0.5*thetaL)))*Co+((2+sigma)*alphaS*(1
/sqrt(rS))*sin(0.5*thetaS)+sigma*alphaS*(1/sqrt(rS))*cos(0.5*thetaS))*Bo+((2+
sigma)*alphaS*(1/sqrt(rS))*cos(0.5*thetaS)-
sigma*alphaS*(1/sqrt(rS))*sin(0.5*thetaS))*Do)+(4+2*sigma*(1-
alphaL^2))*A1+(4*D1*alphaS)+(2*sigma*alphaS*(D1-
B1))+4*K1*((2*sigma+2)*a/(sigma+2)*pi)*qo3*(cosh(pi/a*(b-y)*(1-
(sigma*pi/a)))-pi/a*sinh(pi/a*(b-y)))*r*sin(theta)-
(2+3*sigma)*alpha*T4))/1000000;
SIGMAY4=(mu*((3/4)*((sigma*(1/sqrt(rL))*cos(1/2*thetaL)-
(2*alphaL^2+sigma*alphaL^2)*(1/sqrt(rL))*sin(1/2*thetaL))*Ao-
((2*alphaL^2+sigma*(1+alphaL^2))*(1/sqrt(rL))*sin(1/2*thetaL))*Co+((2*alphaS+
sigma*alphaS)*(1/sqrt(rS))*cos(1/2*thetaS)+sigma*alphaS*(1/sqrt(rS))*sin(1/2*
thetaS))*Bo-
((2*alphaS+sigma*alphaS)*(1/sqrt(rS))*sin(1/2*thetaS)+sigma*alphaS*(1/sqrt(rS
))*cos(1/2*thetaS))*Do)+(2*sigma*(1-alphaL^2)-4*alphaL^2)*A1-
4*B1*alphaS+2*sigma*alphaS*(D1-
```

```
B1)+4*K1*((2*sigma+2)*a/(sigma+2)*pi)*qo3*(cosh(pi/a*(b-y)*(1-(sigma*pi/a)))-
pi/a*sinh(pi/a*(b-y)))*r*sin(theta)-(2+3*sigma)*alpha*T4))/1000000;
TAUXY4=mu*(1.5*Ao*alphaL*(1/sqrt(rL))*sin(1/2*thetaL)+(3/4)*Bo*(1/sqrt(rS))*(
alphaS^2*cos(1/2*thetaS)+sin(1/2*thetaS))+1.5*Co*alphaL*(1/sqrt(rL))*cos(1/2*
thetaL)+(3/4)*Do*(1/sqrt(rS))*(alphaS^2*cos(1/2*thetaS)+sin(1/2*thetaS))+2*(a
lphaS^2*B1-D1)+4*C1*alphaL-
4*K1*((2*sigma+2)*a/(sigma+2)*pi)*qo3*(cosh(pi/a*(b-
y)))*(1+(a/pi)*r*cos(theta))).*sin(theta)/10^8;
%%
SIGMAX5=(mu*((3/4)*(((2+sigma)*(1/sqrt(rL))*cos(1/2*thetaL)-
sigma*alphaS^2*(1/sqrt(rL)*sin(0.5*thetaL)))*Ao-
((2+sigma*(1+alphaL^2))*(1/sqrt(rL)*sin(0.5*thetaL)))*Co+((2+sigma)*alphaS*(1
/sqrt(rS))*sin(0.5*thetaS)+sigma*alphaS*(1/sqrt(rS))*cos(0.5*thetaS))*Bo+((2+
sigma)*alphaS*(1/sqrt(rS))*cos(0.5*thetaS)-
sigma*alphaS*(1/sqrt(rS))*sin(0.5*thetaS))*Do)+(4+2*sigma*(1-
alphaL^2))*A1+(4*D1*alphaS)+(2*sigma*alphaS*(D1-
B1))+4*K1*((2*sigma+2)*a/(sigma+2)*pi)*qo4*(cosh(pi/a*(b-y)*(1-
(sigma*pi/a)))-pi/a*sinh(pi/a*(b-y)))*r*sin(theta)-
(2+3*sigma)*alpha*T5))/1000000;
SIGMAY5=(mu*((3/4)*((sigma*(1/sqrt(rL))*cos(1/2*thetaL)-
(2*alphaL^2+sigma*alphaL^2)*(1/sqrt(rL))*sin(1/2*thetaL))*Ao-
((2*alphaL^2+sigma*(1+alphaL^2))*(1/sqrt(rL))*sin(1/2*thetaL))*Co+((2*alphaS+
sigma*alphaS)*(1/sqrt(rS))*cos(1/2*thetaS)+sigma*alphaS*(1/sqrt(rS))*sin(1/2*
thetaS))*Bo-
((2*alphaS+sigma*alphaS)*(1/sqrt(rS))*sin(1/2*thetaS)+sigma*alphaS*(1/sqrt(rS
))*cos(1/2*thetaS))*Do)+(2*sigma*(1-alphaL^2)-4*alphaL^2)*A1-
4*B1*alphaS+2*sigma*alphaS*(D1-
B1)+4*K1*((2*sigma+2)*a/(sigma+2)*pi)*qo4*(cosh(pi/a*(b-y)*(1-(sigma*pi/a)))-
pi/a*sinh(pi/a*(b-y)))*r*sin(theta)-(2+3*sigma)*alpha*T5))/1000000;
TAUXY5=mu*(1.5*Ao*alphaL*(1/sqrt(rL))*sin(1/2*thetaL)+(3/4)*Bo*(1/sqrt(rS))*(
alphaS^2*cos(1/2*thetaS)+sin(1/2*thetaS))+1.5*Co*alphaL*(1/sqrt(rL))*cos(1/2*
thetaL)+(3/4)*Do*(1/sqrt(rS))*(alphaS^2*cos(1/2*thetaS)+sin(1/2*thetaS))+2*(a
lphaS^2*B1-D1)+4*C1*alphaL-
4*K1*((2*sigma+2)*a/(sigma+2)*pi)*qo4*(cosh(pi/a*(b-
y)))*(1+(a/pi)*r*cos(theta))).*sin(theta)/10^8;
%%
SX1=SIGMAX1.*sigx;
SX2=SIGMAX2.*sigx;
SX3=SIGMAX3.*sigx;
SX4=SIGMAX4.*sigx;
SX5=SIGMAX5.*sigx;
%%
figure(1)
plot(theta, SX1 ,'-dr', theta, SX2,'-og',theta,SX3,'-pb',theta,SX4,'-
^m',theta,SX5,'-sk')
xlabel('theta (radians)')
ylabel('inplane stress in x direction (Mpa)')
legend('qo=0','qo=500','qo=1000','qo=1500','qo=2000')
legend('Location','East')
%%
SY1=SIGMAY1.*sigy;
SY2=SIGMAY2.*sigy;
SY3=SIGMAY3.*sigy;
SY4=SIGMAY4.*sigy;
SY5=SIGMAY5.*sigy;
```

```
%%
figure(2)
plot(theta, SY1 ,'--dr', theta, SY2,'--og',theta,SY3,'--pb',theta,SY4,'--
^m',theta,SY5,'--sk')
xlabel('theta (radians)')
ylabel('inplane stress in y direction (Mpa)')
legend('qo=0','qo=500','qo=1000','qo=1500','qo=2000')
legend('Location','East')
%%
SXY1=abs(TAUXY1.*sigxy);
SXY2=abs(TAUXY2.*sigxy);
SXY3=abs(TAUXY3.*sigxy);
SXY4=abs(TAUXY4.*sigxy);
SXY5=abs(TAUXY5.*sigxy);
%%
figure(3)
plot(theta, SXY1 ,'--dr', theta, SXY2,'--og',theta,SXY3,'--pb',theta,SXY4,'--
^m',theta,SXY5,'--sk')
xlabel('theta (radians)')
ylabel('shear stress in xy direction (Mpa)')
legend('qo=0','qo=500','qo=1000','qo=1500','qo=2000')
legend('Location','East')
%%
KID1=SX1*sqrt(2*pi*r)/Fxx;
KID2=SX2*sqrt(2*pi*r)/Fxx;
KID3=SX3*sqrt(2*pi*r)/Fxx;
KID4=SX4*sqrt(2*pi*r)/Fxx;
KID5=SX5*sqrt(2*pi*r)/Fxx;
%%
figure(4)
plot(theta, KID1 ,'--dr', theta, KID2,'--og',theta,KID3,'--pb',theta,KID4,'--
^m',theta,KID5,'--sk')
xlabel('theta (radians)')
ylabel('KID dynamic stress intensity factor(Mpa.m^(1/2)) for stress in x
direction')
legend('qo=0','qo=500','qo=1000','qo=1500','qo=2000')
legend('Location','East')
%%
KID1=SY1*sqrt(2*pi*r)/Fyy;
KID2=SY2*sqrt(2*pi*r)/Fyy;
KID3=SY3*sqrt(2*pi*r)/Fyy;
KID4=SY4*sqrt(2*pi*r)/Fyy;
KID5=SY5*sqrt(2*pi*r)/Fyy;
%%
figure(5)
plot(theta, KID1 ,'--dr', theta, KID2,'--og',theta,KID3,'--pb',theta,KID4,'--
^m',theta,KID5,'--sk')
xlabel('theta (radians)')
ylabel('KID dynamic stress intensity factor (Mpa.m^(1/2)) for stress in y
direction')
legend('qo=0','qo=500','qo=1000','qo=1500','qo=2000')
legend('Location','East')
%%
KID1=SXY1*sqrt(2*pi*r)/Fxy;
KID2=SXY2*sqrt(2*pi*r)/Fxy;
```

```
KID3=SXY3*sqrt(2*pi*r)/Fxy;
KID4=SXY4*sqrt(2*pi*r)/Fxy;
KID5=SXY5*sqrt(2*pi*r)/Fxy;
%%
figure(6)
plot(theta, KID1 ,'--dr', theta, KID2,'--og',theta,KID3,'--pb',theta,KID4,'--
^m',theta,KID5,'--sk')
xlabel('theta (radians)')
ylabel('KID dynamic stress intensity factor (Mpa.m^(1/2)) for shear stres in
xy plane')
legend('qo=0','qo=500','qo=1000','qo=1500','qo=2000')
legend('Location','East')
```